2011

Kinase pathways underlying muscarinic activation of colonic longitudinal muscle

Charles Dudley Anderson Jr.
Virginia Commonwealth University

Kinase pathways underlying muscarinic activation of colonic longitudinal muscle

A dissertation submitted in partial fulfillment of the requirements for the degree of Doctor of Philosophy at Virginia Commonwealth University.

by

Charles Dudley Anderson, Jr.

B.S., University of Richmond, 1996

M.S., Virginia Commonwealth University, 2004

Director: John R. Grider, Ph.D.
Professor
Physiology and Biophysics

Virginia Commonwealth University

Richmond, Virginia

May, 2011

ACKNOWLEDGMENTS

The author has not the space to thank adequately all those who helped, guided, and supported him through what has been a very long journey. He thanks everyone with his most humble appreciation. The support of his committee and faculty has been invaluable and unyielding; their advice and consideration can never be repaid or forgotten. The love of his friends has made the journey not a lonely one, and the love of his family has ensured that he would never lack comfort.

Specifically and personally, I wish to focus upon but a few of the many. Dr. Joseph Feher has been my academic, philosophical, and spiritual guide for most of the past decade. Dr. Frank Raucci is the best example of a friend a man could have. Dr. Sunila Mahavadi remains the most kind, selfless, and caring teacher that I could ever imagine, despite her denials to the same. Dr. John Grider has inspired me by example to possess balance in my relationship with science, work, and life. Thank you, Jack. I will always be proud to be part of your madness/career. And my dear Novia, who has suffered and has celebrated every step with me, I thank you. I am certain this point in my journey means as much (or more) to you as it does to me. And I am so very lucky our journey does not stop here.

TABLE OF CONTENTS

TABLE OF FIGURES

TABLE OF TABLES

TABLE OF ABBREVIATIONS

AA	Arachidonic Acid
AMP	Adenosine Monophosphate
AMPK	AMP-activated Protein Kinase
ATP	Adenosine Triphosphate
AUC	Area Under Curve
Ca^{2+}	Free Calcium Ion
cADPR	Cyclic ADP-ribose
CaMKI	Calcium-calmodulin Dependent Kinase Type I
CaMKII	Calcium-calmodulin Dependent Kinase Type II
CaMKK	Calcium-calmodulin Dependent Kinase Kinase
cAMP	Cyclic Adenosine Monophosphate
CCh	Carbachol/Carbamylcholine
CPI-17	C-Kinase Potentiated Protein Phosphatase Inhibitor 17 kDa
cPLA2	Cytoplasmic Phospholipase A 2
DAG	Diacylglycerol
eNOS	Endothelial Nitric Oxide Synthase
ENS	Enteric Nervous System
ERK1/2	Extracellular Signal Kinase Type1/2
ICC	Interstitial Cells of Cajal

ILK	Integrin-Linked Kinase
IP_3	Inositol 1,4,5 Trisphosphate
kDa	Kilodalton
LM-MP	Longitudinal Muscle-Myenteric Plexus
M1	Muscarinic Receptor Type 1
M2	Muscarinic Receptor Type 2
M3	Muscarinic Receptor Type 3
MLC_{20}	20 kDa Regulatory Light Chain of Myosin II
MLCK	Myosin Light Chain Kinase
MLCP	Myosin Light Chain Phosphatase
MYPT1	Myosin Phosphatase Target Subunit 1
Na^+	Free Sodium Ion
nM	Nanomolar
NO	Nitric Oxide
PDGF	Platelet-derived Growth Factor
PI	Phosphoinositide
PIP	Phosphatidylinositol-4-bisphosphate
PIP_2	Phosphatidylinositol 4,5 bisphosphate
PKA	cAMP-dependent Protein Kinase
PKG	cGMP-dependent Protein Kinase
PLC	Phospholipase C
PP1	Protein Phosphatase Type 1
Rho kinase	Rho-associated Protein Kinase

SMC	Smooth Muscle Cell
SR	Sarcoplasmic Reticulum
TTX	Tetrodotoxin
μM	Micromolar
VDCC	Voltage-dependent Calcium Channel
VIP	Vasoactive Intestinal Peptide
ZIPK or Zip Kinase	Zipper Interacting Protein Kinase

ABSTRACT

KINASE PATHWAYS UNDERLYING MUSCARINIC ACTIVATION OF COLONIC LONGITUDINAL MUSCLE

By Charles Dudley Anderson, Jr.

A dissertation submitted in partial fulfillment of the requirements for the degree of Doctor of Philosophy at Virginia Commonwealth University.

Virginia Commonwealth University, 2011

Major Director: John R. Grider, Professor, Department of Physiology and Biophysics

The longitudinal muscle layer in gut is the functional opponent to the circular muscle layer during the peristalsis reflex. Differences in innervation of the layers allow for the contraction of one layer that corresponds with the simultaneous relaxation of the other, enabling the passage of gut contents in a controlled fashion. Differences in development have given the cells of the two layers differences in receptor populations,

membrane lipid handling, and calcium handling profiles/behaviors. The kinase signaling differences between the two layers is not as well characterized. Upon activation of cells from the circular muscle layer, it is known that Rho kinase and ERK1/2 promote contraction, while CaMKK/AMPK and CaMKII perform inhibitory/self-inhibitory roles. Such behaviors are poorly understood in the longitudinal muscle layer.

In longitudinal muscle strips, we measured muscarinic receptor-mediated contraction following incubation with kinase inhibitors. Upon comparison to control, contributions of Rho Kinase and ERK1/2 were similar to those seen in circular muscle. Inhibition of both of these enzymes leads to diminished contraction. However, CaMKK/AMPK and CaMKII have effects in longitudinal muscle opposite to their regulation in circular muscle – their inhibition also diminishes the contractile response. These contractile data from strips were supported by immunokinase assay measurements of MLCK activity from strip homogenates with and without kinase inhibition. Therefore, we suggest that the activities of CaMKK/AMPK and CaMKII in longitudinal muscle are indeed different from their regulatory roles in circular muscle, perhaps a consequence of the different calcium handling modalities of the two muscle types.

INTRODUCTION

Function of Gut

Simply, the gut is a muscular tube that allows for the intake, processing, absorption, and elimination of solid and liquid nutrients. The coordination of these roles involves the varied chemical and mechanical abilities of the gut. These abilities in turn require numerous control mechanisms to maintain proper function.

Gut as Agent of digestion/absorption/defense

The primary role of the gut is acquisition of necessary nutrients for the maintenance of overall structural integrity and energy supply, fueling the metabolic processes of the body. As food and drink are ingested, regions of the gut play specific roles in the mechanical and chemical breakdown of food (digestion). Mechanically, the muscular tube can collapse upon its contents, physically compressing them to render the contents into smaller pieces, leading to a suspension (or emulsion) of the various ingested substances. Different types of mechanical activity ensure both this disassembly of ingesta and the coordinated movement of ingesta through the gut, where a variety of place-specific chemical processes can occur [1].

Chemically, the gut releases agents into its lumen, where mixing with the contents leads to chemical reactions that reduce large polymer molecules (e.g. starches, proteins, triglycerides) into smaller constitutive pieces (e.g. sugars, peptides, fatty acids). This chemistry facilitates the absorption of these ingested materials by non-muscular components. The epithelium facing the lumen possesses membrane bound enzymes that offer final digestion of proteins and carbohydrates and the absorption into the cells of the epithelium. Lipid digestion products also enter the epithelial cells by diffusion. After entry into the cells, the absorbed nutrients enter the blood stream as gut tissue is highly served by both the circulatory and lymphatic systems. Digestion products that remain unabsorbed continue passage through the gut for elimination from the organism.

The gut interior is contiguous with the external environment and possesses considerable surface area. Because of its high exposure, the gut has intricate immunological roles and abilities to prevent introduction of harmful substances or life forms into the body. These functions are carried out by cells or tissues that are distinct from the cells or tissues charged with the mechanical and chemical duties already mentioned. These cells and tissues offer regulation of gut function, including motility, and their roles in maintenance of basic

functions is beginning to find appreciation in the literature[2]. Under normal conditions, beyond immunological threat, the gut itself possesses sensory functions upon its exposure to contents of a meal. Such sensory cells can perhaps feed into a control network that manipulates motility, secretory, and absorptive behaviors. Altered behaviors could optimize the efficiency of the gut when the contents warrant, or prevent inefficiency when stimuli communicate harmful or wasteful contents [3, 4].

Transit of Gut Contents

The movement of contents through the gut and the mechanical treatment of contents while inside the lumen are critical for efficient absorption of nutrients. Two general patterns of gut motility accomplish these roles. Both motility patterns require coordinated activity of the two muscular layers of the gut, the circular muscle layer and the longitudinal muscle layer.

The circular muscle layer consists of muscle cells oriented around the circumference of the gut lumen, forming adjacent rings of muscle that extend throughout the gut. Upon local activation of these cells, the circular muscle tissue contracts, and these muscular rings decrease their diameter and therefore the caliber of the gut lumen. The longitudinal muscle layer is comprised of cells oriented along the long axis of the gut,

parallel to the overall direction of the movement of contents. Upon local activation, the contraction of longitudinal muscle causes the gut lumen to increase its diameter in a manner that shortens the gut at that location. Because of their opposing actions on the gut lumen, the two muscular layers will not normally activate at the same location simultaneously. However, when these opposing actions occur at adjacent locations, the contents of the lumen can be manipulated in a controlled fashion [5].

Gut Anatomy

Gut structure varies along the length of the canal, but generally possesses a consistent layered organization. Outer layers provide for structural integrity and muscular activity, and inner layers secrete substances into the lumen and have mechanisms that allow for the absorption of ingested nutrients. In addition, there are neural connections and vascular pathways throughout all gut tissue.

Gross Anatomy

The innermost layer of the gut is the mucosa, containing both the epithelial cells necessary for final digestion and assimilation of the ingested material, and the *lamina propria*, a layer of connective tissue with capillaries and lacteals to convey absorbed nutrients. In addition, the mucosal layer

possesses glands able to secrete substances into the gut lumen, cells with sensory capabilities, and the *muscularis mucosae*, a thin layer of smooth muscle that aids in enhanced contact of the epithelium with luminal contents as a result of its contractile function. Outside of the mucosal layer lies the submucosa, another layer of connective tissue that possesses connections to the vasculature, inflammatory cells, and in some cases, glands. The submucosa contains a neural plexus, the submucosal plexus which has interconnections within the nervous system of the gut (enteric nervous system), as well as connections to the autonomic nervous system. This submucosal plexus is important in controlling the secretory functions of the mucosa through innervation of the epithelium, and may play a role in the coordination of muscularis mucosae and muscularis externa activity with secretory activity[6].

External to the submucosa is the circular muscle layer, a layer of smooth muscle cells oriented circumferentially to the central axis of the gut lumen. When cells in this muscle layer contract, the overall effect is the narrowing of the lumen at this location. When properly coordinated, this narrowing of the lumen can propel the luminal substances within forward in the gut. This contraction can also mix the contents of the lumen at the contraction locale. Because of its muscular activity, this

layer also contains blood vessels and neural connections, but does not contain the nerve bodies themselves[7]. Continuing outward radially, the adjacent layer contains neurons and organized connections among these neurons within the enteric nervous system, as well as external connections to the autonomic nervous system. This myenteric plexus plays a chief role in controlling the muscular activity of the circular muscle layer beneath it, and the longitudinal muscle layer above it[8]. The longitudinal muscle layer consists of smooth muscle cells oriented in parallel with the long axis of the lumen. The longitudinal muscle layer is substantially thinner than the circular muscle layer and varies in its receptor population, calcium handling, and signaling chemistry[9]. When longitudinal muscle contracts, the lumen of the gut is dilated at the contraction site and the gut shortened, in contrast to the actions of the circular muscle. The neural connections provided by the myenteric plexuses between the longitudinal and circular muscle layers coordinate activity ensuring that longitudinal muscle and circular muscle do not simultaneously contract at the same location in gut[10, 11].

Beyond the longitudinal muscle layer there exists a serous membrane, the serosa, which serves as an outer containment membrane for the gut tube. The epithelial cells of this layer

secrete a serous fluid to lubricate the outer surfaces of the gut. The layers of the gut are depicted in Figure 1 [12].

Figure 1. Structure of the Gut Wall. Adapted from Furness.

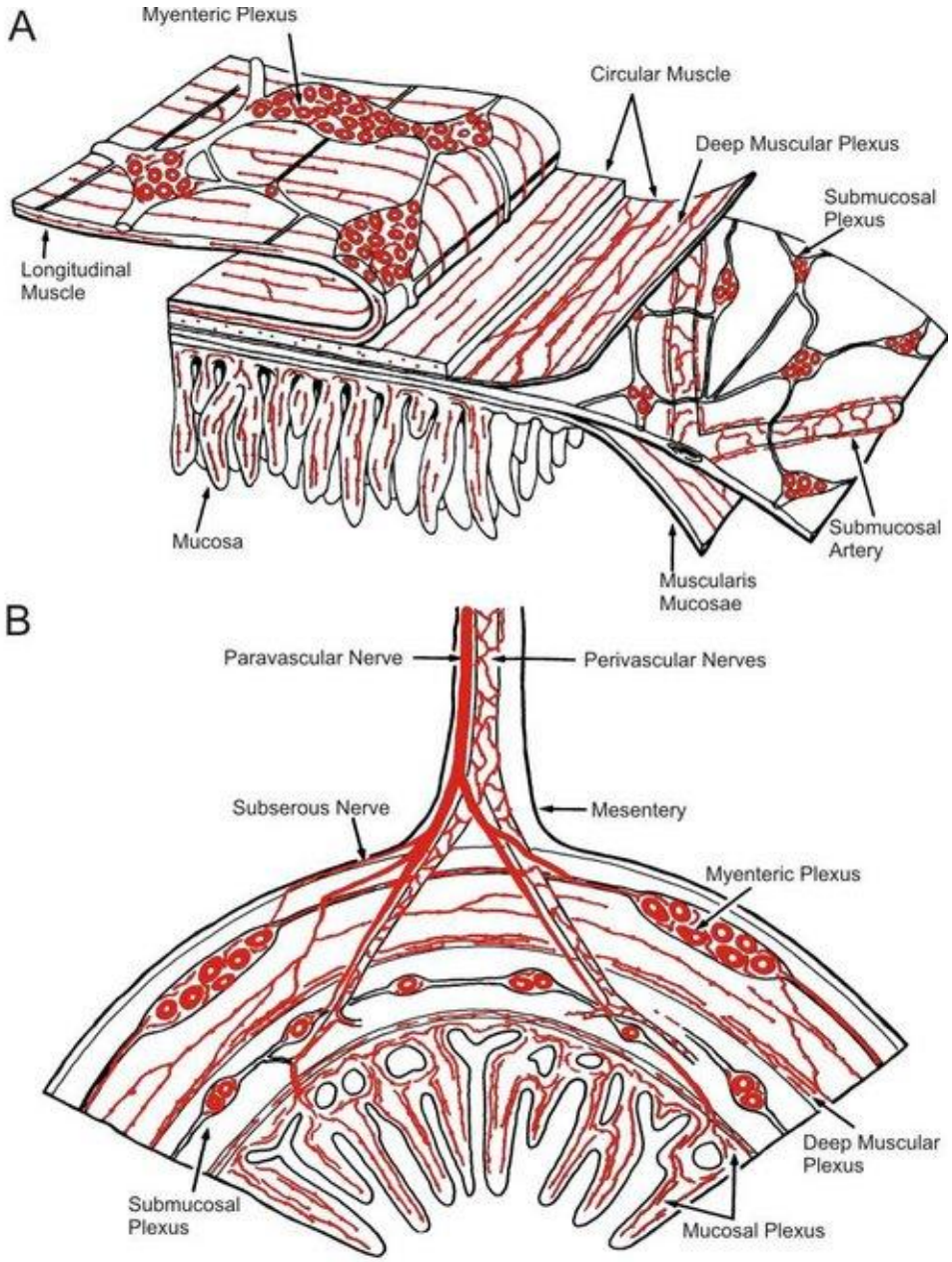
A
Myenteric Plexus
Circular Muscle
Deep Muscular Plexus
Submucosal Plexus
Longitudinal Muscle
Mucosa
Submucosal Artery
Muscularis Mucosae
B
Paravascular Nerve
Perivascular Nerves
Subserous Nerve
Mesentery
Myenteric Plexus
Deep Muscular Plexus
Submucosal Plexus
Mucosal Plexus

Cell Types

Two cell types dominate the population of gut cells – smooth muscle cells and epithelial cells. The smooth muscle cells, located in the circular muscle layer and longitudinal muscle layer, are responsible for motility patterns of the gut, both the propulsive pattern and the non-propulsive segmentation pattern. Smooth muscle cells also are found in the muscularis mucosa layer, aiding in exposure of the epithelial cells with the gut contents[6].

The epithelial cells are critical for the absorption of nutrients for the luminal contents. Epithelial cells also possess enzymes necessary for the final digestion of the same. Beyond these two dominant cell types, there exist several types of enteroendocrine cells that serve sensory/control functions through monitoring of gut contents and relaying of hormonal signals that may affect overall motility, secretory, and absorptive action[4, 13].

The presence of immune cells and tissue within the gut is extensive, a consequence of exposure of the tremendous surface area of gut mucosa to the environment. As such, the entry into the body of most antigens occurs through this epithelial barrier. Defending this barrier from pathogenic invasion, while recognizing critical resident flora, requires an immune system

distinct from the rest of the body[14]. The gut immune system initiates responses that cooperate with the general immune system. The gut is also highly served by lymphatic vessels, which play a role in lipid absorption. Because of the size and importance of the gut as an immune organ, it possesses a population of immune cells greater than the spleen, skin, and lymph nodes combined[2].

Innervation

The enteric nervous system (ENS) is contained within the two anatomical plexuses, the myenteric and submucosal plexuses. These structures provide the motor control for the muscle layers, secretory control of the mucosal layers, and control for the circuitry offered by a variety of sensory mechanisms. The enteric nervous system can stand alone, performing its duties independent of the central nervous system, but is normally modulated by inputs from the autonomic nervous system. Parasympathetic influences upon the ENS originate in the vagal nuclei of the brain stem that synapse upon the ENS plexus of the esophagus, stomach, and upper intestine, and also from sacral parasympathetic nuclei, synapsing upon the plexuses of the colon[15]. Parasympathetic activity promotes overall gut function, exciting extant motor and secretory pathways. Sympathetic activity incident on the gut travels from

prevertebral ganglia onto the ENS plexuses. Such activity reduces the actions of the ENS overall, slowing motility and secretion. Sympathetic activity also excites sphincteric muscle, preventing organized movement of ingesta through the gut[16].

As in the central nervous system, the ENS consists of not only neurons of various types, but also glial cells that protect and maintain the intricate networks of neurons, as well as providing modulatory input to neurons of all types. Complicated interconnections of motor and sensory neurons and interneurons allow for local control of the sophisticated motor behaviors of the gut. As mentioned, circular muscle contraction must occur orad to gut contents (with longitudinal relaxation), and circular muscle relaxation caudad to the contents (with longitudinal contraction). Differences in the innervation and functions of the circular and longitudinal muscle layers allow for this coordination.

ICCs/Fibroblast-like cells

In addition to the connections displayed in the above diagram, other cells participate in the shaping of electrical activity. The interstitial cells of Cajal (ICC) are neuron-like interstitial cells located through the gut. These cells are capable of depolarizing themselves to threshold potential and initiating depolarization in surrounding gut muscular tissue. The mechanism of their self-depolarization, involving intracellular Ca stores and mitochondrial Ca uptake is inherently rhythmic, and this rhythmic depolarization is seen within the gut musculature that the ICCs influence. Beyond the basic rhythms which are specific to specific gut regions, the overall excitability of ICCs can be affected by stretch/distention, furthering their contribution to motility, as increased frequency of firing promotes both segmentation and peristaltic behaviors[17, 18]. Microscopic studies using electrically sensitive dyes show that the ICCs may play a role in the electrical coupling of the longitudinal and circular muscle layer. This connection is specialized to promote coordination without destroying the intrinsic electrical identity of the two layers [19, 20]. Another cell type, the fibroblast-like cell, appears to co-exist with the ICCs in the plexus and muscle layers. They possess great similarity with ICCs, but are reported to be distinguishable via microscopy.

These cells are in close proximity to terminals of enteric neurons, ICCs, and smooth muscle cells. Their high current densities and apparent gap junction formation with SMC loosely suggest that fibroblast-like cells may be involved in a modulation role in transmission to and perhaps between the muscle layers [21-23]. These results, however, remain highly controversial.

Innervation of Circular and Longitudinal Muscle

From the neural plexus, processes travel to the muscle layers. However, the population of nerves that are efferent to the longitudinal muscle layer and the circular muscle layer are different in type and quantity. The motor neurons incident upon longitudinal muscle are overwhelmingly excitatory and the vast majority of these excitatory neurons contain acetylcholine as a neurotransmitter. Approximately half of these neurons can also possess excitatory peptide neurotransmitters, such as the tachykinins substance P and neurokinin A[24].

The lack of a robust population of neurons with inhibitory neurotransmitters suggests that inhibition of longitudinal muscle is mediated through the control of these existing excitatory pathways. The interneurons that modulate the excitatory motor neurons of longitudinal muscle possess receptors for typically inhibitory neurotransmitters, such as

vasoactive intestinal peptide (VIP) and nitric oxide (NO)[25]. However, these interneurons excite upon exposure to these typical inhibitory agents, and stimulate the release of Ach and tachykinins from the downstream motor neurons. Whereas VIP and NO would promote relaxation if directly incident upon muscle cells, when incident upon interneurons, contraction is fostered. It is thought that these interneurons, specific to longitudinal muscle, contribute to the coordinated inverse behaviors of circular and longitudinal muscle at the specific site of gut activity.

In circular muscle, a more direct, and yet more involved, scheme exists. The muscle tissue itself is densely innervated with both excitatory and inhibitory neurons. Inhibition of circular muscle cells can be elicited by direct neuronal release of inhibitory neurotransmitters, whereas a specialized interneuron is necessary for the majority of longitudinal muscle inhibition. The receptor population in circular muscle is richer in variety and number. Circular muscle cells possess receptors that longitudinal muscle does not, including opioid receptors, somatostatin receptors, and neuropeptide Y2 and Y4 receptors [26-28]. No receptors have been identified that exist in longitudinal muscle cells that do not exist in circular muscle cells. Circular muscle can be signaled to contract or

relax by a variety of neurotransmitters and circulating agents, both peptide and non-peptide in nature. The control of contraction of longitudinal muscle is primarily cholinergic, and the control of relaxation in longitudinal muscle is responsible to a unique subset of myenteric interneurons which do not innervate circular muscle.

Muscle Contraction

Muscle activity is driven by the interaction of the proteins actin and myosin. Actin maintains two primary roles in the cell, forming both the microfilaments that are critical to cytoskeletal structure and the thin filaments in muscle cells that provide structure against which the motor protein myosin can exert force. The alpha isoform of actin is the actin associated with muscular contraction, whereas the beta and gamma isoforms of actin play more important roles in the cytoskeletal arrangement[29]. There are several classes of myosin proteins, most playing a role in a form of movement, ranging from muscular contraction to vesicular transport. Myosin class II is the useful form in muscle, interacting with actin to generate force[30].

Myosin itself is composed of several “chains”, domains of this very large protein. The heavy chains are important in muscle contraction, and the light chains important in structure and

regulation of the activity of the heavy chains. The interaction of actin and myosin facilitates the inherent ATPase activity of the heavy chains of myosin. Regulation of myosin activity and muscle contraction is accomplished by either the regulation of the association of actin with myosin or by direct manipulation of the catalytic activity of the myosin protein. The three general types of muscle - skeletal, cardiac, and smooth muscle each possess differing mechanisms to achieve this regulation[31]. However, all mechanisms involve manipulation of intracellular levels of free calcium which precede any actions of actin and myosin, and all mechanisms involve specific proteins that interact directly with either actin or myosin.

Skeletal

In skeletal muscle, a nerve impulse is transmitted to a muscle fiber by means of the neuromuscular junction. The action potential travels down the sarcolemmal membrane and into the T-tubules that penetrate into the body of the muscle fiber. Dihydropyridine receptors (voltage-gated calcium channels) are activated by the depolarization of the action potential upstroke and are electrically coupled to the ryanodine receptors on the sarcoplasmic reticulum. Ryanodine receptor activation leads to release of calcium from the sarcoplasmic reticulum, and intracellular calcium is elevated. This free calcium binds to

the protein troponin, which is in a protein complex with tropomyosin. In low calcium (relaxed) state, the tropomyosin within this complex is positioned in a manner that prevents the binding of actin and myosin, preventing contraction. When calcium is bound to troponin, however, the troponin-tropomyosin complex undergoes a conformational change that removes the steric inhibition of actin by tropomyosin, exposing the active sites on actin, and permitting actin-myosin interactions. The termination of contraction occurs as the intracellular calcium is reduced through the activity of Ca^{2+} ATPases on the sarcoplasmic reticular membrane. Unbound troponin reinstates the inhibition of actin sites by tropomyosin.

Cardiac

Cardiac muscle contraction is similar to skeletal muscle in the manner of troponin-tropomyosin-actin interactions. The mechanism that leads to the increase of intracellular free calcium that enables these reactions is profoundly different. An action potential on the membrane of a cardiomyocyte is not of neural origin, but from specialized muscle cells at an alternate location in the heart. The depolarization that led to calcium channel activation (and ryanodine receptor activation) in skeletal muscle leads to actual calcium entry through similar channels in heart. This calcium entry triggers a large release

of calcium from sarcoplasmic reticular stores (Ca-induced Ca-release), and this sarcoplasmic calcium is responsible for troponin binding and the removal of inhibition from actin. The contraction of cardiac muscle is dependent upon the entry of extracellular calcium, and the strength of contraction is a consequence of the amount of calcium influx and its modulation/activation of the ryanodine receptors[32]. Relaxation is similar, involving the uptake of calcium into and its sequestration in the cardiac sarcoplasmic reticulum.

Smooth

Smooth muscle contraction has few similarities to the excitation-contraction coupling mechanisms in striated muscle. Ultimately, contraction is permitted when the regulatory light chains of myosin are appropriately phosphorylated. There is no steric interference of the actin and myosin filaments as in cardiac and skeletal muscle; troponin is absent in smooth muscle, but the thin filaments protein calponin and caldesmon have been implicated in similar regulatory roles[33].

The phosphorylation of the myosin regulatory light chain at a serine residue at position 19 is sufficient to cause cross-bridge formation and cycling, ATP hydrolysis, and muscle contraction[34]. Phosphorylation of the regulatory light chain in striated muscle does occur, but it is neither sufficient nor

necessary for contraction as in smooth muscle. Such phosphorylation in striated muscle, will, however, increase force production and speed of contractions[35].

Smooth muscle has a more dynamic control mechanism than striated muscle, as the phosphorylation level of myosin is affected by the action of scores of kinases and phosphatases. Furthermore, other protein targets exist within smooth muscle that can shape the forces developed by the actin-myosin interaction dynamics, independent of the myosin phosphorylation level. Investigation of those other mechanisms in general smooth muscle and the differences among smooth muscle types are the ultimate goal and drive of this study.

Regulation of smooth muscle contraction

As stated, the contraction of smooth muscle is driven by the control of the phosphorylation level of the 20 kDa regulatory light chain of myosin II (MLC_{20}). Membrane receptor activation leads to the initiation of second messenger signaling cascades, and, ultimately, an increase in intracellular calcium. The calcium binding protein calmodulin complexes with the sudden increase in intracellular calcium, and a host of Ca^{2+}/calmodulin dependent processes are launched. Of primary interest is the Ca^{2+}/calmodulin-dependent enzyme myosin light chain kinase (MLCK), a dedicated protein kinase of which MLC_{20} is its only

substrate[35]. Phosphorylation levels of MLC_{20} rise and the uninhibited actin/myosin interactions initiate contraction. Phosphorylation levels of MLC_{20} can remain high even as the initial Ca2+ transient diminishes, as MLC_{20} is targeted by kinase other than MLCK. In addition, maintained phosphorylation levels and contractile force can be achieved through inhibition of myosin light chain phosphatase (MLCP), an enzyme dedicated to the dephosphorylation of MLC_{20}. Ultimately, relaxation occurs as the phosphatase activity predominates and phosphorylation levels of MLC_{20} fall, reducing the interaction and enzymatic activities of actin/myosin[36].

Receptors/Membrane-Mediated Processes

A large variety of receptor types enable a wider variety of chemical agents to initiate or modulate smooth muscle contraction. These agents via membrane receptor-mediated processes will affect muscle tone through either the manipulation of calcium levels (and the Ca^{2+}-dependent processes MLCK and MLCP), the activation of enzymes outside of the standard Ca^{2+}-dependent pathways that affect MLC_{20} phosphorylation levels (critical for sustained contraction and relaxation), or through the manipulation of the motor proteins themselves (altering their affinities for each other or for their assigned enzyme effectors)[37]. The enteric nervous system is capable of

generating numerous excitatory agents, specific to location, motility patterns, and in response to perceived stimuli[38]. The smooth muscle cells themselves may release agents that can elicit local responses, and endocrine agents may bring modulation through the general circulation[39].

Ligands for membrane receptors in gut can be classic non-peptide neurotransmitters (acetylcholine, dopamine), peptide transmitters (somatostatin, vasoactive intestinal peptide), peptide hormones (cholecystokinin), or atypical ligands with plant-based origins that arrive by ingestion and diffusion to the muscle layers[3, 13, 27, 40-43]. Receptor profiles for smooth muscle vary among types and even vary within the same type at different locations. Also, identical ligand-receptor pairs can elicit differing effects in alternative locations of smooth muscle [40, 44, 45]. Most receptors responsible for contraction in smooth muscle are coupled to transmembrane G-proteins, although receptor tyrosine kinase pathways are important to growth factor-induced contraction [46, 47]. These G-proteins then activate second messengers or directly activate specific kinase cascades in the cytosol. The G-proteins, associated second messengers, and kinase cascades are often specific to smooth muscle type and function, and may differ within the same organ system[45].

Calcium

The elevation of intracellular calcium is physiologically necessary for the initiation of contraction in smooth muscle. The primary source for this calcium is the sarcoplasmic reticulum of the smooth muscle cell. Within the SR of smooth muscle cells, calcium is primarily bound to the sequestering protein calreticulin, and not calsequestrin as in striated muscle [48, 49]. Preceding smooth muscle contraction, receptors on the SR membrane must be activated so that stored calcium may be released into the cytosol. Here, differences exist between smooth muscle types. In circular smooth muscle of the gut, IP_3 receptors exist on the SR membrane and as levels of the second messenger rise, these receptors are activated, and calcium release channels open. In longitudinal muscle of the gut, IP_3 receptors are absent from the SR – external calcium entry is the signal to ryanodine receptors for SR calcium release[50]. This mechanism of Ca^{2+}-induced Ca^{2+} release bears strong resemblance to cardiac muscle excitation-contraction coupling, and is specific to longitudinal gut smooth muscle.

The entry of calcium from the extracellular space is another mechanism of control. In longitudinal muscle, this entry is coupled to the calcium release from the SR that permits contraction. In both circular and longitudinal muscle, the entry of calcium is an important component of the electrical

excitability of the muscle. In both gut muscle types, the voltage-dependent calcium channel (VDCC) $Ca_V1.2$ is expressed[51]. Upon depolarization of the sarcolemmal membrane by agonist-induced inward currents (or local electrotonic depolarization), these channels carry the inward calcium current responsible for the action potential upstroke[52]. The gating behavior and sensitivities of these channels are regulated by various kinases upon receptor activation, inflammation, and a host of cellular metabolic events [53-55]. The calcium that enters via these channels is coupled to SR calcium release in longitudinal muscle, as well as the enhancement of kinase pathway activation, gene expression, and energy metabolism in both muscle types [56, 57]. There is also significant interplay between calcium entry through these VDCCs and the membrane ion channels (K_{Ca} and Cl_{Ca}) responsible for cellular repolarization [58, 59].

MLCK

Myosin light chain kinase (MLCK) is a dedicated serine-threonine kinase that has the 20 kDa regulatory light chain of myosin II (MLC_{20}) as its sole substrate. Upon binding with the calcium-calmodulin complex, MLCK phosphorylates MLC_{20} at serine 19, permitting the actin-myosin interaction that allow for smooth muscle contraction. Also, phosphorylated MLC_{20} (MLC_{20}-p) is involved in other processes related to cytoskeletal

manipulation such as motility, apoptosis, and secretion[35]. Many studies have shown that MLC_{20} can be phosphorylated by other kinases, and this phosphorylation is important during the sustained contraction of tonic smooth muscle, but it is the phosphorylation of MLC_{20} by MLCK that is the predominant effector of initial contraction[34, 60, 61]. The activity of MLCK itself can be affected by its phosphorylation at several site; kinases that phosphorylate can increase or decrease MLCK activity, and may do so by either altering the rate of enzyme activity or the affinity of MLCK for Ca^{2+}-calmodulin [62-66].

MLCP

Myosin light chain phosphatase (MLCP) is the opposing enzyme to MLCK, removing the phosphate from Serine 19 on MLC_{20}. It is a trimer composed of protein phosphatase 1c-δ, the myosin phosphatase target subunit 1 (MYPT1), and a small 20kDa unit M20[67]. The PP1 family of enzymes is expressed widely in tissues and is a non-specific serine/threonine phosphatase. PP1 enzymes are typically bound to a targeting subunit to direct this non-specific enzymatic action here by MYPT1. MYPT1 targets the phosphatase subunit to MLC_{20}, while increasing the specificity of PP1c-δ through a conformational change that occurs when bound to MYPT1[68]. The M20 subunit is of unknown function.

The overall level of MLC_{20} phosphorylation is closely tied to the activity level of these two opposing enzymes, notwithstanding the MLCK-independent phosphorylation of MLC_{20}. As MLCK activity can be modified by select kinases, MLCP can also be reduced in its activity by interaction with two of its subunits. When the subunit MYPT1 is phosphorylated at threonine 696 (human), the phosphatase subunit can no longer be directed properly to its myosin target [69]. Rho kinase was the first studied kinase to phosphorylate MYPT1 in this manner, but several kinases have been identified as effectors of MYPT1. Some phosphorylate in a manner similar to Rho kinase, and others target residues that prevent the Rho Kinase-like inhibition[70]. The wide range of kinases that target MYPT1 invites discussion of perhaps a greater role in cellular functions for MLCP[30]. The phosphatase subunit PP1c-δ has an endogenous inhibitor, C-kinase potentiated protein phosphatase-1 inhibitor (CPI-17). The phosphorylation of CPI-17 at serine 12 and threonine 38 enabled its blocking of PP1c-δ activity and this phosphorylation is performed by many of same kinases that phosphorylate MYPT1 [71-75].

Initial/Sustained

Contraction in some smooth muscles type is biphasic – an initial transient contraction of relatively high amplitude,

followed by a lowering of tone to a reduced but sustained contraction. Other muscle types maintain moderate levels of tone for extended periods of time. An initial contraction and the initial partial decline agree with the transient change in intracellular calcium. Following the release of calcium by any specific mechanism, MLCK activity will increase as it binds to calcium-calmodulin complexes. Following the transient increase, calcium uptake by the SR reduces intracellular calcium levels to pre-contraction values. Tone in the muscle can still be maintained at a lower degree despite a calcium level that would not alone develop such tone. This phenomenon of elevated tone with low calcium is termed calcium sensitization [36, 76].

Two general mechanisms are responsible for sustained tone. Calcium sensitization has been studied extensively in preparations where calcium levels are held constant. Studies have shown that both MLCK activity may be altered at constant calcium and that MLC_{20} can be phosphorylated by kinases other than MLCK at all levels of calcium[44, 61, 77-79]. These Ca^{2+}-independent processes are partially responsible for the enhanced tone of the sustained phase of contraction. MLC_{20} phosphorylation levels are also affected by activity of MLCP, and inhibition of this phosphatase activity contributes to maintained tone. Both inhibitors of MLCP activity,

phosphorylated CPI-17 and MYPT1, have been implicated in the sustained phase, either individually or in concert [80-82]. CPI-17 and MYPT1 are expressed to different degrees across smooth muscle types, and this ratio of expression can be connected to general phasic (initial and sustained contractile behavior) or tonic (extended sustained contractile with no initial peak) motility patterns[83]. Many kinases that offer Ca-independent phosphorylation of MLC_{20} (through either enhanced MLCK activity or direct phosphorylation) also phosphorylate the inhibitors of MLCP[39, 81]. Agonists that cause standard Ca-dependent increases in MLCK activity may also promote phosphatase inhibition through the same or alternate subtypes of their receptors [84, 85].

Circular Muscle

Receptors/G-Proteins/Second Messengers

Circular muscle in gut expresses an extensive array of receptors for both neurotransmitters released by the enteric nervous system, agents from gut tissue, and agents in the circulation. Muscarinic receptors are in the greatest number, with muscarinic type 2 (M_2) outnumbering muscarinic type 3 (M_3), but only M_3 is thought to participate directly in contraction[86]. A majority of identified receptors operate through G-proteins, but receptor tyrosine kinase activity has been seen in intestinal muscle with exposure to members of the growth factor family[87]. Though these effects can couple downstream with cascades that start at G-proteins, they are mainly seen during proliferation and may be primarily pathophysiological in presence[88].

G-protein activation in circular muscle stimulates phosphoinositide (PI) hydrolysis by members of the phospholipase C (PLC) family. The beta isoforms predominate in activity with PLC-beta1 downstream of M_3 activation (via $G\alpha_q$) and PLC-β3 downstream of M_2 activation (via $G\beta\gamma_i$)[89]. Activation of M_3 is critical for contraction, and leads to hydrolysis of phosphatidylinositol 4,5-bisphosphate (PIP_2) into inositol 1,4,5-trisphosphate (IP_3) and diacylglycerol (DAG)[90, 91]. Both IP_3

and DAG have downstream effects that shape contraction. G-proteins activated in circular muscle may also have downstream effects of adenylate cyclase, Rho kinase, PI-3 kinase, and other members of the phospholipase family[39]. It is, however, M_3 activation leading to IP_3 formation that is essential in the initial contraction. Activation of M_2 has downstream effects on contraction (primarily inhibitory), but mostly operate on a time scale beyond the M_3/IP_3 consequences[84].

IP3/SR Ca release

With agonist-induced IP_3 formation via PLCβ, IP_3 receptors (IP_3R) are activated on the SR of circular muscle. These receptors are SR membrane calcium channels, have high affinity for IP_3, and are inhibited by heparin[92]. When IP_3 binds to these receptors, calcium stored in the SR is released into the cytosol[93]. This transient increase in intracellular calcium causes binding sites on calmodulin to be occupied, and the calcium-calmodulin complexes then activate MLCK, initiating contraction. Other calcium dependent enzymes are also activated which may modulate the activities of MLCK and MLCP. The rise in intracellular calcium is short-lived, as pumps on the SR membrane re-accumulate the released calcium, and with the actions of the cell membrane Ca^{2+}-ATPases, restore the levels of calcium to previous values. These IP_3 receptors/Ca channels are

modulated by association with other receptors on the SR membrane, protein kinases, and the level of intracellular calcium that these channels manipulate. All these effects can shape the kinetics of release, and consequently the effects of the calcium transient [58, 94-97].

Ca-Independence

Following the decline of the calcium transient, Ca-independent processes allow for a degree of sustained tone to be maintained. Ca-independent kinases such as Integrin-Linked Kinase (ILK) and Zipper-interacting protein kinase (ZIPK) phosphorylate MLC_{20} in manner similar to the Ca-dependent MLCK [98-100]. MLC_{20} phosphorylation levels are also kept at an elevated level by inhibition of the myosin phosphatase, either through phosphorylation of MYPT1 or CPI-17. It is not uncommon for agents to initiate the Ca^{2+}-independent phosphorylation of myosin while simultaneously inhibiting the phosphatase, nor it is uncommon for pathways to activate both known mediators of phosphatase inhibition [74, 75, 81, 82].

Relaxation

Relaxation is fostered when phosphatase activity exceeds active MLC_{20} phosphorylation. Both protein kinase A (PKA) and protein kinase G (PKG) are implicated in the relaxation of smooth muscle. Inhibitory neurotransmitters such as VIP

activate Gs proteins, increasing cAMP levels through adenylate cyclase stimulation, and leading to increased PKA activity. PKA can target membrane ion channels leading to hyperpolarization, phosphorylate upstream molecules to inhibit contractile pathways, and directly phosphorylate MYPT1 in a fashion that precludes its role as an inhibitor of MLCP [101-103]. Nitric oxide (NO), another inhibitory transmitter, can elevate PKG activity through stimulation of soluble guanylate cyclase. Protein Kinase G has similar targeting as PKA to inhibit contraction/promote relaxation, and has been shown definitively also to phosphorylate CPI-17 at a site that precludes its involvement in MLCP inhibition [72, 104, 105]. Whether PKA targets CPI-17 directly to promote relaxation finds conflict in the literature [101, 105].

Rho Kinase

Rho-associated kinase (Rho Kinase) is a serine-threonine kinase widely expressed in tissues and implicated in a wide array of cytoskeletal processes, including cell motility, cell proliferation, neurite growth, and apoptosis[106]. Rho Kinase is speculated to be a promising target in treatments of Alzheimer's disease, stroke, multiple sclerosis, and pain [107]. Its physiological interaction with cytoskeletal structures also leads to a role in muscle contraction, and the inhibition of Rho

kinase finds clinical uses in treatment of asthma and hypertension [108-110].

Effects on contraction by Rho kinase mainly involve its phosphorylation of the targeting subunit MYPT1, preventing MLCP from removing activating phosphates on MLC_{20} [111]. This role is considered critical in the sustained contraction seen in many tissue types, and Rho kinase is seen to be expressed to a higher level in those tissues that exhibit more tonic contractile behavior [112]. However, studies also demonstrate that the pro-contractile effects of Rho Kinase may be mediated through inhibition of NO synthesis, indirect phosphorylation of MLC_{20} through activation of Ca^{2+}-independent ZIP kinase, and perhaps direct phosphorylation of myosin [113-115].

ERK1/2

Extracellular signal-kinase types 1 and 2 (ERK1/2) are common and prevalent participants in signaling cascades connected to cellular activities of growth, differentiation, survival, and metabolism. A large portion of the downstream effects of ERK1/2 effect changes in gene expression in response to extracellular signals or events [116]. ERK1/2 is also often involved in acute effects or responses and its parent pathways are numerous and well-described, and its targets of phosphorylation as varied.

Effects on smooth muscle activity are easily connected to the role of ERK1/2 in cell proliferation, as cytoskeletal rearrangement is crucial to mitotic, differentiation, and motile behaviors. Phosphorylation of the putative contractile regulators caldesmon and calponin by ERK1/2 enhance contraction [54, 117]. ERK1/2 expression is heightened in models of inflammatory disease of the gut, which often present with hypercontractility [87, 118]. ERK activity is implicated in the physiological contraction of gut and vascular smooth muscle [78, 119]. These effects of ERK1/2 can be mediated by phosphorylation of participants in existing contractile pathways incident upon MLCK or by direct phosphorylation of MLCK, enhancing MLC_{20} phosphorylation [65, 66, 120].

CaMKII

Calcium-Calmodulin dependent kinase II (CaMKII) is a serine/threonine kinase that is expressed widely in excitable tissue. Upon binding with calcium-calmodulin (following a transient increase in intracellular calcium), CaMKII autophosphorylates at threonine 286 and can maintain its activity after dissociating from calcium-calmodulin complexes [37]. The kinase can modulate membrane channels and engage with downstream kinases such as ERK1/2 [121-124]. CaMKII associates with motor proteins in cell migration and hypertrophy, and has

receptors and transport proteins of the sarcoplasmic reticulum as targets [125-128].

In smooth muscle cells, inhibition of CaMKII can enhance contraction, and this effect has been attributed to the effect of CaMKII on MLCK [129] Phosphorylation of MLCK by CaMKII reduces the affinity of MLCK for calcium-calmodulin, decreasing its phosphorylation of MLC_{20}, and this phosphorylation has been specifically blocked by inhibitors of CaMKII [130, 131]. However, other studies have indicated a possible link to CaMKII activity and tone maintenance in vascular smooth muscle [132, 133]. These conflicting findings, along with the involvement of CaMKII with proteins important in calcium handling (ryanodine receptors, phospholamban) indicate the role of this enzyme in calcium handling could be complex and not constant across tissues with different calcium handling characteristics.

CaMKK/AMPK

Adenosine Monophosphate Activated Kinase (AMPK) is an important regulator of cellular metabolism, involved in adaptation of cellular processes to changes in metabolic level (AMP:ATP ratio). As AMP levels rise, enhanced AMPK activity causes changes in glucose transport, lipid metabolism, and mitochondrial activity [134-136]. Under normal conditions, AMPK can be activated through receptor activation via calcium-

calmodulin kinase kinase (CaMKK), with the beta isoform of CaMKK being the most prevalent upstream mediator [137-139]. Inhibition of CaMKK is closely correlated with AMPK inhibition and is the typical path of pharmacological manipulation [139-141].

AMPK also associated with motor proteins. AMPK interacts with actin filaments of the cytoskeleton in osmotic stress models, changing their affinity for other cytoskeletal proteins [142]. And studies have shown that MLCK is a substrate of AMPK, with the phosphorylation of MLCK at a site close to the CaMKII phosphorylation site, and resulting in a similar reduction in affinity for calcium-calmodulin [143]. AMPK can phosphorylate fragments of MLC_{20}, but this is not thought to be part of the normal activity of AMPK [144].

Putative Circular Muscle Model

Most gut smooth muscle studies are performed upon smooth muscle cells or tissue from the circular muscle layer, presumably because of its thickness and perceived dominant role in gut motility. Considering the literature regarding kinase manipulations of MLCK/MLCP/MLC_{20}, the following model is offered (Figure 2). Not all possible kinases or kinase targets were mentioned and are beyond the scope of this study. This model is similar to many found in reviews and texts [39, 145-147].

Figure 2. Putative Model for Circular Muscle Regulation

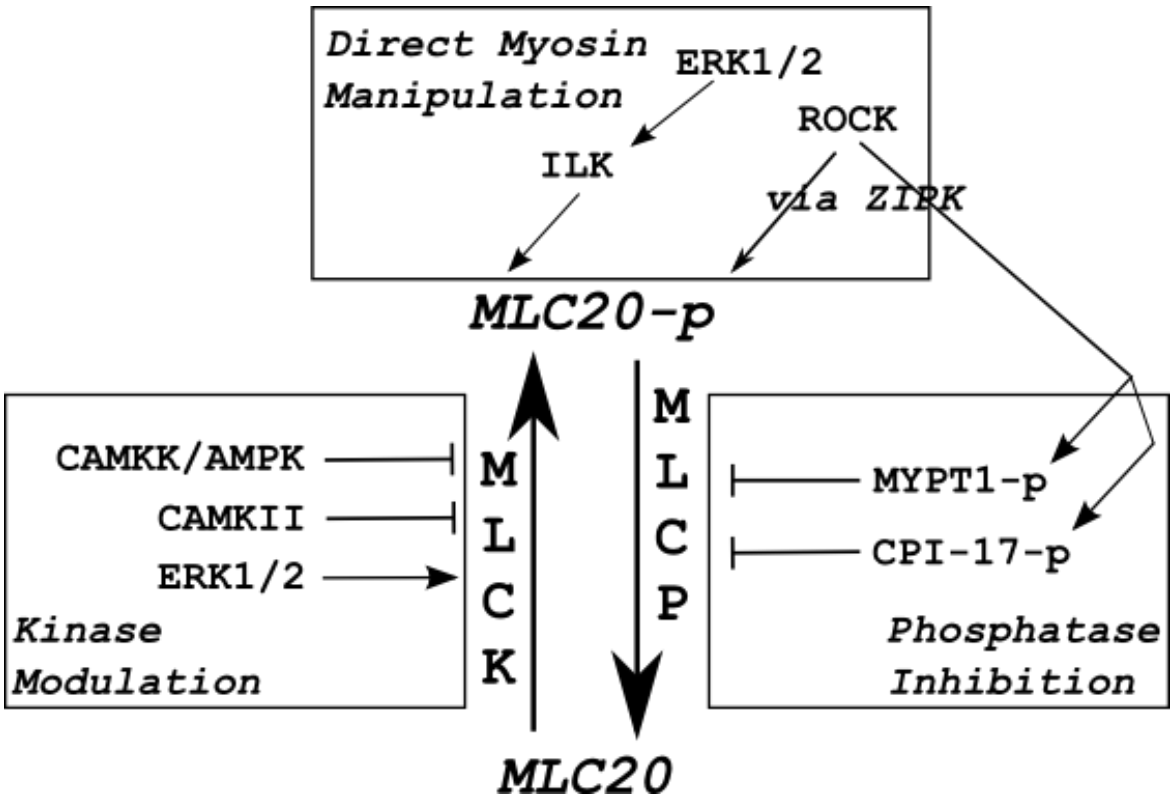
Direct Myosin Manipulation
ERK1/2
ROCK
ILK
via ZIPK
MLC20-p
CAMKK/AMPK
CAMKII
ERK1/2
Kinase Modulation
MLCK
MLCP
MYPT1-p
CPI-17-p
Phosphatase Inhibition
MLC20

Longitudinal Muscle

Longitudinal muscle in gut possesses many differences from the circular muscle with which it works in opposition. These differences begin during development and lead to a muscle phenotype that possesses a different receptor profile, membrane lipid handling, and a mechanism of cytoplasmic calcium handling more similar to striated cardiac muscle than any other form of muscle, smooth or striated.

Development

The epithelium of the gut is derived from embryonic endoderm, and the muscle from splanchnic mesoderm. Neural precursor cells of ectodermal origin begin to populate the gut almost immediately, and their presence enables the mesenchyme to begin to differentiate into what would become the circular muscle layer [148]. There is debate on the origin of what will become the longitudinal layer. Some believe that longitudinal muscle develop from circular muscle cells, others from a common precursor that gives rise to both the ICCs and the longitudinal muscle layer [149, 150]. Regardless, the development of the longitudinal muscle is delayed relative to the circular, as this is seen in both mouse model and human embryo [151]. ICCs are often characterized by their expression of c-kit, a receptor tyrosine kinase, as ICCs and mast cells are the only cells in the gut that express c-kit. Blockade of c-kit signaling in the

gut abolishes the development of both the ICCs and the longitudinal muscle, intimating that at the very least, ICC signaling is necessary for longitudinal muscle development. The possibility the ICCs and longitudinal muscle cells come from the same progenitor agrees with this finding [152]. Known organogenetic proteins such as *Shh*, *BMP*, *forkhead*, and *Wnt* are suspected to play roles in the radial patterning of the gut, it seems that platelet derived growth factor (PDGF) may be the most important [153]. Studies report that the cells destined to be the longitudinal muscle layer express receptors for PDGF, which is released by more internal parts of the gut. This receptor development could be caused by a gradient of these other signaling proteins, but the combination of a substantive PDGF receptor and appropriate ligand allows for longitudinal muscle to differentiate from the c-kit expressing layer [154].

Receptors/Phosphoinositides

As stated earlier, the receptor population of circular muscle cells and longitudinal muscle cells are different. Longitudinal muscle lacks receptors for opioids, somatostatin, and neuropeptides Y_2 and Y_4 [27, 28, 42]. This variance in receptor population coincides with a lesser degree of innervation that longitudinal muscle possesses – the innervating neurons are fewer in number, almost completely excitatory, and primarily

cholinergic (secondary are the tachykinins). Circular muscle is innervated by excitatory and inhibitory neurons that offer a greater variety of ligands to match the receptor variety.

Muscarinic receptors are common between the two muscle types, and M_3 activation in both muscle layers leads to activation of PLC-β1. Other agonists and the M_2 receptors can operate to increase PLC-β3 via $G\beta\gamma_i$ mechanism in both muscle types. PLC then turns upon membrane lipids as substrate for the generation of second messengers. Here, another variation is seen; in circular muscle, the primary target of PLC is PIP_2, and the generated second messenger is IP_3. In longitudinal muscle, the primary substrate is PIP and the generated second messenger IP_2 [90, 93].

In circular muscle, the IP_3 generated from PLCβ activity is the ligand responsible for calcium liberation into the cytosol. IP_3 receptors on the sarcoplasmic reticulum bind to cytoplasmic IP_3, opening channels and increasing intracellular calcium, enabling the contractile mechanism. Longitudinal muscle generates little IP_3, and the sarcoplasmic reticula of longitudinal muscle have very few IP_3 receptors [50]. Yet, contraction occurs in longitudinal muscle despite the signaling differences.

Calcium Handling

Longitudinal muscle does not generate IP_3 nor does it have IP_3 receptors on its sarcoplasmic reticular membrane. A fundamentally different mechanism is utilized to usher calcium release into the cytosol. The sarcoplasmic reticula of longitudinal muscle possess ryanodine receptors, which are insensitive to IP_3. These ryanodine receptors exist elsewhere in the gut, even in circular muscle, but only in longitudinal muscle is their contribution physiologically relevant and necessary for contraction [155-157]. Sarcoplasmic reticula with high populations of ryanodine receptors resemble a cardiac muscle paradigm, and longitudinal muscle also shares with cardiac muscle the mechanism by which the release of calcium from the SR is regulated.

Studies with calcium channel blockers have shown that contraction in circular muscle is not hindered by removal of extracellular calcium or the block of sarcolemmal calcium channels. Eventually, contractions do decline in amplitude, but this is a consequence of normal cellular extrusion of calcium. Without entry of extracellular calcium, such stores will eventually exhaust. In longitudinal muscle, however, removal of extracellular calcium or blockade of calcium entry diminishes contractions immediately. Just as in heart, the entry of calcium into the cell is obligatory for the release of calcium

from the sarcoplasmic reticulum in longitudinal muscle [158] Such release is possible in circular muscle, but the necessary concentration to trigger release is very high, and is primarily seen in permeabilized cell preparations where such concentrations can be realized [50]. Under physiological conditions, calcium-induced calcium release is not seen in circular muscle.

The mechanism that modulates calcium entry in longitudinal muscle differs from its cardiac counterpart. In heart, the depolarization of the action potential is sufficient to gate surface membrane calcium channels, allowing for the calcium entry that triggers SR calcium release. This is not necessary for contraction in longitudinal smooth muscle, yet the membrane must depolarize before the VDCCs can open. As an excitable tissue, it is reasonable that depolarization could spread electrotonically from a distant locale, bringing the membrane to threshold for the calcium channels, allowing calcium entry. But agonists can initiate contraction in isolated conditions with no external depolarizing effort. A second messenger must be responsible. The agent was discovered to be arachidonic acid (AA), a polyunsaturated fatty acid that can be liberated from membrane lipids by phospholipase A2 (PLA2) in the cytosol (cytoplasmic PLA2, cPLA2) [159]. AA activates chloride

channels, causing the inward current that depolarizes the membrane and gates the calcium channels. Similar experiments in circular muscle showed no connection between chloride channels, AA, and calcium entry [160]. Further regulation is conveyed by cyclic ADP-ribose (cADPR), an endogenous nucleotide known to modulate calcium release from ryanodine-sensitive calcium stores. Circulating levels of cADPR can be increased through receptor activation and stimulation of ADP-ribosyl cyclase, enhancing SR ca efflux. Circular muscle demonstrated no such similar mechanism.

Rationale

Given the differences in development, receptor population, lipid chemistry, and in particular, calcium handling, it is hypothesized that the actions of the kinases known to modulate MLC_{20} phosphorylation in circular muscle may have different actions in longitudinal muscle. Following the model in Figure 2, and using longitudinal muscle strips from rat colon, changes in contractile behavior was measured in the presence and absence of inhibitors for Rho Kinase (Y27632), ERK1/2 (PD98059), CaMKII (KN-62), and CaMKK/AMPK (STO-609). Contraction was be elicited by carbachol (m2 and m3 activation). Molecular techniques illustrated direct effects of the kinases on MLCK.

MATERIALS AND METHODS

Materials

Unless otherwise noted, all chemicals were obtained from Sigma-Aldrich (St. Louis, MO). Kinase Inhibitors Y27632 (Rho kinase), PD98059 (ERK1/2), STO-609 (CaMKK/AMPK), and KN62 (CaMKII) were purchased from Calbiochem (La Jolla, CA). 15% Tris-HCl Ready Gels and DC Protein Assay Kit were products of Bio-Rad (Hercules, CA), Myelin Basic Protein was purchased from Upstate Biotechnology (now Millipore, Billerica, MA) and [γ-^{32}P]ATP from Perkin Elmer Life Sciences (Boston, MA). Antibody for MLCK and protein A/G agarose beads are products of Santa Cruz Biotechnology (Santa Cruz, CA).

Sprague-Dawley Rats were purchased from Charles River Laboratories (Wilmington, MA) and housed in the animal facility of the Division of Animal Resources, Virginia Commonwealth University. All procedures followed guidelines of and were in accordance with the Institutional Animal Care and Use Committee of Virginia Commonwealth University.

Animal Preparation

Rats were euthanized by CO_2 asphyxiation under approved protocols. The colon was dissected out, emptied of contents and placed in a warmed (37°C) oxygenated Krebs solution of the following composition (in mM): 118 NaCl, 4.75 KCl, 1.19 KH_2PO_4, 1.2 $MgSO_4$, 2.54 $CaCl_2$, 25 $NaHCO_3$, 11 mM glucose (pH 7.4). 2-3 cm sections of colon were removed and threaded onto a glass rod, where the longitudinal muscle/myenteric plexus (LM-MP) was removed by radial abrasion with a lab wipe. The resultant strip of muscle was freed of excess fat and mesenteric attachments and held in oxygenated Krebs buffer until use for tension recording or molecular assay.

Strip Preparation

Strips destined for recordings of contractile behavior were tied at both ends with surgical silk – on one end a simple loop for attachment to a glass hook, the other end to a length of silk tied to a brass ring. The strip was then placed in a vertical orientation with the loop secured to a glass hook and the brass ring to a Model FT03C Force Transducer (Grass Technologies, Quincy, MA). An organ bath (Radnoti, Monrovia, CA) was raised to submerge the strip in 5 mL of continuously oxygenated and warmed Krebs solution. Force recordings were amplified by a 15A12 model amplifier (contained within a Model 15LT Amplifier System), relayed to a PVA-16 Polyview Adaptor

Unit (A/D-D/A converter), and displayed/stored by a PC running Polyview Version 1.3 (Grass Technologies, Quincy, MA). Force was recorded in grams per the software specifications. All analysis of data traces was performed within the Polyview software itself, as exportation of usable raw data was limited by software design.

Strips destined for molecular assay were treated as those intended for recordings – time scales for inhibitor incubation and agonist exposure were identical. Following prescribed incubation times, tissue strips were submerged in a bath of Krebs with 1 μM carbachol. After 60 seconds of immersion in carbachol/Krebs (corresponding to a normal vigorous response seen in strips), strips were flash frozen in liquid nitrogen and placed into TPER (Tissue Protein Extraction Reagent, Pierce, Rockford, IL) or lysis buffer with composition 50 mM Tris-HCl (pH 7.5), 150 mM NaCl. 0.1% SDS, 0.5% sodium deoxycholate, 1% NP-40, 10 mM sodium pyrophosphate. Into either vehicle, a protease/phosphatase cocktail (100 μg/mL PMSF, 10 μg/mL leupeptin, 30 mM sodium fluoride and 3 mM sodium vanadate) was added at a concentration of 2 μL/mL. Tissue was homogenized and solubilized in the above solutions. Following centrifugation at 20000 *g* for 15 min at 4°C, the protein concentration of the supernatant was assessed with a DC protein assay kit. These

supernatant lysates were stored at -80°C until needed for immunokinase assay.

Isometric Force Measurement

Force experiments were conducted in the following manner. Following hanging of the strip and submersion in the organ bath, strips were subjected to approximately 1 gram of pre-tension via the mounting rack-and-pinion. Strips were allowed to equilibrate for no less than 30 minutes before experiments were conducted and data collected. Exposure to inhibitors, blockers, and carbachol (sole agonist) occurred within the organ bath. Concentrations were appropriate and in agreement with current literature and are noted in the results.

Following an experiment, strip data were reviewed and analyzed from within the Polyview software suite. All experiments were designed to compare treatment to control conditions. Paired t-tests were conducted in GraphPad (GraphPad Software, La Jolla, CA), and significance assumed at $P < 0.05$. Often in summary, treatment conditions were displayed as compared to control, but significance relays to the raw data paired t-test.

Data Analysis

Contractile data was viewed from several perspectives as to the effects of kinase inhibition: changes to basal tone upon kinase inhibitor administration, peak contractile amplitude

following agonist exposure, and an area under the curve measurement to quantify the contraction as viewed during the first two minutes of the contraction in an effort to determine differences in force development/decay. All numerical values are offered as mean ± SEM.

Basal Tension

Basal tension was measured as the mean tension during a 3 minute period following at least 30 min of equilibration (control conditions) or 10 min of inhibitor incubation (basal recording obtained in interval proceeding carbachol administration). Such measurements were made in multiple strips from multiple animals, and paired t-tests conducted to demonstrate a significantly appreciable effect.

Peak Contraction

Peak contraction (amplitude) was defined to be the greatest amplitude of tone above basal during the two minute period following agonist administration. This two minute period is taken to begin when tone appreciably elevates from basal value. Differing geometries of the shape of the contraction waveform allows for this peak measurement to occur at varying time indices following carbachol administration. An example of such a measurement (utilizing a constructed model curve) is displayed in Figure 3.

Figure 3. Peak Amplitude Measurement.

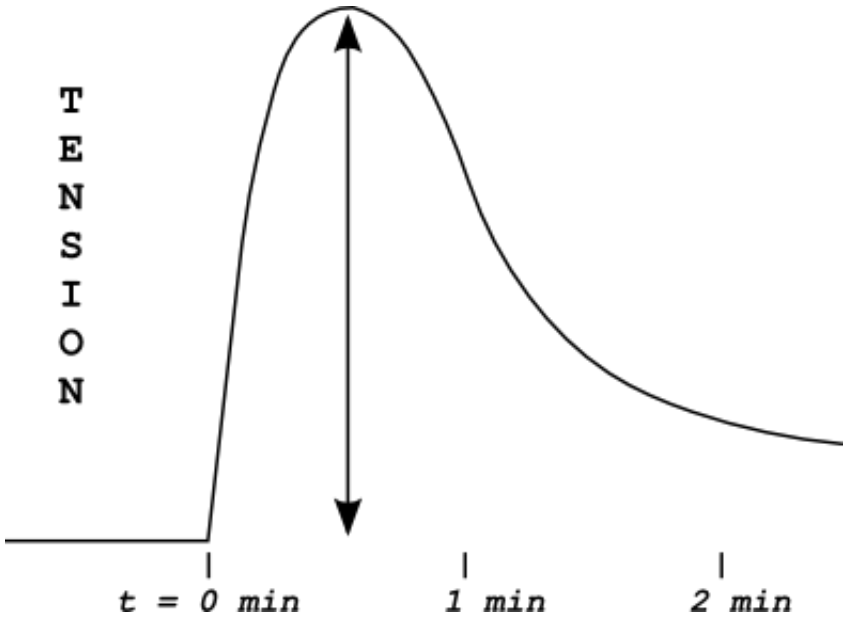
TENSION
t = 0 min
1 min
2 min

Contraction at 1 min and 2 min post exposure

In strips that developed an early peak that subsided quickly, the amplitude of the contraction above basal was also recorded at 1 minute and 2 minutes following the initial increase in tone due to agonist administration (the beginning of the studied interval). An example of such measurements (utilizing constructed model curves) is displayed in Figures 4 and 5.

AUC for first minute and first two minutes of exposure

The area underneath a curve representing force versus time has no physical definition in an isometric contraction. Energy expenditure cannot be quantified without a displacement. But along with the values of the contraction at 1 min and 2 min as percentage of peak, these quantities do speak to the development and maintenance of the tension, and do help describe the decay of the same. This is a typical method used to describe contraction curves in muscle strips. Examples of these measurements: AUC 0-1 min, AUC 1-2 min, and AUC 0-2 min (utilizing constructed model curves) are offered in Figures 6-8.

Figure 4. Contraction at t = 1 minute.

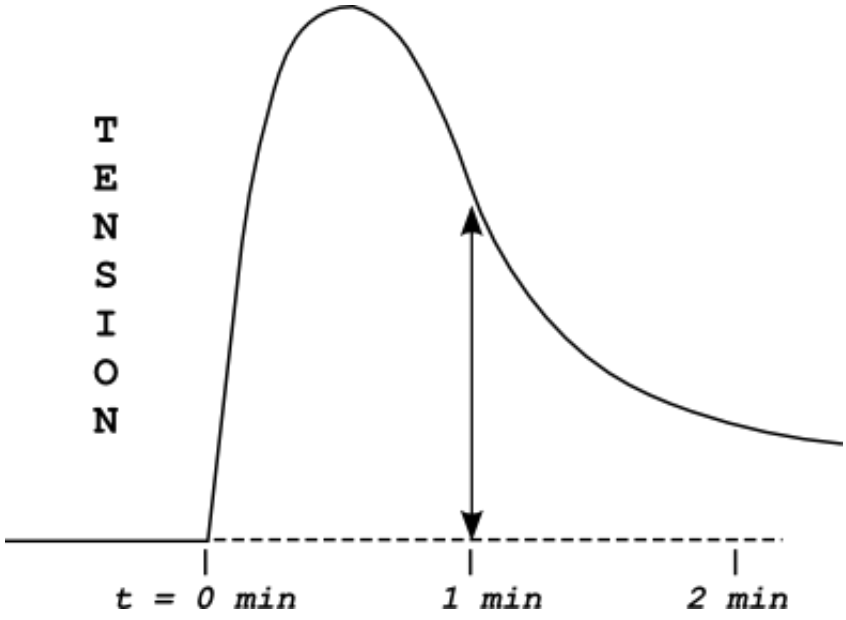
TENSION
t = 0 min
1 min
2 min

Figure 5. Contraction at t = 2 minutes.

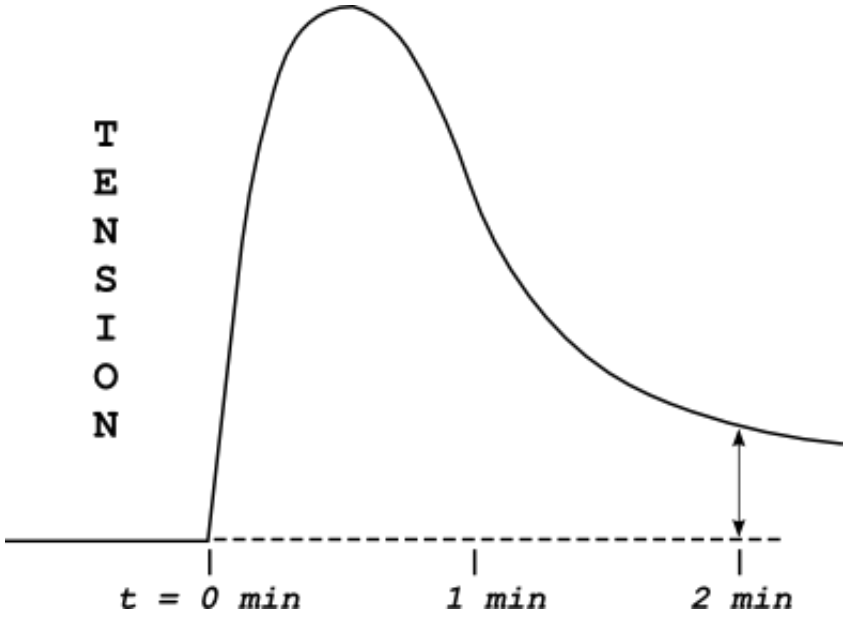
TENSION
t = 0 min
1 min
2 min

Figure 6. Area under the curve, 0-1 minute.

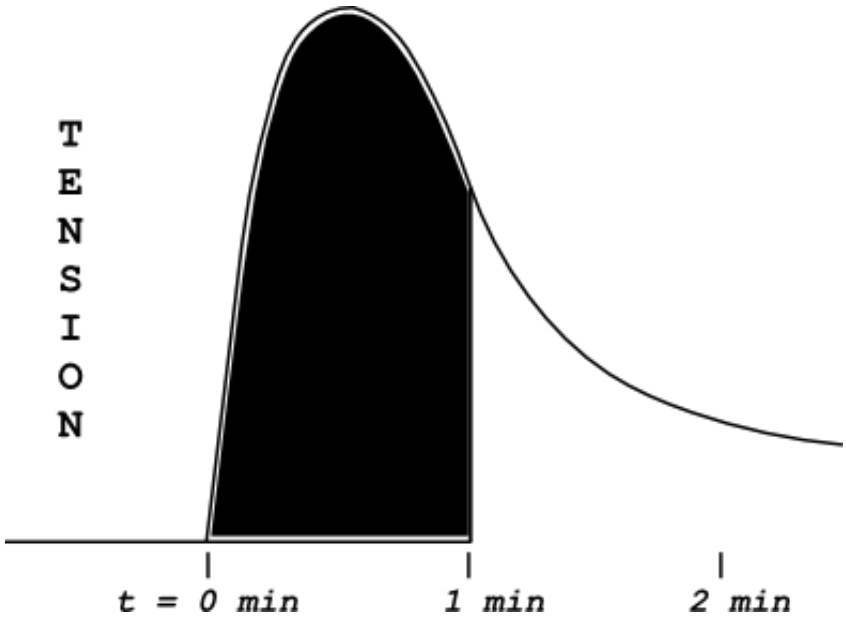
TENSION
t = 0 min
1 min
2 min

Figure 7. Area under the curve, 1-2 minutes.

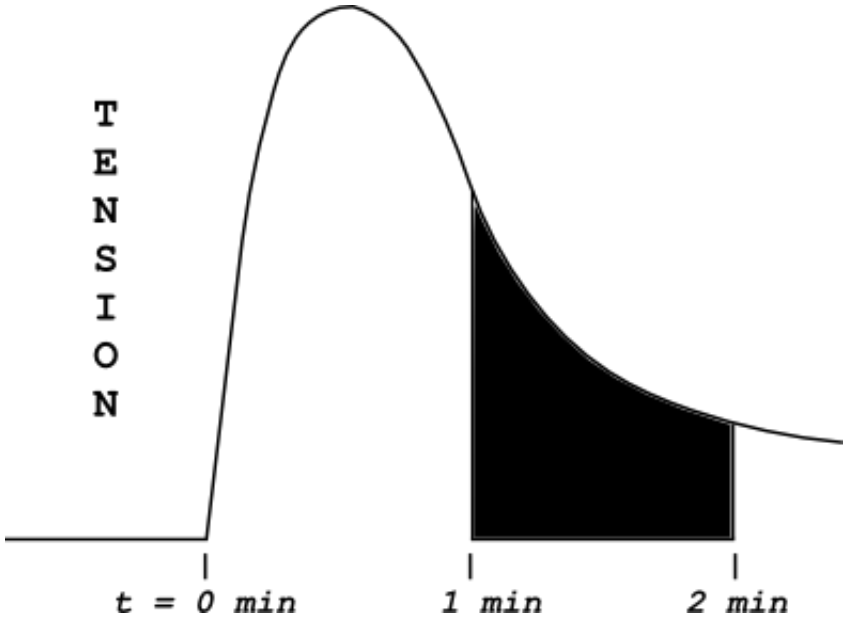
TENSION
t = 0 min
1 min
2 min

Figure 8. Area under the curve, 0-2 minutes.

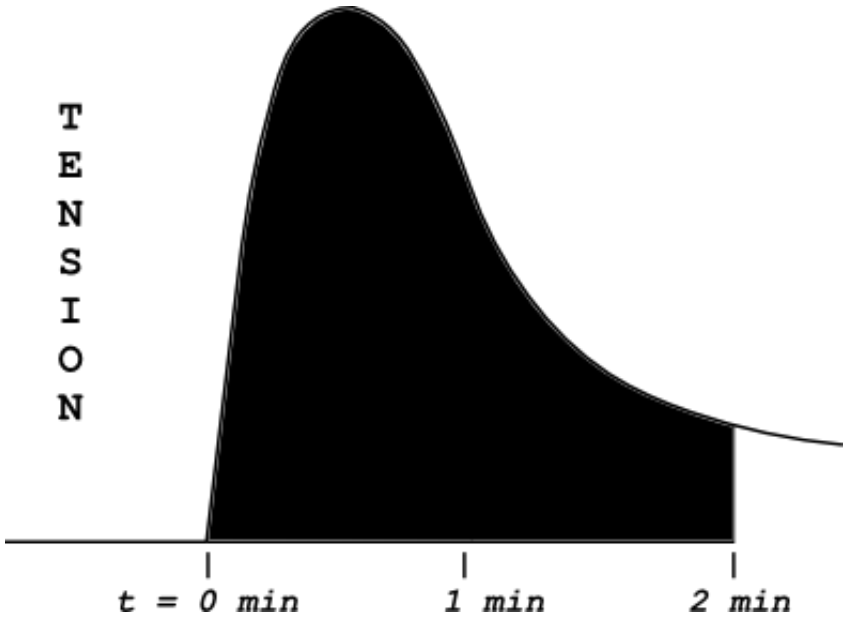
TENSION
t = 0 min
1 min
2 min

Kinase Assay

Activities of MLCK activity were measured by an immunokinase assay as performed in earlier studies from the lab [85, 88, 161, 162]. 100 μg of protein was transferred from the supernatant of prepared tissue sample to a designated tube and 1 μg of MLCK goat antibody was added. At 4°C, this mixture was incubated for 2 hours. Protein A/G agarose beads were added to each sample, and the mixture again incubated at 4°C overnight. Following centrifugation, supernatants were withdrawn and the beads/protein washed with lysis buffer three times.

The bead/protein pellets were resuspended in kinase buffer with composition (in mM): 100 tris-HCl, 1000 KCl, 50 $MgCl_2$, 10 EDTA, and 1 DTT. Twenty microliters of this mixture were added to a reaction mixture of (in mM): 100 tris-HCl, 1 KCl, 50 $MgCl_2$, 1 DTT, 1 ATP, and 10 μCi of [γ-^{32}P]ATP (3000 Ci/mol) with 5 μg myelin basic protein as kinase target substrate. This mixture was incubated for 15 min at 37°C. Twenty microliters of this mixture (and the accompanying myelin basic protein phosphorylated with γ-^{32}P) was absorbed onto phosphocellulose filter paper disks, and free radioactivity washed away by repeated immersion in 75 mM H_3PO_4. Radioactivity was then measured by liquid scintillation, and values expressed as counts/minute per microgram of protein.

RESULTS

Sample Traces

Sample traces are offered to demonstrate the variety of contraction waveforms. Most contractions studied (~75%) possess a waveform similar to the top panel of Figure 9 – a sharp rise in developed tension, followed by a decrease to a sustained level within 60-90 seconds. Other contractions (~20%) may show a rise in tension without appreciable decay, maintaining an elevated tone, as in the bottom panel of Figure 9. Contractions that demonstrated little decline following an early peak were not utilized in measurements that attempted to quantify the decay in tension (t = 1 min, t = 2 min studies).

In addition, contractions may exhibit phasic activity superimposed upon the described waveforms. An example of such a waveforms in displayed in Figure 10. For waveforms with prominent phasic components, contraction values at 1 min and 2 min were interpolated values. Area under the curve values were utilized as recorded, unless phasicity was extreme enough to take the minima of contractions to values below the initial baseline tension. Polyview software would treat such as negative areas under the curve and complicate the analysis. Such tracings were not utilized for AUC data.

Figure 9. Sample traces from main Polyview screen.

Top Panel: Trace indicative of early peak tension development and substantial decay to sustained level. Trace line enhanced for ease of viewing

Bottom Panel: Trace indicative of little decay following peak tension. Trace line enhanced for ease of viewing.

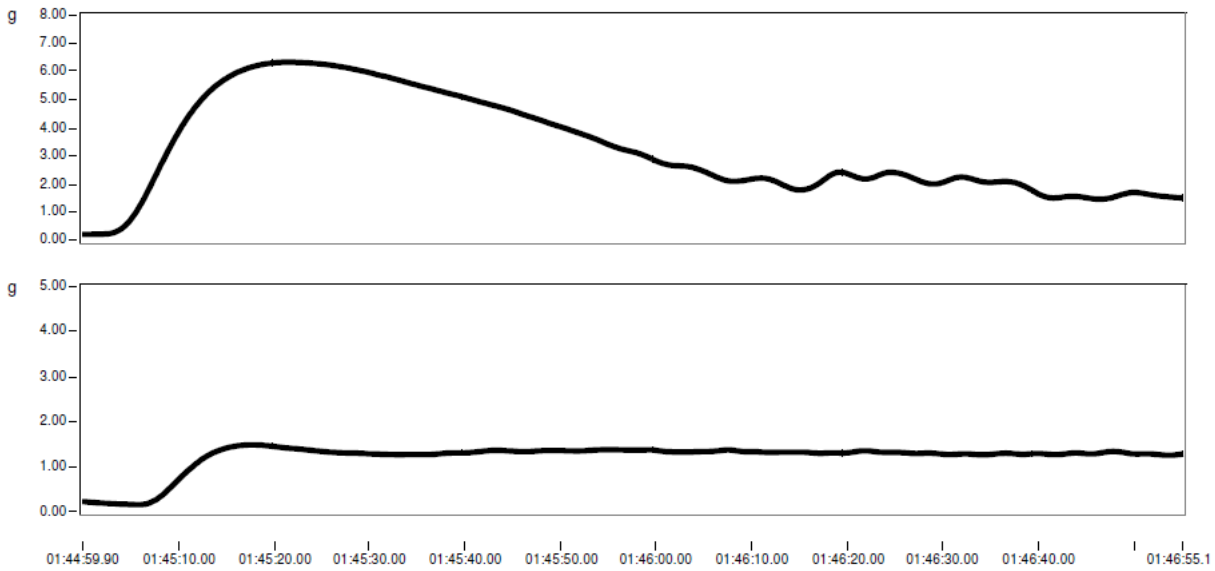
g
8.00
7.00
6.00
5.00
4.00
3.00
2.00
1.00
0.00
g
5.00
4.00
3.00
2.00
1.00
0.00
01:44:59.90
01:45:10.00
01:45:20.00
01:45:30.00
01:45:40.00
01:45:50.00
01:46:00.00
01:46:10.00
01:46:20.00
01:46:30.00
01:46:40.00
01:46:55.1

Figure 10. Sample partial trace from Zoom screen of Polyview Software suite.

Trace indicative of strips that exhibit phasic activity superimposed upon standard decay. Zoom feature of Polyview automatically filters and smoothes resultant data. Calculations are performed on original raw data.

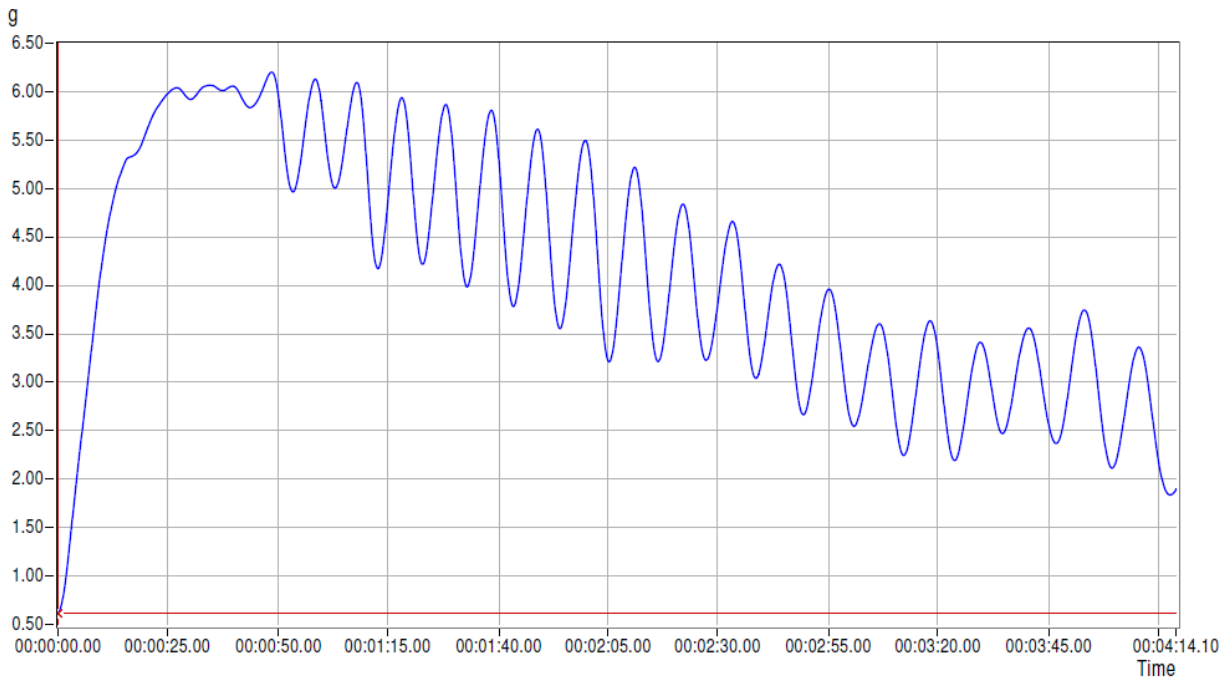
g
6.50
6.00
5.50
5.00
4.50
4.00
3.50
3.00
2.50
2.00
1.50
1.00
0.50
00:00:00.00
00:00:25.00
00:00:50.00
00:01:15.00
00:01:40.00
00:02:05.00
00:02:30.00
00:02:55.00
00:03:20.00
00:03:45.00
00:04:14.10
Time

Control Behavior of Strips due to carbachol

Strips were exposed to carbachol (CCh) at concentrations of 10 nM, 1 μM, and 100 μM. 10 nM elicited contraction in strips approximately 50% of the time, and data from these responsive strips were utilized. 1 μM CCh consistently produced robust responses, and 100 μM CCh reliably produced a maximal response. These doses are consistent with similar studies conducted using strips [40, 163].

Circular muscle strips were not viable preparations in this study. Although circular muscle strips can be prepared from human tissue reliably, in rat it is apparent that the longitudinal muscle layer provides needed integrity to the muscle strip – in its absence, circular muscle tears easily (along its physiological orientation) when subjected to tension. Similar difficulties have been noted in the literature [163, 164].

Contraction Dose response

The grand mean of control responses by carbachol dose are displayed in Figure 11. Contractile responses were 0.51 ± 0.06 grams at 10 nM CCh (n=40), 1.00 ± 0.12 grams at 1 μM CCh (n=50) and 1.80 ± 0.18 grams at 100 μM CCh (n=54). These force measurements are not normalized by mass and demonstrate the variability among strips used in the experiments. However, all

strips serve as individual controls for the experimental treatments, and all statistical tests are suitably conducted on repeated measurements.

Contraction at 1 and 2 min post exposure

Measured tension at time points 1 minute and 2 minutes following the initial tension increase were compared to peak values and expressed as a percentage At t=1 minute, the percentages of peak tension were 74.28% ± 4.32% for 10 nM CCh (n=16), 74.97% ± 3.09% for 1 μM CCh (n=23), and 64.69% ± 4.23% for 100 μM CCh (n=29). At t=2 minutes, the percentage values respectively were 65.56% ± 6.67% (n=15), 62.85% ± 4.96% (n=26), and 47.87% ± 4.13% (n=29). These data are summarized in Figure 12.

Area under the curve for control contractions

Areas under the response curves were calculated for the first minute (AUC 0-1 min), second minute (AUC 1-2 min), and first two minutes (AUC 0-2 min). For AUC 0-1 min, values were 16.79 ± 2.83 gram-seconds at 10 nM CCh (n=35), 38.86 ± 5.09 gram-seconds at 1 μM CCh (n=42), and 77.25 ± 8.65 gram-seconds at 100 μM CCh (n=46). For AUC 1-2 min, values were 22.85 ± 4.01 gram-seconds at 10 nM CCh (n=35), 46.89 ± 7.42 gram-seconds at 1 μM CCh (n=38), and 53.00 ± 7.09 gram-seconds at 100 μM CCh (n=44). For AUC 0-2 min, values were 34.44 ± 5.84 gram-seconds at 10 nM CCh

(n=34), 83.62 ± 11.35 gram-seconds at 1 µM CCh (n=42), and 133.25 ± 14.67 gram-seconds at 100 µM CCh (n=45). A summary of this data is displayed in Figure 13.

Figure 11. Control contractile response to carbachol.

Grand mean of all responses. (n=40 for 10 nM CCh, n=50 for 1 µM CCh, and n=54 for 100 µM CCh).

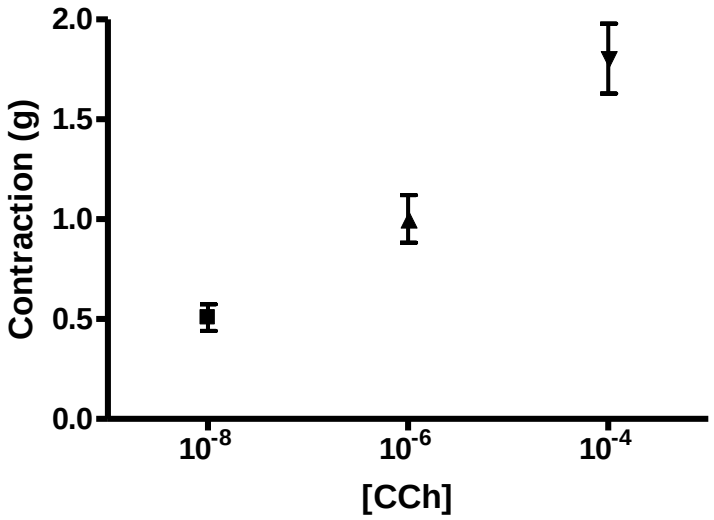
2.0
1.5
1.0
0.5
0.0
Contraction (g)
10-8
10-6
10-4
[CCh]

Figure 12. Percentage of Peak Amplitude remaining at t = 1 min and t = 2 min for control responses.

Sample sizes for t=1 minute: for 10 nM CCh (n=16), for 1 μM CCh (n=23), and for 100 μM CCh (n=29). At t=2 minutes, respective sample sizes: n=15, n=26, and n=29.

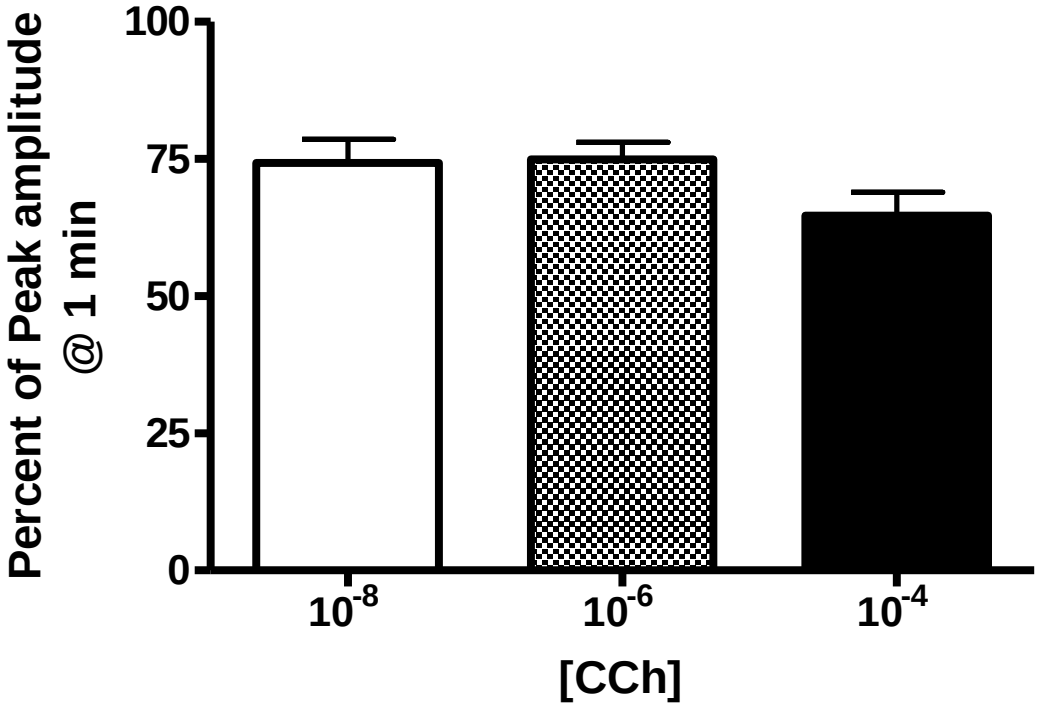
Percent of Peak amplitude @ 1 min
100
75
50
25
0
10-8
10-6
10-4
[CCh]

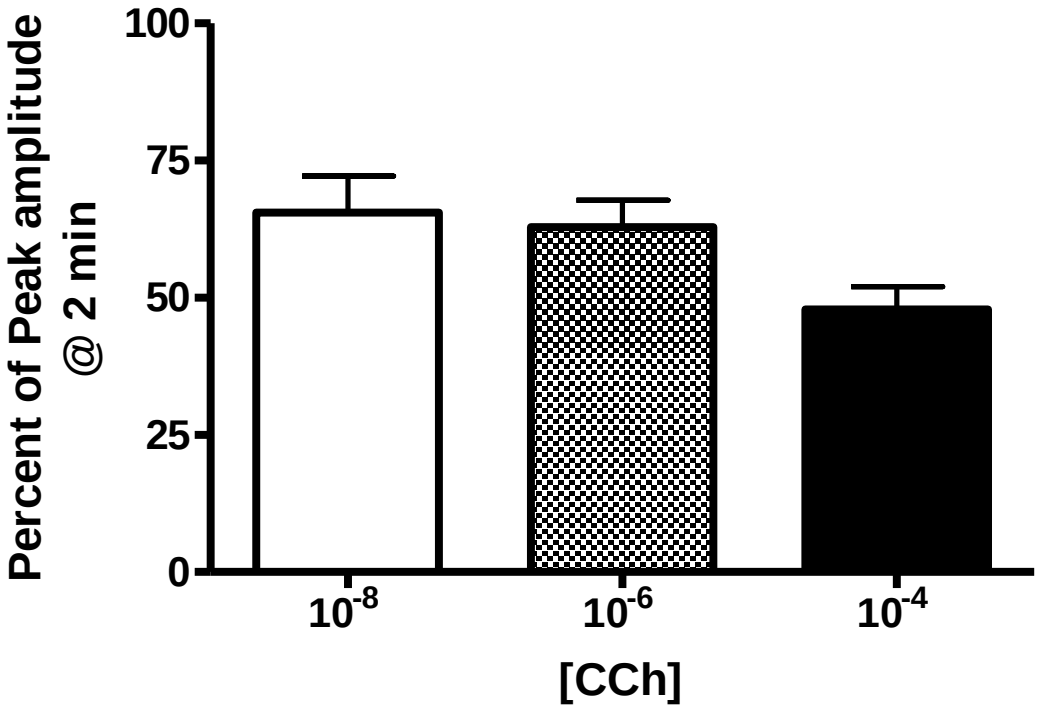
Percent of Peak amplitude @ 2 min
100
75
50
25
0
10-8
10-6
10-4
[CCh]

Figure 13. AUC 0-1 min, AUC 1-2 min, and AUC 0-2 min data for control responses.

Sample sizes range from 32 to 45 among the three metrics.

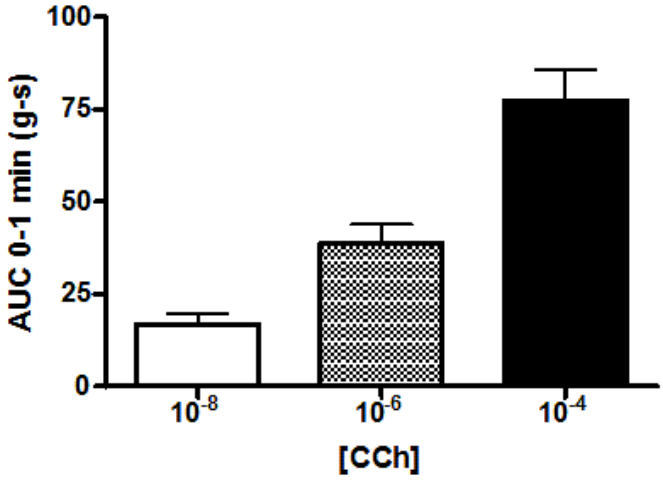
AUC 0-1 min (g-s)
100
75
50
25
0
10-8
10-6
10-4
[CCh]

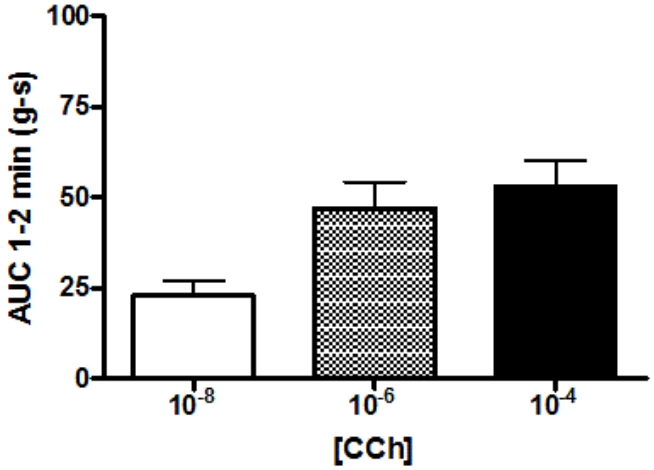
AUC 1-2 min (g-s)
100
75
50
25
0
10-8
10-6
10-4
[CCh]

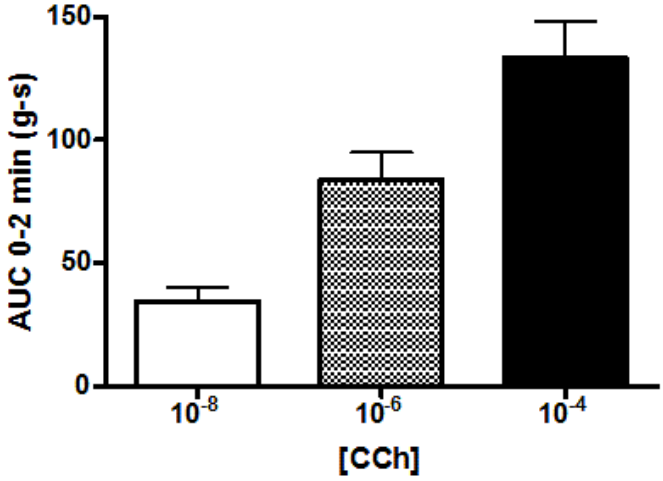
AUC 0-2 min (g-s)
150
100
50
0
10-8
10-6
10-4
[CCh]

Repeated Measurements

Repeated measurements of peak amplitude and area under the curve were conducted on strips in absence of kinase inhibition. This was to ensure that any change in contractile behavior is not an artifact of de-sensitization to agonist or strip fatigue. Strips were exposed to 1 µM CCh, contractions measured. Following a wash, strips were incubated for 15 min in Krebs solution, and dosed again with 1 µM CCh, to mimic the incubation period with kinase inhibitors. Data are expressed as percentage of initial contraction/AUC. Paired t-tests were conducted to assess significance between initial and repeated measurements.

Peak Amplitude/Area under the curve repeated measurements

Following a 15 min incubation after initial contraction, peak recorded tension in strips was 98.29% ± 3.99% of the initial recording (n=13, 5 animals). Summary data displayed in Figure 14. Following a 15 min incubation period, strips exhibited contractions with AUC 0-1 min and AUC 0-2 min that were 99.00% ± 2.148% (n=13, 5 animals) and 102.1% ± 1.881% (n=13, 5 animals) respectively. No significant differences were seen with repeated measures (all $P > 0.05$). These data are summarized in Figure 15.

Figure 14. Peak Contractions of Repeated Measurements.

Repeated peak recorded tension in strips was 98.29% ± 3.99% of the initial recording (n=13, 5 animals). No significance noted.

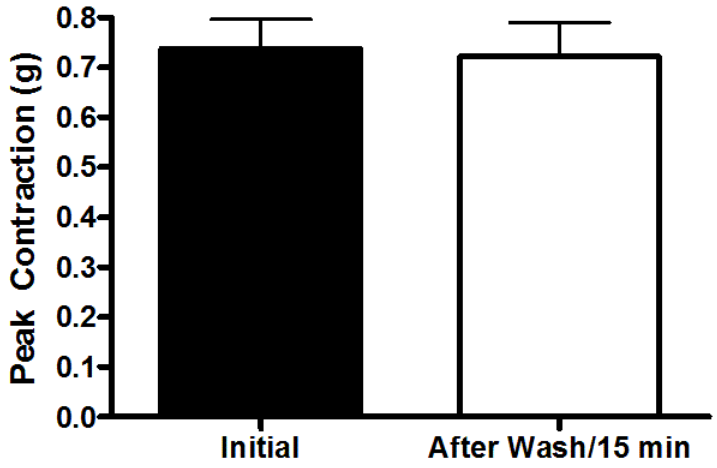
Peak Contraction (g)
0.8
0.7
0.6
0.5
0.4
0.3
0.2
0.1
0.0
Initial
After Wash/15 min

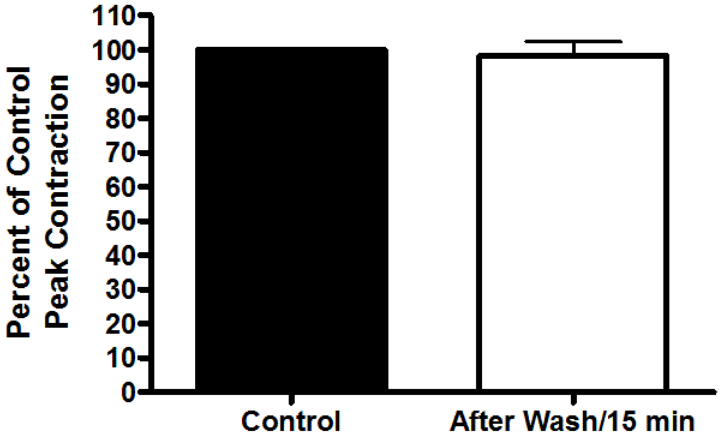
Percent of Control
Peak Contraction
110
100
90
80
70
60
50
40
30
20
10
0
Control
After Wash/15 min

Figure 15. AUC 0-1 min and AUC 0-2 min values for repeated measurements.

Repeated AUC 0-1 min and AUC 0-2 min values were 99.00% ± 2.148% (n=13, 5 animals) and 102.1% ± 1.881% (n=13, 5 animals) of the original recordings. No significance noted.

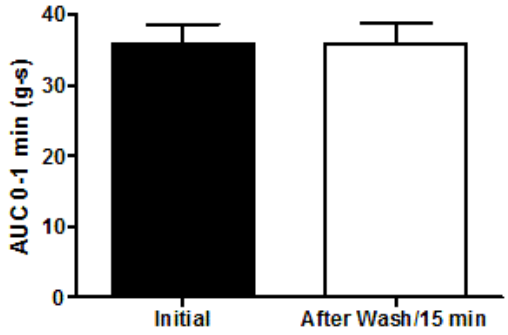
AUC 0-1 min (g-s)
40
30
20
10
0
Initial
After Wash/15 min

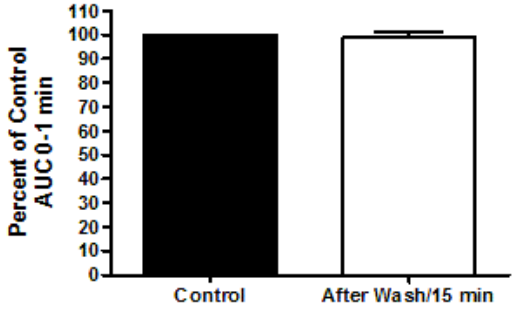
Percent of Control AUC 0-1 min
110
100
90
80
70
60
50
40
30
20
10
0
Control
After Wash/15 min

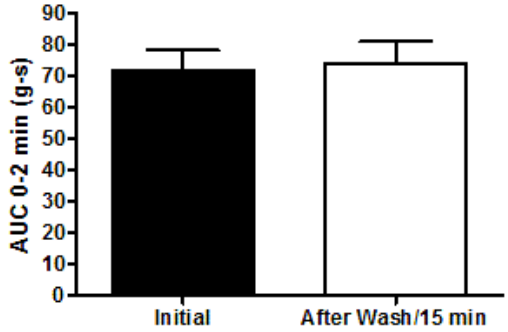
AUC 0-2 min (g-s)
90
80
70
60
50
40
30
20
10
0
Initial
After Wash/15 min

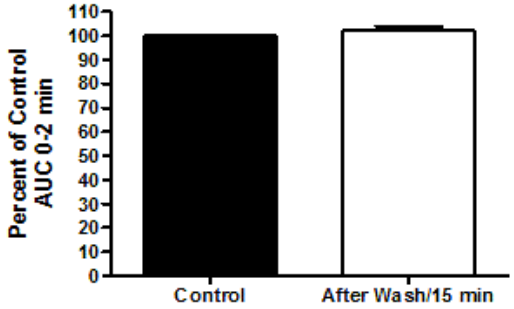
Percent of Control AUC 0-2 min
110
100
90
80
70
60
50
40
30
20
10
0
Control
After Wash/15 min

Effects of Muscarinic Antagonism

Contraction in longitudinal muscle is mediated primarily by m3 receptors. Smooth muscle cells expressed a greater number of m2 receptors, but these receptors are not definitively involved in acute contractile behavior. Strips were subjected to 1 µM CCh before and after incubation with methoctramine (m2 receptor antagonist) and 4-DAMP (m3 receptor antagonist). Incubation with 1 µM methoctramine caused no significant changes to peak contraction, AUC 0-1 min, or AUC 0-2 min induced by 1 µM carbachol (all $P > 0.05$, n=7 from 4 animals). Incubation with 1 µM 4-DAMP prevented all responses to 1 µM carbachol (n=6). Results are summarized in Figure 16.

Figure 16. Effect of muscarinic antagonists on CCh-induced contraction.

1 µM methoctramine showed no significant effect upon 1 µM CCh induced contraction. 1 µM 4-DAMP completed blocked all contraction induced by CCh. n=7 from 4 animals.

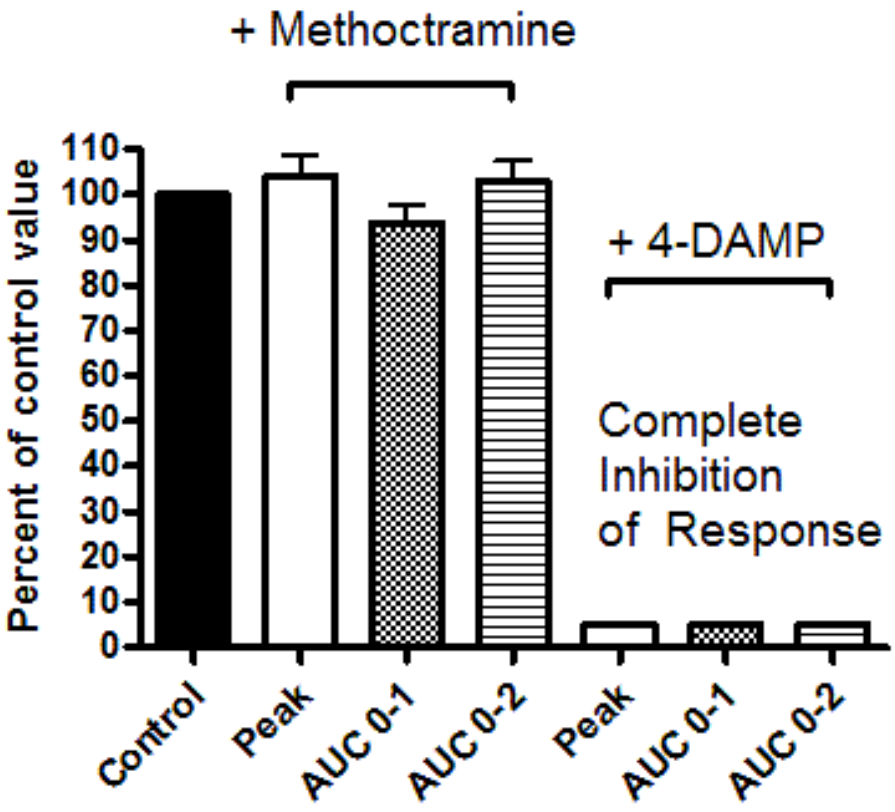
+ Methoctramine
+ 4-DAMP
Complete
Inhibition
of Response
Percent of control value
110
100
90
80
70
60
50
40
30
20
10
0
Control
Peak
AUC 0-1
AUC 0-2
Peak
AUC 0-1
AUC 0-2

Effects of Neural Inhibition (TTX)

Repeated measurements were conducted in the presence of 1 µM tetrodotoxin (TTX), a Na^+ channel blocker, in order to investigate any neural influence on contractile behavior. Peak contractions, contractions at 1 minute and 2 minutes, and area under the curve data were collected after 15 min incubation with TTX and compared to control contractions.

Peak Contraction due to carbachol

The peak contraction elicited by all concentrations of CCh was not significantly affected by TTX administration. Viewed as percentage of control contraction, TTX exposure led to contractions 102.8% ± 5.98% of the control value at 1 µM CCh (n=7), 113.2% ± 8.6% at 10 µM CCh (n=7), and 110.5% ± 9.02% at 100 µM CCh (n=7). Again, although mean contractions were increased with TTX incubation, the values only approached significance (all P-Values > 0.05). Summary data for Peak contraction in the presence of TTX is offered in Figure 17.

Contraction at 1 min and 2 min minutes post exposure

Contraction at 1 min and 2 minute was recorded under control conditions and after incubation with TTX. Raw values and percent of peak contraction are offered. As with the peak contraction, 1 µM TTX cause no significant change in the amplitude of contraction at t = 1 minute and t = 2 minutes. A t

= 1 minute, control versus TTX had amplitudes (in grams) of 1.85 ± 0.13 versus 1.78 ± 0.12 for 1 µM CCh (n=5), 2.14 ± 0.20 versus 2.04 ± 0.16 grams for 10 µM CCh (n=5), and 2.39 ± 0.19 versus 2.10 ± 0.14 grams for 100 µM CCh (n=5). At t = 2 minutes, control versus TTX had amplitudes (in grams) of 1.67 ± 0.05 versus 1.49 ± 0.07 for 1 µM CCh (n=5), 1.79 ± 0.21 versus 1.62 ± 0.07 grams for 10 µM CCh (n=5), and 1.76 ± 0.08 versus 1.80 ± 0.11 grams for 100 µM CCh (n=5). These data and percent summaries are included in Figure 18.

Area under curve for first two minutes

Similarly, 1 µM TTX has no significant effect upon the area under the curve for the first minute and first two minutes of contractions elicited by CCh at all tested concentrations. For AUC 0-1 min, control versus TTX had values (in gram-seconds) of 63.25 ± 10.64 for versus 60.42 ± 9.23 for 1 µM CCh (n=5), 104.3 ± 13.28 versus 121.2 ± 18.82 grams for 10 µM CCh (n=5), and 112.9 ± 13.27 versus 128.5 ± 27.21 grams for 100 µM CCh (n=5).

For AUC 0-2 min, control versus TTX had values (in gram-seconds) of 106.5 ± 18.73 for versus 98.44 ± 12.09 for 1 µM CCh (n=5), 149.3 ± 23.02 versus 183.2 ± 31.53 grams for 10 µM CCh (n=5), and 192.5 ± 32.68 versus 220.0 ± 38.89 grams for 100 µM CCh (n=5). These data and percent summaries are included in Figure 19.

Figure 17. Peak Contraction Data in the presence of TTX versus control.

102.8% ± 5.98% of control at 1 µM CCh (n=7), 113.2% ± 8.6% at 10 µM CCh (n=7), and 110.5% ± 9.02% at 100 µM CCh (n=7). No significance determined.

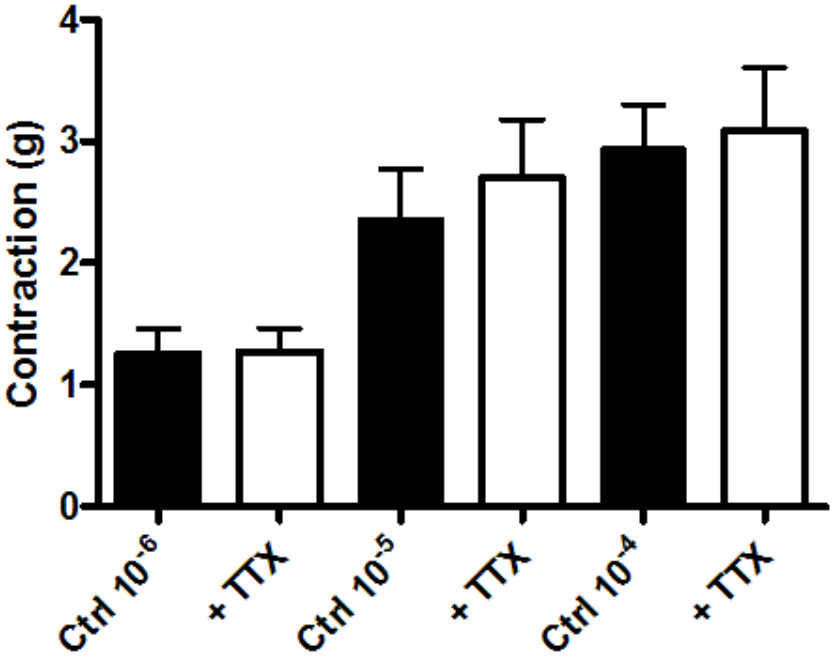
Contraction (g)
4
3
2
1
0
Ctrl 10-6
+ TTX
Ctrl 10-5
+ TTX
Ctrl 10-4
+ TTX

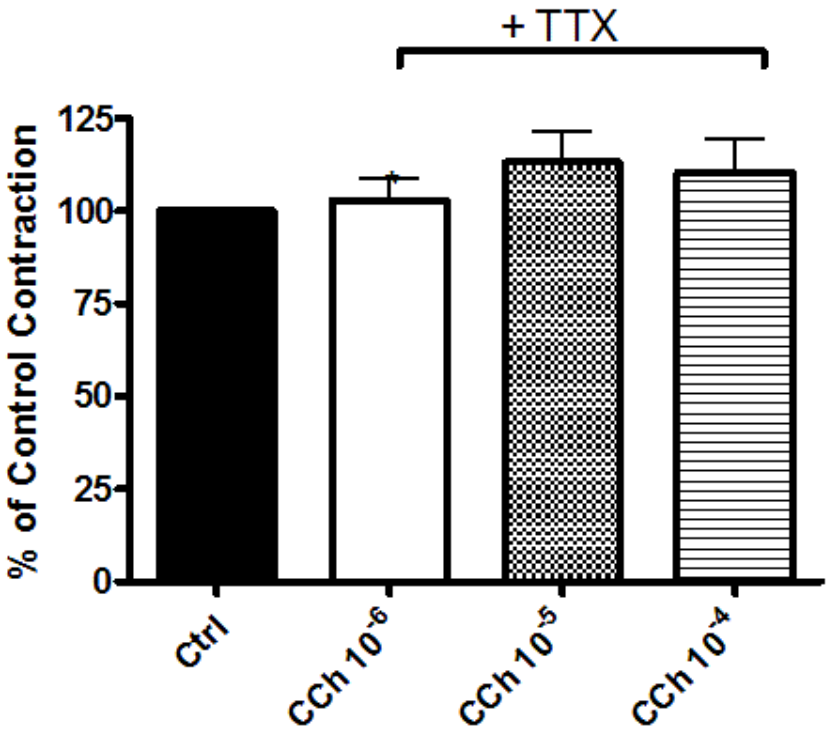
+ TTX
% of Control Contraction
125
100
75
50
25
0
*
Ctrl
CCh 10-6
CCh 10-5
CCh 10-4

Figure 18. Contractions at 1 min and 2 min in the presence of TTX versus control.

No significant difference in contractions at 1 min and 2 min post carbachol in TTX-incubated group versus control group. n = 5 from at least three animals.

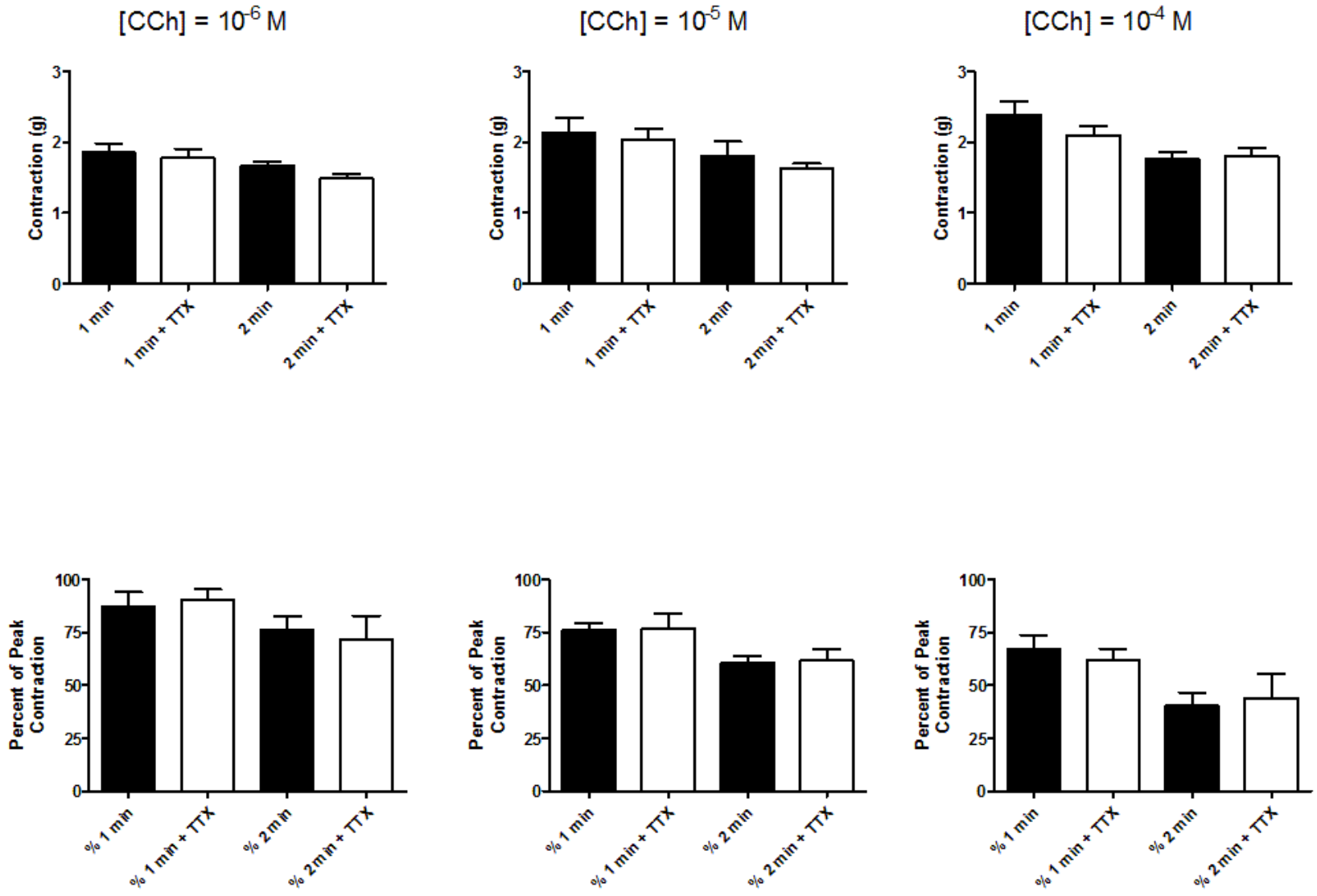
[CCh] = 10-6 M
[CCh] = 10-5 M
[CCh] = 10-4 M
Contraction (g)
0
1
2
3
1 min
1 min + TTX
2 min
2 min + TTX
Percent of Peak Contraction
0
25
50
75
100
% 1 min
% 1 min + TTX
% 2 min
% 2 min + TTX

Figure 19. AUC 0-1 min and AUC 0-2 min values in the presence of TTX versus control.

No significant differences noted in AUC values between TTX group and carbachol group. n = 5 minimum from at least 3 animals.

AUC 0-1 min (g-s)
200
150
100
50
0
CCh 10-6
+ TTX
CCh 10-5
+ TTX
CCh 10-4
+ TTX
AUC 0-2 min (g-s)
300
200
100
0
CCh 10-6
+ TTX
CCh 10-5
+ TTX
CCh 10-4
+ TTX
% of Control AUC 0-1 min
150
125
100
75
50
25
0
Ctrl
CCh 10-6
CCh 10-5
CCh 10-4
+ TTX
% of Control AUC 0-2 min
150
125
100
75
50
25
0
Ctrl
CCh 10-6
CCh 10-5
CCh 10-4
+ TTX

Effects of Rho Kinase Inhibition (Y27632)

Rho kinase is known to affect the phosphatase leg of contractile regulation through its direct phosphorylation of MYPT1 and its indirect phosphorylation of CPI-17 via PLD-DAG-PKC. Incubation of strips for 15 minutes in 10 μM Y27632 (a powerful Rho Kinase inhibitor) allows for comparison of Rho-kinase inhibited contraction to control conditions. Rho kinase inhibition was viewed from the contractile perspectives of basal tone regulation, peak contraction, contraction at one and two minutes post CCh exposure, and area under the curve values. The possible effect of Rho kinase inhibition on MLCK activity was studied via molecular methods.

Basal Activity

Rho kinase inhibition led to a significant decrease in basal tone after 10 minutes of incubation. In studied strips (n=15), administration of Y27632 (Rho kinase inhibition) resulted in a change of basal tone from 0.82 ± 0.07 grams to 0.73 ± 0.06 grams. A conducted paired t-test returned $P < 0.01$; the inhibition of Rho kinase reduces basal tone. Data summarized and displayed in Figure 20.

Figure 20. Effect of Rho Kinase inhibition on basal tone.

Administration of 10 µM Y27632 for 10 min resulted in a reduction of basal tone from 0.82 ± 0.07 grams to 0.73 ± 0.06 grams (* indicates $P < 0.05$, n=12).

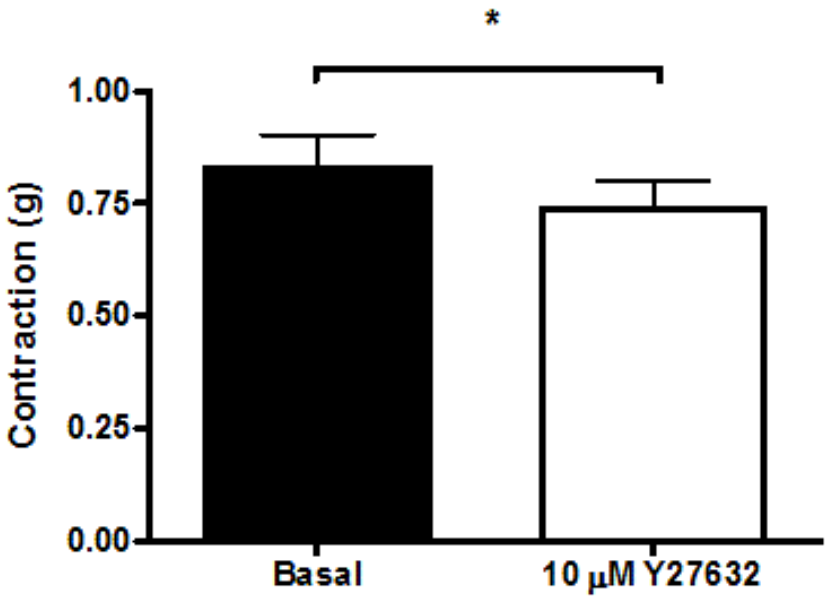
*
1.00
0.75
0.50
0.25
0.00
Contraction (g)
Basal
10 μM Y27632

Peak Contraction due to carbachol

Rho kinase inhibition (via Y27632 incubation) significantly reduced contraction for carbachol concentrations of 1 µM and 100 µM. Control peak contraction values (in grams) versus contractions following Y27632 incubation are 0.80 ± 0.30 versus 0.30 ± 0.08 ($P > 0.05$, n=4) at 10 nM CCh; 1.13 ± 0.28 versus 0.71 ± 0.19 ($P < 0.01$, n=15) for 1 µM CCh; and 2.17 ± 0.38 versus 1.21 ± 0.23 ($P < 0.05$, n=16) at 100 µM CCh. Summary data are displayed in Figure 21.

Contraction at 1 min and 2 min minutes post exposure

Rho kinase inhibition reduced the contraction at both 1 min and 2 min post CCh exposure for all concentrations of CCh. With 10 nM CCh, 1 minute control values (in grams) versus Y27632 incubation were 1.34 ± 0.17 versus 0.72 ± 0.15 ($P < 0.05$), 2 minute values were 1.11 ± 0.06 for control versus 0.64 ± 0.08 for Y27632 incubation ($P < 0.01$, both n=3); for 1 µM CCh, 1 minute control values (in grams) were 1.76 ± 0.31 versus 0.83 ± 0.11 ($P < 0.05$), 2 minute values were 1.45 ± 0.22 for control versus 0.77 ± 0.10 grams for Y27632 incubation ($P < 0.05$, both n=6); for 100 µM CCh, 1 minute control values (in grams) versus Y27632 incubation were 1.70 ± 0.21 versus 1.14 ± 0.18 ($P < 0.01$), 2 minute control values were 1.48 ± 0.16 versus 1.08 ± 0.15 for Y27632 incubation ($P < 0.01$, both n=9). Data summarized in Figure 22.

Figure 21. Effect of Rho Kinase Inhibition on Peak Contraction.

Top Panel: Rho Kinase inhibition significantly reduced peak contraction elicited by 1 µM CCh (1.13 ± 0.28 versus 0.71 ± 0.19 grams, n=15) and by 100 µM CCh (2.17 ± 0.38 versus 1.21 ± 0.23 grams, n=16). (* = $P < 0.05$)

Bottom Panel: Summary data expressed as percentage of control. (* = $P < 0.05$)

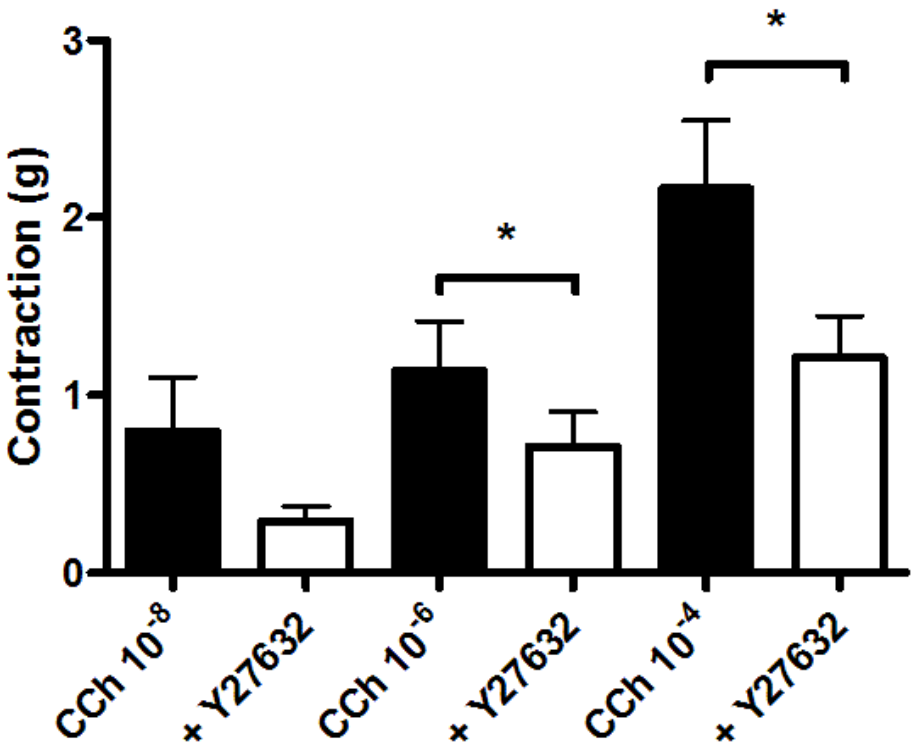
Contraction (g)
3
2
1
0
*
*
CCh 10-8
+ Y27632
CCh 10-6
+ Y27632
CCh 10-4
+ Y27632

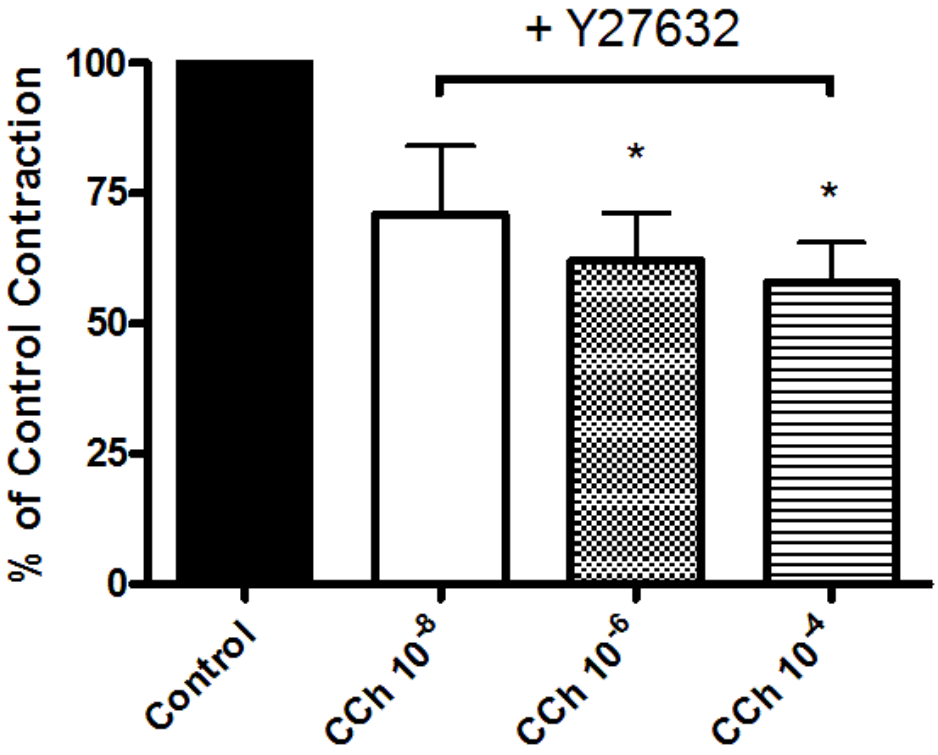
+ Y27632
% of Control Contraction
100
75
50
25
0
*
*
Control
CCh 10-8
CCh 10-6
CCh 10-4

Figure 22. Effect of Rho Kinase Inhibition at 1 min and 2 min post CCh exposure.

Top Panel: Tone was reduced at t = 1 min and t = 2 min with Rho kinase inhibition. Sample Sizes range from 3 to 9. (* = $P < 0.05$)

Bottom Panel: t = 1 min and t = 2 min data expressed by percentage of control.

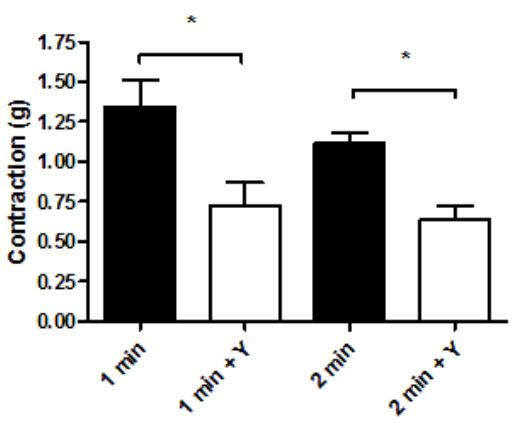
Contraction (g)
1.75
1.50
1.25
1.00
0.75
0.50
0.25
0.00
*
*
1 min
1 min + Y
2 min
2 min + Y

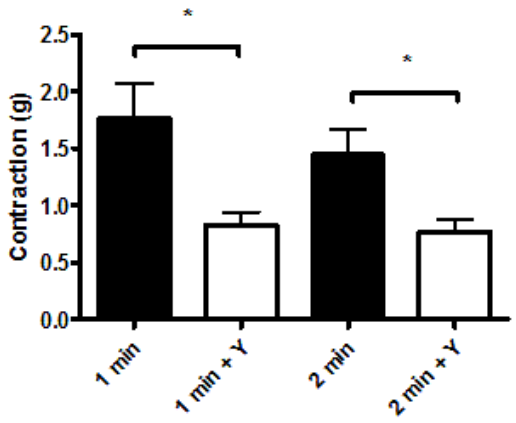
Contraction (g)
2.5
2.0
1.5
1.0
0.5
0.0
*
*
1 min
1 min + Y
2 min
2 min + Y

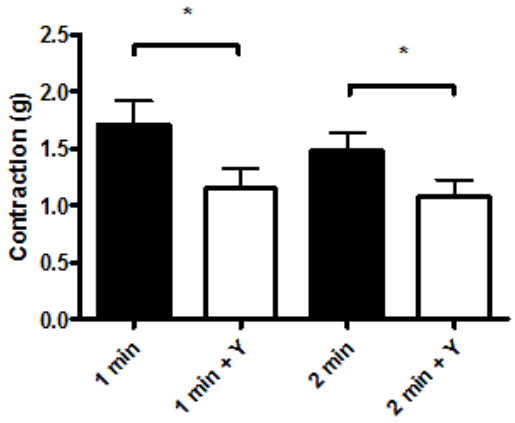
Contraction (g)
2.5
2.0
1.5
1.0
0.5
0.0
*
*
1 min
1 min + Y
2 min
2 min + Y

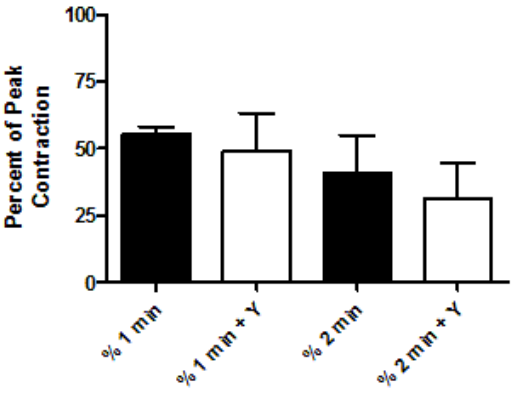
Percent of Peak Contraction
100
75
50
25
0
% 1 min
% 1 min + Y
% 2 min
% 2 min + Y

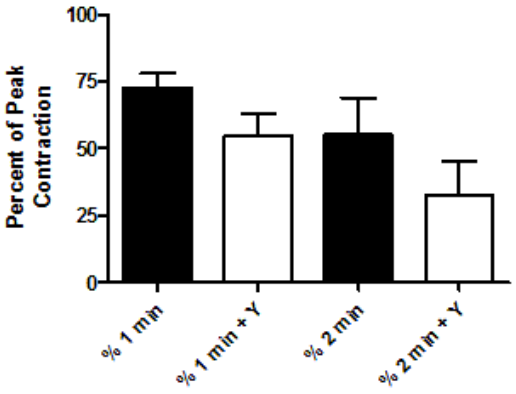
Percent of Peak Contraction
100
75
50
25
0
% 1 min
% 1 min + Y
% 2 min
% 2 min + Y

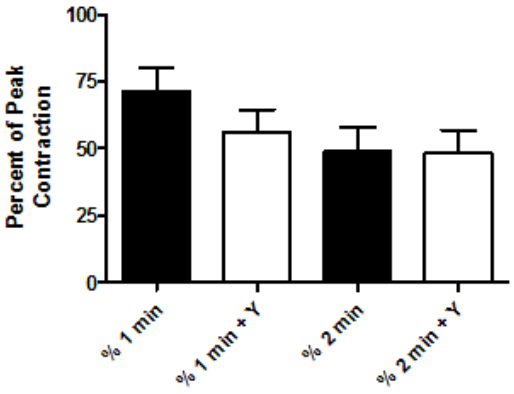
Percent of Peak Contraction
100
75
50
25
0
% 1 min
% 1 min + Y
% 2 min
% 2 min + Y

Area under curve for first two minutes

Rho Kinase inhibition caused a significant decrease in the area under the curve metric in the first (AUC 0-1), second (AUC 1-2), and first two minutes (AUC 0-2) for contractions elicited by 1 µM and 100 µM CCh. AUC data for 10 nM CCh contractions were not significantly reduced. For AUC 0-1 min, control versus Y27632 incubation values (in gram-seconds): for 100 nM CCh, 13.08 ± 8.85 versus 3.608 ± 2.00 ($P > 0.05$, n=5); for 1 µM CCh, 46.05 ± 9.86 versus 15.02 ± 3.56 ($P < 0.01$, n=13); for 100 µM CCh, 85.81 ± 15.41 versus 42.86 ± 7.68 ($P < 0.01$, n=16). For AUC 1-2 min, control versus Y27632 incubation values (in gram-seconds): for 100 nM CCh, 14.93 ± 9.17 versus 3.917 ± 1.87 ($P > 0.05$, n=3); for 1 µM CCh, 64.13 ± 15.90 versus 21.83 ± 5.48 ($P < 0.01$, n=13); for 100 µM CCh, 56.82 ± 12.61 versus 31.06 ± 6.07 ($P < 0.05$, n=15). For AUC 0-2 min, control versus Y27632 incubation values (in gram-seconds): for 100 nM CCh, 35.54 ± 24.26 versus 9.503 ± 5.223 ($P > 0.05$, n=3); for 1 µM CCh, 120.8 ± 25.15 versus 39.90 ± 9.417 ($P < 0.01$, n=10); for 100 µM CCh, 142.7 ± 26.03 versus 74.87 ± 13.31 ($P < 0.01$, n=15). Summary data for AUC values is presented in Figure 23.

Figure 23. Effect of Rho kinase inhibition on AUC values.

Top Panel: Raw data values of AUC 0-1 min, AUC 1-2 min, and AUC 0-2 min for CCh concentrations of 10 nM, 1 µM, and 100 µM. Sample sizes range from 5 to 16. (* indicates $P < 0.05$)

Bottom Panel: Data expressed as percentage of control.

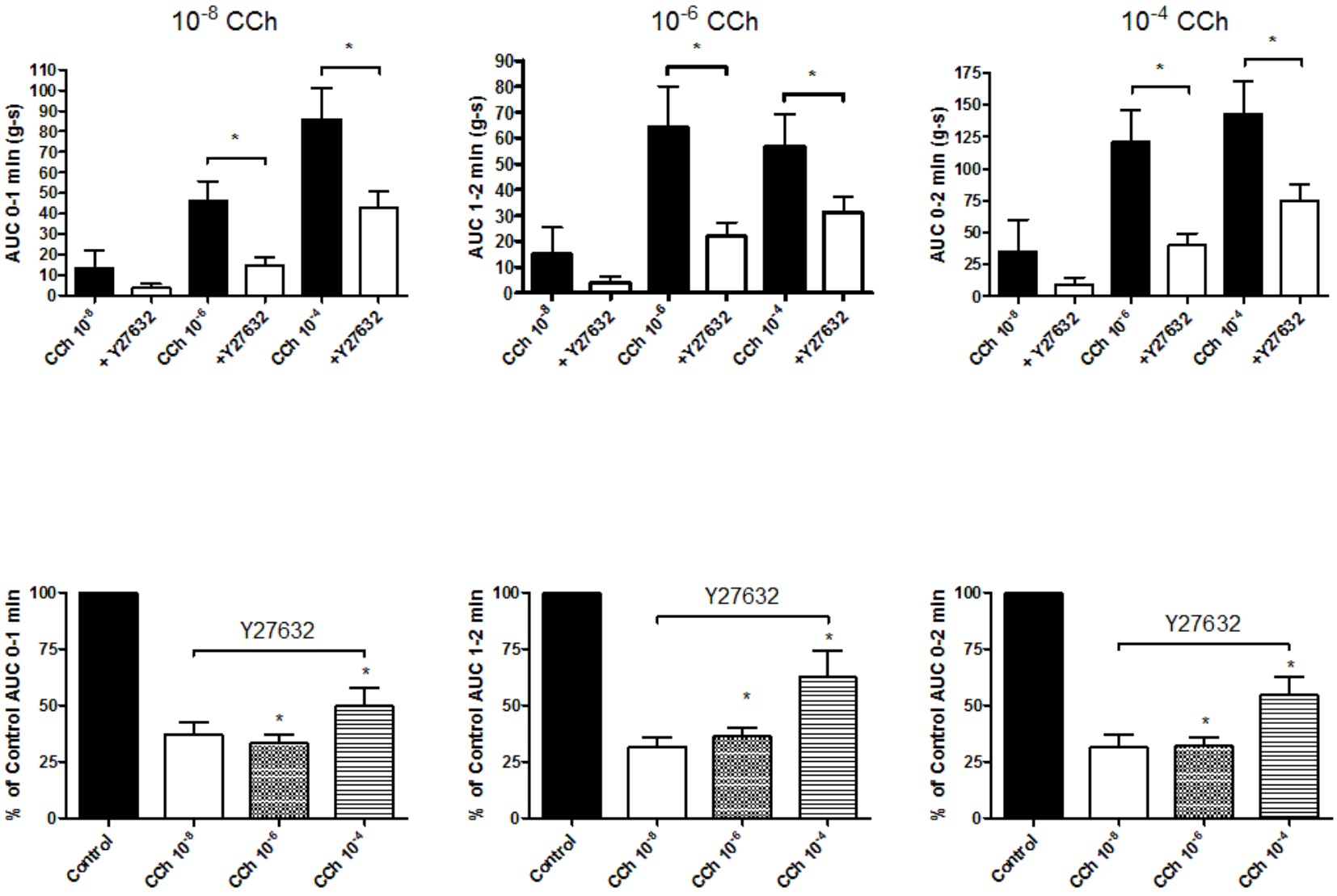
10-8 CCh
10-6 CCh
10-4 CCh
AUC 0-1 min (g-s)
AUC 1-2 min (g-s)
AUC 0-2 min (g-s)
CCh 10-8
+Y27632
CCh 10-6
+Y27632
CCh 10-4
+Y27632
% of Control AUC 0-1 min
% of Control AUC 1-2 min
% of Control AUC 0-2 min
Y27632
Control
CCh 10-8
CCh 10-6
CCh 10-4

MLCK activity

The effect of Rho kinase inhibition on MLCK activity was measured using immunokinase assay. MLCK activity was measured in longitudinal muscle-myenteric plexus (LM-MP) strip homogenates of four groups: control, following 10 min incubation of 10 µM Y27632, 1 min post 1 µM CCh exposure, and 1 min post 1 µM CCh exposure following 10 min incubation with 10 µM Y27632. 1 µM CCh increased MLCK activity to 167% ± 21% of control activity ($P < 0.05$ versus control, $n = 12$). Incubation for 10 min with Y27632 reduced CCh-induced activity to 122% ± 11% of control activity ($P < 0.05$ versus control, $n = 8$). Incubation of Y27632 alone did not differ MLCK from control ($n = 12$ for control, $n = 4$ for Y27632 alone). CCh-induced activity was not significantly varied between strips with and without Rho Kinase inhibition ($n = 12$ for CCh, $n = 8$ for CCh with Y27632 incubation). Results are shown in Figure 24.

Figure 24. Effect of Rho Kinase Inhibition on CCh-evoked MLCK activity.

1 µM CCh-induced MLCK activities with and without Rho Kinase inhibition are presented. Values expressed as percentage ± SEM of control MLCK activity. Control, n = 12. CCh-induced activity is 167% ± 21% of control ($P < 0.05$, n = 12). CCh activity in the presence of 10 µM Y27632 reduces CCh-induced activity to 122% ± 11% of control ($P < 0.05$, n = 8).

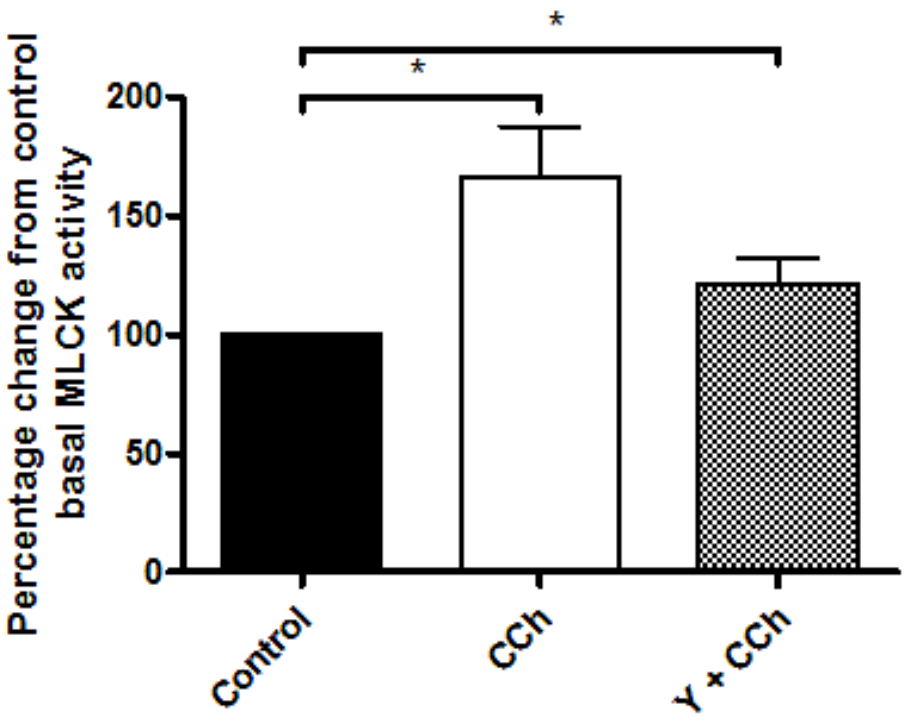
Percentage change from control basal MLCK activity
200
150
100
50
0
*
*
Control
CCh
Y + CCh

Effects of ERK1/2 Inhibition (PD98059)

Incubation of strips for 15 minutes in 10 µM PD98059 (an ERK1/2 inhibitor) allows for comparison of ERK1/2 inhibited contraction to control conditions. ERK1/2 inhibition was viewed from the contractile perspectives of basal tone regulation, peak contraction, contraction at one and two minutes post CCh exposure, and area under the curve values. Possible additive effects of ERK1/2 inhibition (postulated to work as kinase regulator) and Rho Kinase inhibition (known phosphatase regulator) are studied. The effect of ERK1/2 inhibition on MLCK activity was studied via molecular methods.

Basal Activity

ERK1/2 inhibition led to no significant change in basal tone after 10 minutes of incubation. In studied strips (n=12), administration of PD98059 (ERK1/2 inhibition) resulted in a change of basal tone from 0.79 ± 0.06 grams to 0.81 ± 0.05 grams. A conducted paired t-test returned $P > 0.05$; the inhibition of ERK1/2 does not affect basal tone. Data summarized and displayed in Figure 25.

Peak Contraction due to carbachol

ERK1/2 inhibition (via PD98059 incubation) significantly reduced contraction for all carbachol concentrations. Control peak contraction values (in grams) versus contractions following

PD98059 incubation are 0.47 ± 0.13 versus 0.28 ± 0.08 ($P < 0.05$, n=6) at 10 nM CCh; 0.86 ± 0.13 versus 0.49 ± 0.09 ($P < 0.01$, n=9) for 1 µM CCh; and 2.06 ± 0.38 versus 1.40 ± 0.32 ($P < 0.001$, n=9) for 100 µM CCh. Summary data are displayed in Figure 26.

Contraction at 1 min and 2 min minutes post exposure

ERK1/2 inhibition reduced the contraction at both 1 min and 2 min post CCh exposure for all concentrations of CCh. With 10 nM CCh, 1 minute control values (in grams) versus PD98059 incubation were 1.07 ± 0.15 versus 0.90 ± 0.14 ($P < 0.01$), 2 minute values were 0.88 ± 0.09 for control versus 0.77 ± 0.09 for PD98059 incubation ($P < 0.01$, both n=4); for 1 µM CCh, 1 minute control values (in grams) were 1.56 ± 0.12 versus 1.13 ± 0.08 ($P < 0.01$), 2 minute values were 1.36 ± 0.14 for control versus 1.01 ± 0.05 grams for PD98059 incubation ($P < 0.01$, both n=4); for 100 µM CCh, 1 minute control values (in grams) versus PD98059 incubation were 1.86 ± 0.13 versus 1.45 ± 0.11 ($P < 0.01$), 2 minute control values were 1.54 ± 0.12 versus 1.15 ± 0.09 for PD98059 incubation ($P < 0.01$, both n=4). Data summarized in Figure 27.

Area under curve for first two minutes

ERK1/2 inhibition caused a significant decrease in the area under the curve metric in the first (AUC 0-1), second (AUC 1-2),

and first two minutes (AUC 0-2) for contractions elicited by 1 µM and 100 µM CCh. AUC values for 10 nM CCh contractions were significantly reduced only for the AUC 0-1 min segment. For AUC 0-1 min, control versus PD98059 incubation values (in gram-seconds): for 10 nM CCh, 18.92 ± 4.19 versus 11.07 ± 2.25 ($P > 0.05$, n=4); for 1 µM CCh, 42.06 ± 8.11 versus 22.18 ± 4.70 ($P < 0.05$, n=6); for 100 µM CCh, 83.18 ± 14.69 versus 54.59 ± 10.46 ($P < 0.01$, n=9). For AUC 1-2 min, control versus PD98059 incubation values (in gram-seconds): for 10 nM CCh, 19.27 ± 4.56 versus 11.73 ± 2.78 ($P < 0.05$, n=4); for 1 µM CCh, 48.45 ± 10.45 versus 24.58 ± 3.25 ($P < 0.05$, n=7); for 100 µM CCh, 58.07 ± 10.41 versus 33.06 ± 7.19 ($P < 0.01$, n=9). For AUC 0-2 min, control versus PD98059 incubation values (in gram-seconds): for 10 nM CCh, 31.22 ± 9.69 versus 18.78 ± 5.57 ($P > 0.05$, n=7); for 1 µM CCh, 87.82 ± 17.61 versus 47.16 ± 6.56 ($P < 0.01$, n=7); for 100 µM CCh, 141.3 ± 23.86 versus 87.66 ± 16.69 ($P < 0.01$, n=9). Summary data for AUC values is presented in Figure 28.

Figure 25. Effect of ERK1/2 Inhibition on Basal Tone.

Administration of 10 µM PD98059 for 10 min resulted in no significant reduction of basal tone (0.79 ± 0.06 grams versus 0.81 ± 0.05 grams, n=12).

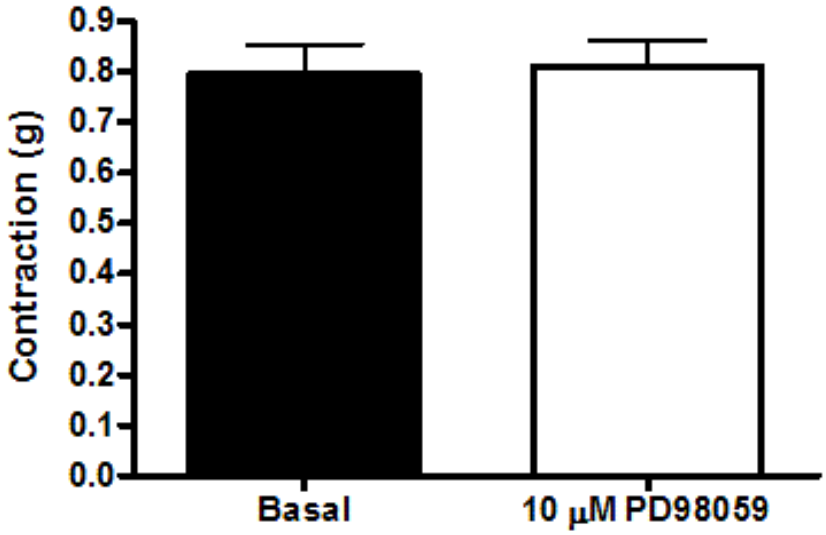
Contraction (g)
0.9
0.8
0.7
0.6
0.5
0.4
0.3
0.2
0.1
0.0
Basal
10 μM PD98059

Figure 26. Effect of ERK 1/2 Inhibition on Peak Contraction.

Top Panel: Summary data expressed as percentage of control. (* = P < 0.05)

Bottom Panel: ERK1/2 inhibition significantly reduced peak contraction elicited by 10 nM CCh (0.47 ± 0.13 versus 0.28 ± 0.08, n=6), 1 µM CCh (0.86 ± 0.13 versus 0.49 ± 0.09 grams, n=9) and by 100 µM CCh (2.06 ± 0.38 versus 1.40 ± 0.32 grams, n=9. (* = P < 0.05)

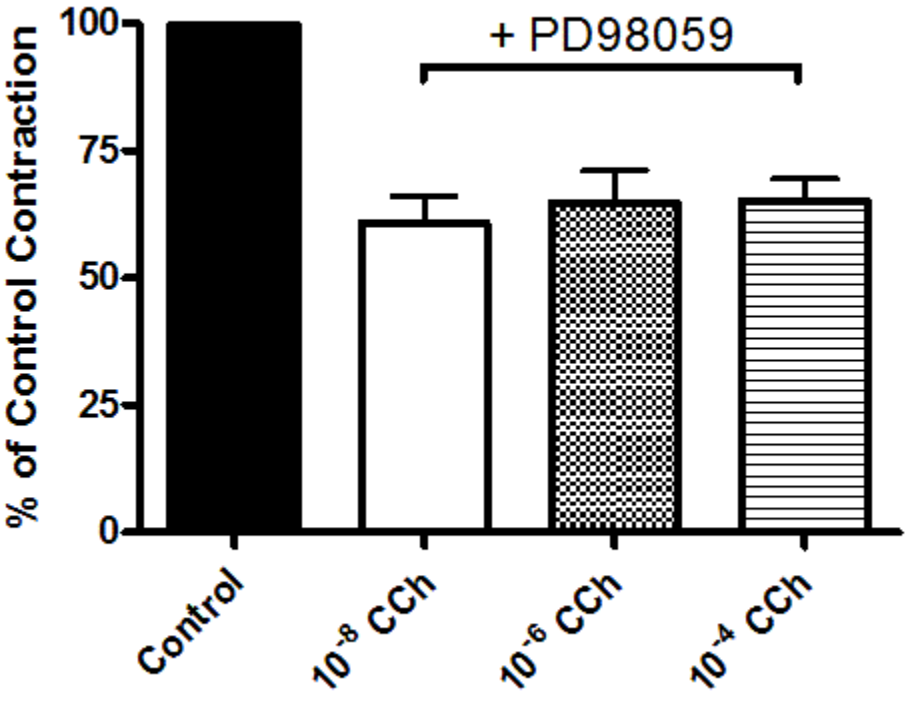
% of Control Contraction
100
75
50
25
0
+ PD98059
Control
10-8 CCh
10-6 CCh
10-4 CCh

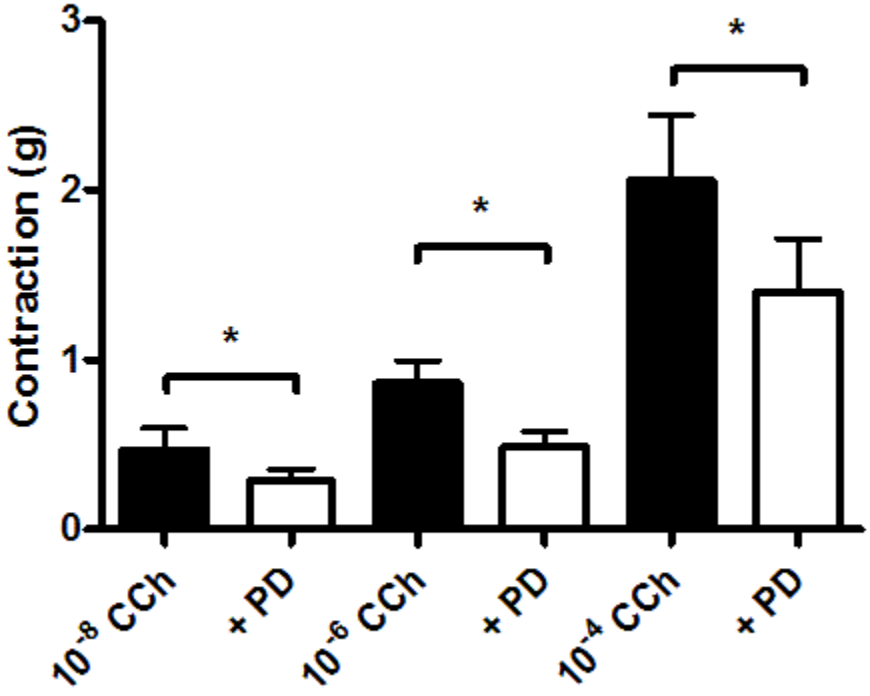
Contraction (g)
3
2
1
0
*
*
*
10-8 CCh
+ PD
10-6 CCh
+ PD
10-4 CCh
+ PD

Figure 27. Effect of ERK 1/2 Inhibition on contraction at 1 min and 2 min post CCh exposure.

Top Panel: Tone was reduced at t = 1 min and t = 2 min with ERK1/2 inhibition. n=4 for all sets. (* = $P < 0.05$)

Bottom Panel: t = 1 min and t = 2 min data expressed by percentage of control.

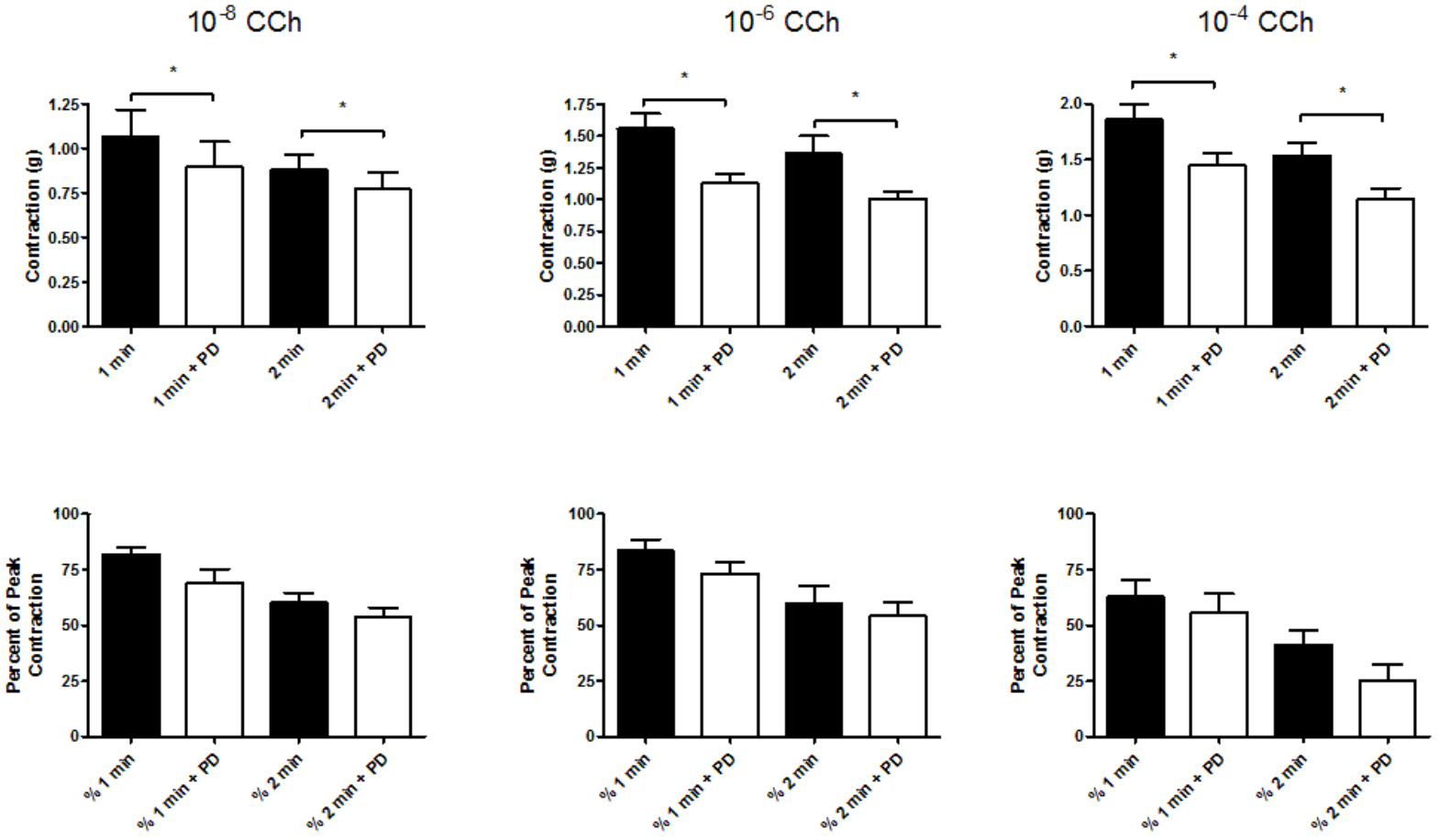
10-8 CCh
10-6 CCh
10-4 CCh
Contraction (g)
Percent of Peak Contraction
1 min
1 min + PD
2 min
2 min + PD
% 1 min
% 1 min + PD
% 2 min
% 2 min + PD
*

Figure 28. Effects of ERK1/2 Inhibition on AUC Values.

Top Panel: Raw data values of AUC 0-1 min, AUC 1-2 min, and AUC 0-2 min for CCh concentrations of 10 nM, 1 µM, and 100 µM. Sample sizes range from 4 to 9. (* indicates $P < 0.05$)

Bottom Panel: Data expressed as percentage of control.

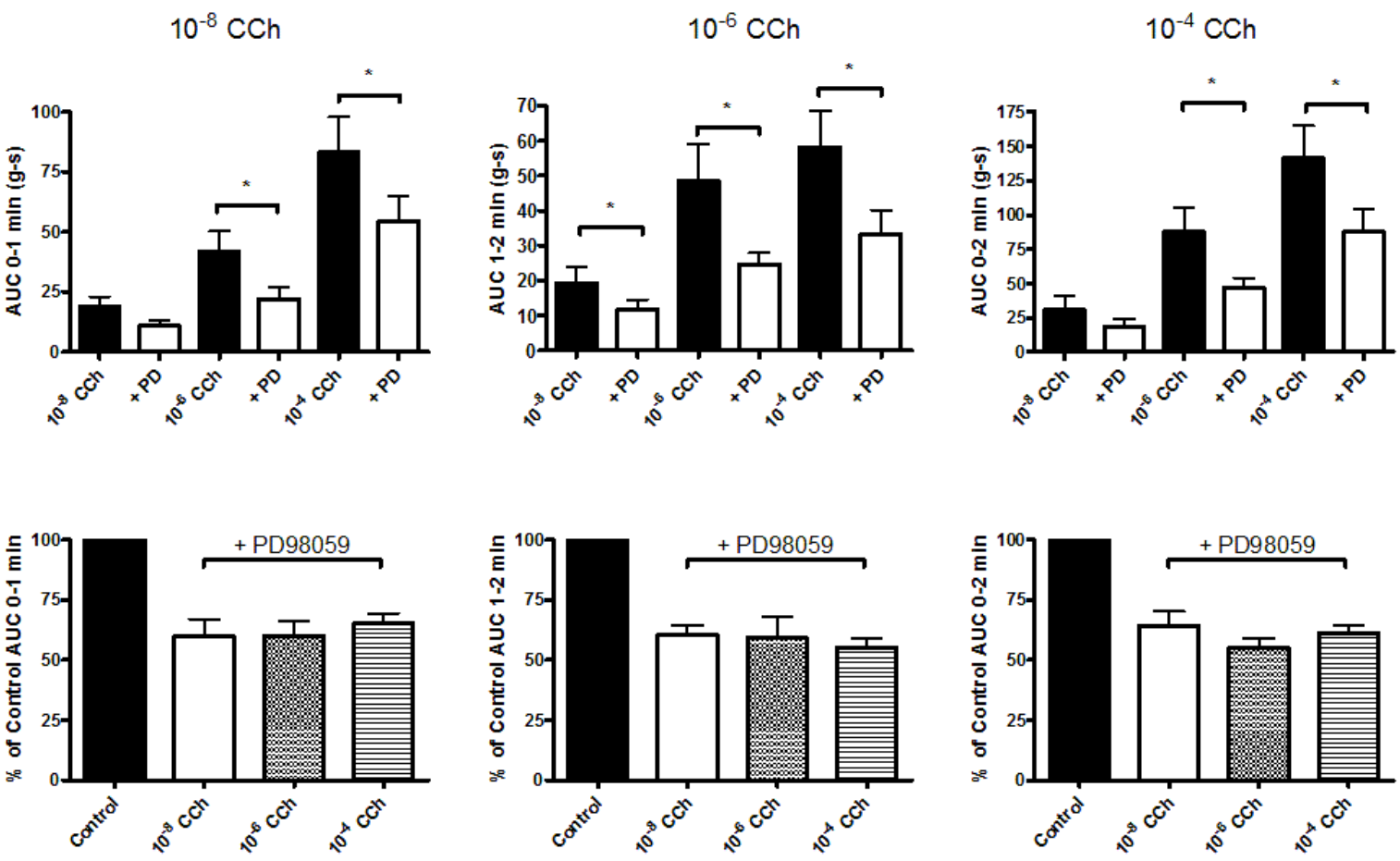
10-8 CCh
10-6 CCh
10-4 CCh
AUC 0-1 min (g-s)
AUC 1-2 min (g-s)
AUC 0-2 min (g-s)
10-8 CCh
+ PD
10-6 CCh
+ PD
10-4 CCh
+ PD
+ PD98059
% of Control AUC 0-1 min
% of Control AUC 1-2 min
% of Control AUC 0-2 min
Control
10-8 CCh
10-6 CCh
10-4 CCh

Combination Effects with Rho Kinase inhibition

ERK1/2 inhibitor PD98059 was used in concert with Rho Kinase inhibitor Y27632 to observe any additive effect. In 6 strips so tested, both 10 µM PD98059 alone and 10 µM PD98059 with 10 µM Y27632 significantly inhibited contraction elicited by 1 µM CCh: 1.17 ± 0.19 grams for Control, 0.96 ± 0.14 grams for PD98059 alone ($P < 0.05$), 0.85 ± 0.13 grams for both inhibitors ($P < 0.05$). However, there was no significant difference between the single inhibitor PD98059 and the use of both inhibitors simultaneously. These results are displayed in Figure 29.

Figure 29. Combination effects of ERK1/2 and Rho Kinase Inhibition on Amplitude.

10 µM PD98059 alone and with 10 µM Y27632 (Rho kinase inhibition) significantly reduced peak contraction as compared to control. Additive effects were not observed. (n=6, * indicates $P < 0.05$)

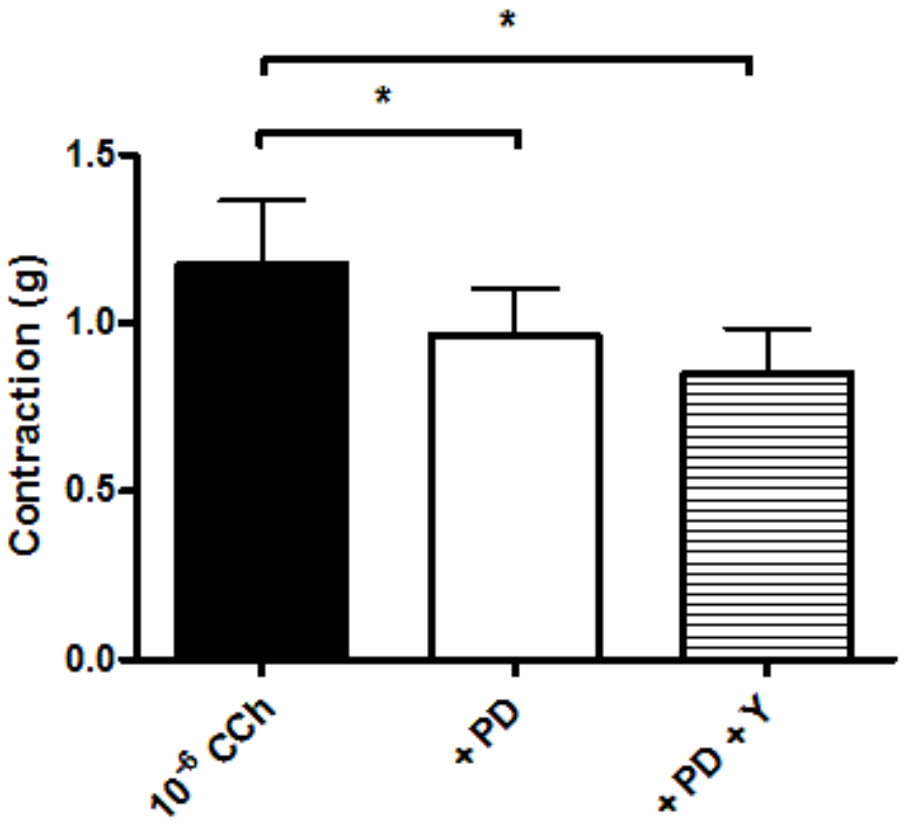
*
*
1.5
1.0
0.5
0.0
Contraction (g)
10-6 CCh
+PD
+PD+Y

MLCK activity

The effect of ERK1/2 inhibition on MLCK activity was measured using immunokinase assay. MLCK activity was measured in longitudinal muscle-myenteric plexus (LM-MP) strip homogenates of four groups: control, following 10 min incubation of 10 µM PD98059, 1 min post 1 µM CCh exposure, and 1 min post 1 µM CCh exposure following 10 min incubation with 10 µM PD98059. 1 µM CCh increased MLCK activity to 167% ± 21% of control activity ($P < 0.05$ versus control, $n = 12$). Incubation for 10 min with PD98059 lead to CCh-induced activity that was 119% ± 21% of control activity ($P > 0.05$, $n = 8$). Incubation of PD98059 alone did not differ MLCK from control ($n = 12$ for control, $n = 4$ for PD98059 alone). CCh-induced activity was not significantly varied between strips with and without ERK1/2 inhibition ($n = 12$ for CCh, $n = 8$ for CCh with ERK1/2 incubation). Results are shown in Figure 30.

Figure 30. Effect of ERK1/2 Inhibition on CCh-evoked MLCK activity.

1 µM CCh-induced MLCK activities with and without ERK1/2 inhibition are presented. Values expressed as percentage ± SEM of control MLCK activity. Control, n = 12. CCh-induced activity is 167% ± 21% of control ($P < 0.05$, n = 12). CCh-induced activity in the presence of 10 µM PD98059 was 122% ± 11% of control ($P > 0.05$, n = 8).

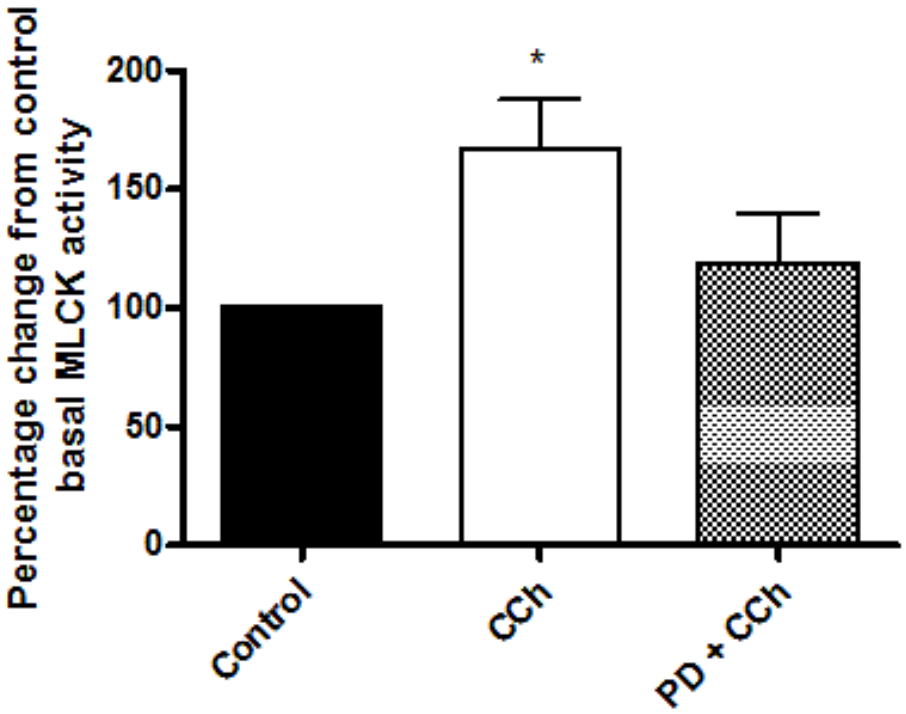
Percentage change from control basal MLCK activity
200
150
100
50
0
*
Control
CCh
PD + CCh

Effects of CaMKK/AMPK Inhibition (STO-609)

Incubation of strips for 15 minutes in 10 µM STO-609 (a CaMKK/AMPK inhibitor) allows for comparison of CaMKK/AMPK inhibited contractions to control conditions. CaMKK/AMPK inhibition was viewed from the contractile perspective in basal tone regulation, peak contraction, contraction at one and two minutes post CCh exposure, and area under the curve values. The effect of CaMKK/AMPK inhibition on MLCK activity was studied via molecular methods.

Basal Activity

CaMKK/AMPK inhibition led to no significant change in basal tone after 10 minutes of incubation. In strips so studied (n=7), administration of STO-609 (CaMKK/AMPK inhibition) resulted in a change of basal tone from 0.76 ± 0.10 grams to 0.74 ± 0.10 grams. A conducted paired t-test returned $P > 0.05$; the inhibition of CaMKK/AMPK has no effect upon basal tone. Data summarized and displayed in Figure 31.

Peak Contraction due to carbachol

CaMKK/AMPK inhibition (via STO-609 incubation) significantly reduced contraction for carbachol concentrations of 1 µM and 100 µM. Control peak contraction values (in grams) versus contractions following STO-609 incubation are 0.51 ± 0.16 versus 0.32 ± 0.14 ($P > 0.05$, n=6) at 10 nM CCh; 1.31 ± 0.20 versus 0.81 ± 0.15 ($P < 0.01$, n=23) for 1 µM CCh; and 1.96 ± 0.37 versus 1.22 ± 0.20 ($P < 0.05$, n=16) for 100 µM CCh. Summary data are displayed in Figure 32.

Contraction at 1 min and 2 min minutes post exposure

CaMKK/AMPK inhibition significant reduced the contraction at both 1 min and 2 min post CCh exposure for CCh concentrations of 10 nM and 1 µM. With 10 nM CCh, 1 minute control values (in grams) versus STO-609 incubation were 1.18 ± 0.16 versus 0.86 ± 0.09 ($P < 0.05$), 2 minute values were 1.15 ± 0.17 for control versus 0.86 ± 0.10 for STO-609 incubation ($P < 0.05$, both n=4); for 1 µM CCh, 1 minute control values (in grams) were 1.54 ± 0.19 versus 1.29 ± 0.18 ($P < 0.01$), 2 minute values were 1.37 ± 0.18 for control versus 1.17 ± 0.16 grams for STO-609 incubation ($P < 0.05$, both n=16); for 100 µM CCh, 1 minute control values (in grams) versus STO-609 incubation were 1.63 ± 0.23 versus 1.33 ± 0.29 ($P > 0.05$), 2 minute control values were 1.31 ± 0.25

versus 0.98 ± 0.19 for STO-609 incubation ($P > 0.06$, both n=6). Data summarized in Figure 33.

Area under curve for first two minutes

CaMKK/AMPK inhibition caused a significant decrease in the area under the curve metric in the first (AUC 0-1), second (AUC 1-2), and first two minutes (AUC 0-2) for all CCh contractions. AUC values for 10 nM CCh contractions were not significantly reduced. For AUC 0-1 min, control versus STO-609 incubation values (in gram-seconds): for 10 nM CCh, 28.99 ± 3.03 versus 15.23 ± 1.59 ($P < 0.01$, n=5); for 1 µM CCh, 52.88 ± 10.26 versus 38.36 ± 7.19 ($P < 0.01$, n=13); for 100 µM CCh, 91.68 ± 20.41 versus 48.86 ± 8.78 ($P < 0.05$, n=9). For AUC 1-2 min, control versus STO-609 incubation values (in gram-seconds): for 10 nM CCh, 33.5 ± 5.57 versus 22.39 ± 3.58 ($P < 0.05$, n=4); for 1 µM CCh, 52.06 ± 10.40 versus 35.00 ± 5.54 ($P < 0.05$, n=17); for 100 µM CCh, 56.69 ± 13.85 versus 36.90 ± 6.71 ($P < 0.05$, n=9). For AUC 0-2 min, control versus STO-609 incubation values (in gram-seconds): for 10 nM CCh, 62.64 ± 5.40 versus 40.46 ± 4.61 ($P < 0.01$, n=7); for 1 µM CCh, 85.42 ± 13.77 versus 54.67 ± 7.92 ($P < 0.01$, n=15); for 100 µM CCh, 114.6 ± 16.23 versus 81.29 ± 13.01 ($P < 0.01$, n=9). Summary data for AUC values is presented in Figure 34.

Figure 31. Effect of CaMKK/AMPK inhibition on basal tone.

Administration of 10 μM STO-609 for 10 min resulted in no significant reduction of basal tone (0.76 ± 0.10 grams versus 0.71 ± 0.10 grams, n=7).

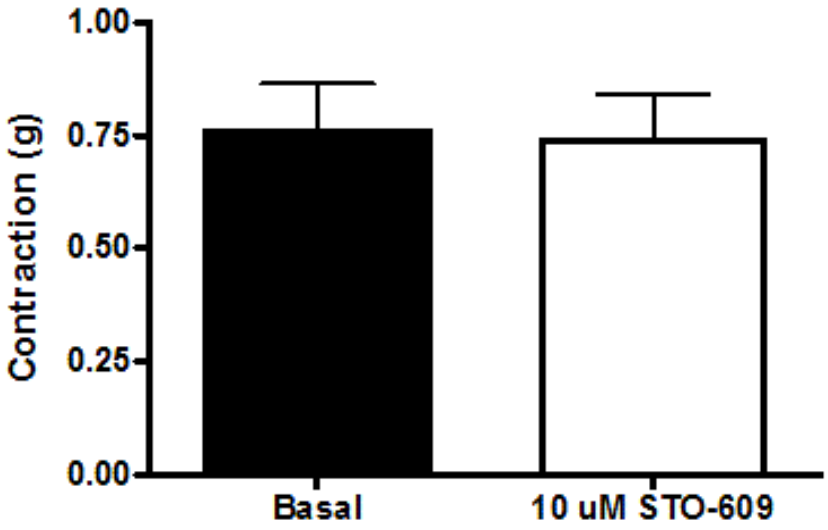
1.00
0.75
0.50
0.25
0.00
Contraction (g)
Basal
10 uM STO-609

Figure 32. Effect of CaMKK/AMPK inhibtion on peak contraction.

Top Panel: CaMKK/AMPK inhibition significantly reduced peak contraction elicited by 1 µM CCh (1.31 ± 0.20 versus 0.81 ± 0.15 grams, n=9) and by 100 µM CCh (1.96 ± 0.37 versus 1.22 ± 0.20 grams, n=9. (* = $P < 0.05$)

Bottom Panel: Summary data expressed as percentage of control. (* = $P < 0.05$)

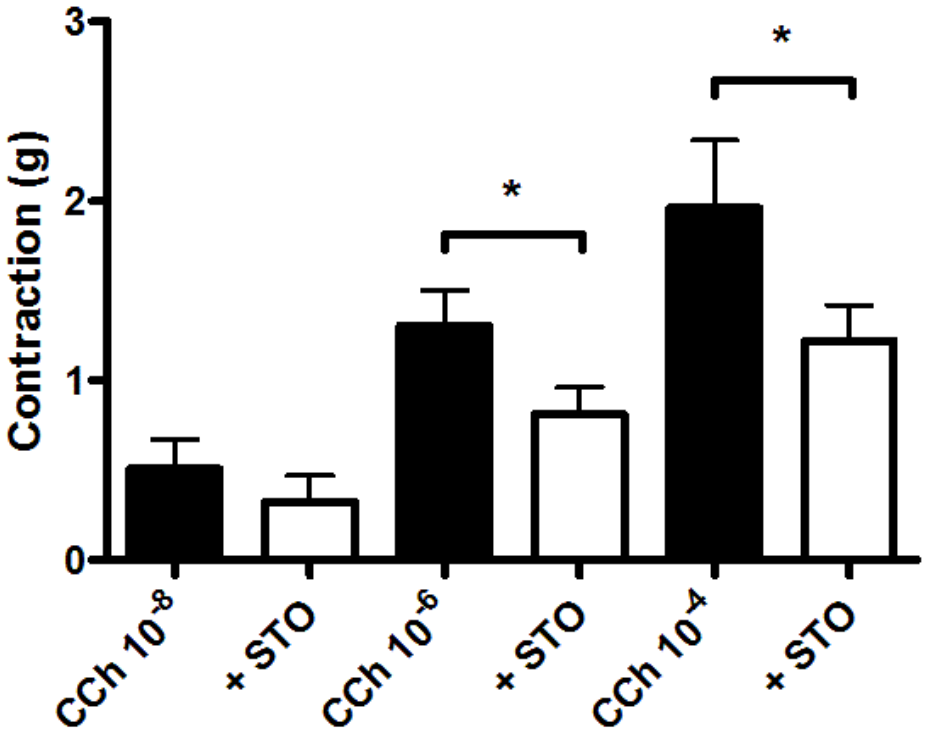
Contraction (g)
3
2
1
0
*
*
CCh 10-8
+ STO
CCh 10-6
+ STO
CCh 10-4
+ STO

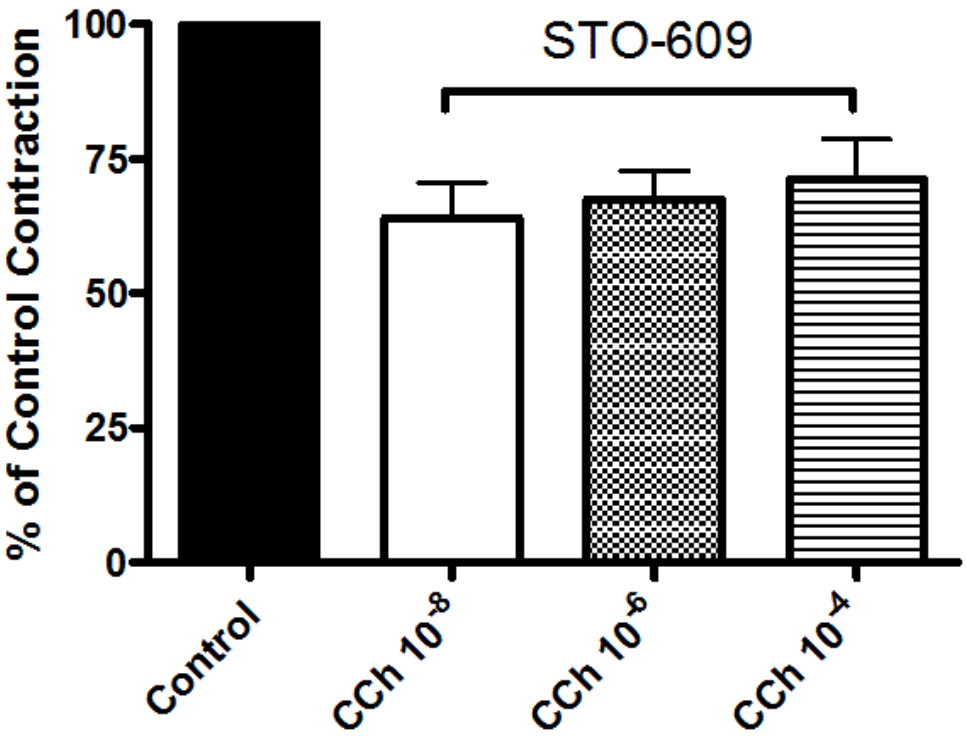
% of Control Contraction
100
75
50
25
0
STO-609
Control
CCh 10-8
CCh 10-6
CCh 10-4

Figure 33. Effect of CaMKK/AMPK inhibition on contractions at 1 min and 2 min post CCh exposure.

Top Panel: Tone was reduced at t = 1 min and t = 2 min with Rho kinase inhibition. Sample Sizes range from 4 to 16. (* = $P < 0.05$)

Bottom Panel: t = 1 min and t = 2 min data expressed by percentage of control.

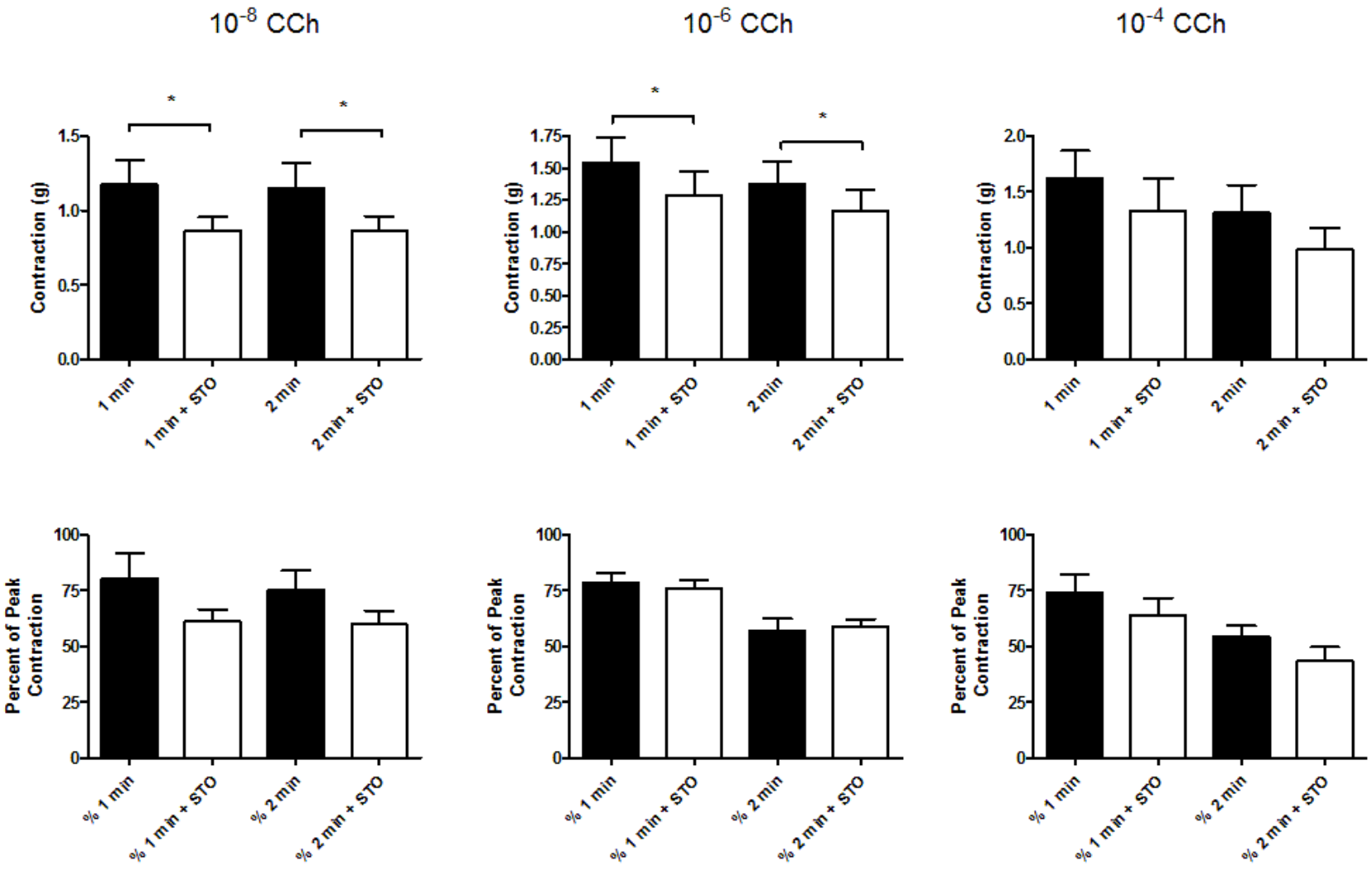
10-8 CCh
10-6 CCh
10-4 CCh
Contraction (g)
Percent of Peak Contraction
1 min
1 min + STO
2 min
2 min + STO
% 1 min
% 1 min + STO
% 2 min
% 2 min + STO
*

Figure 34. Effects of CaMKK/AMPK Inhibition on AUC values.

Top Panel: Raw data values of AUC 0-1 min, AUC 1-2 min, and AUC 0-2 min for CCh concentrations of 10 nM, 1 µM, and 100 µM. Sample sizes range from 5 to 16. (* indicates $P < 0.05$)

Bottom Panel: Data expressed as percentage of control.

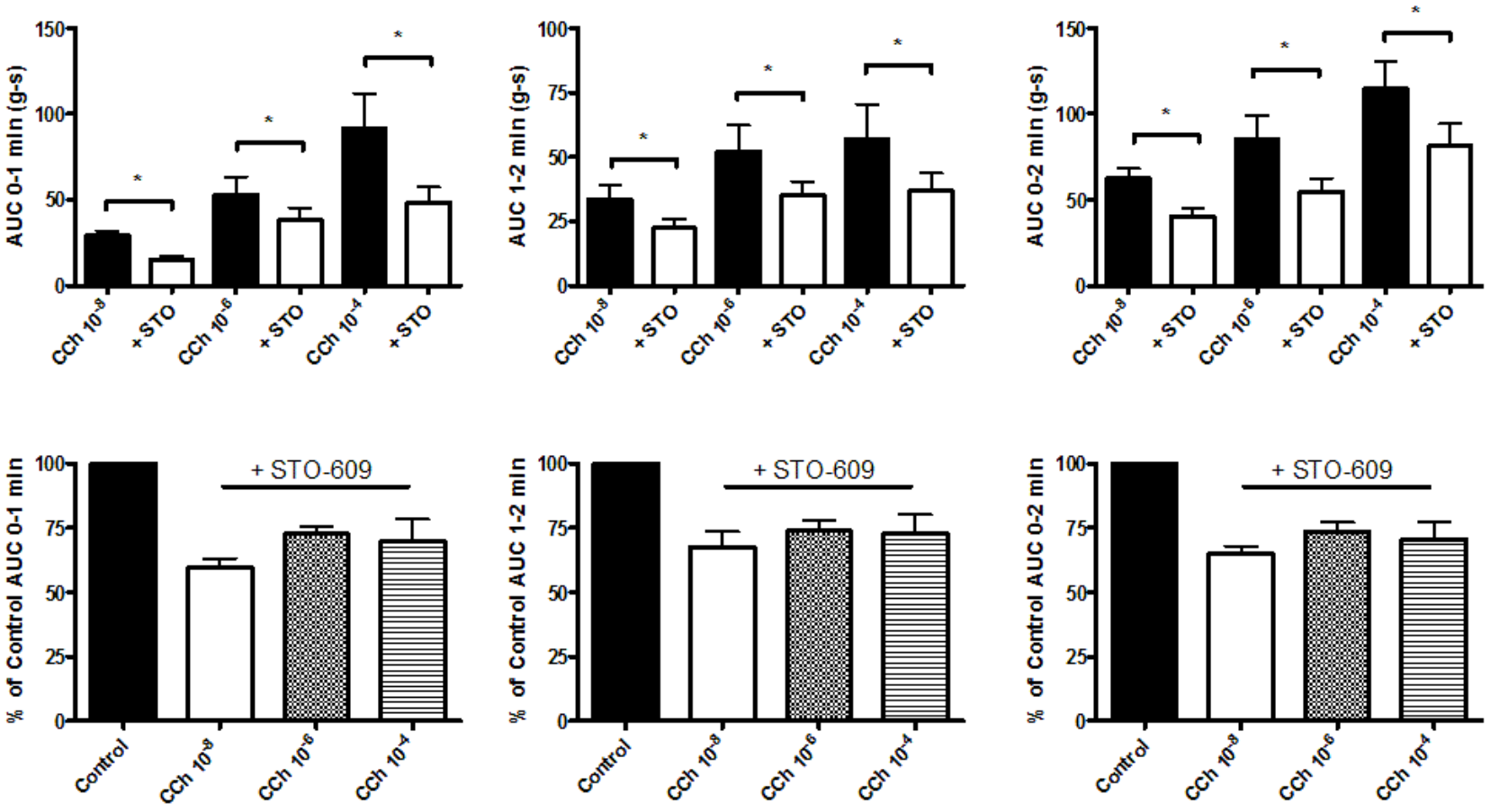
AUC 0-1 min (g-s)
AUC 1-2 min (g-s)
AUC 0-2 min (g-s)
CCh 10-8
+ STO
CCh 10-6
+ STO
CCh 10-4
+ STO
% of Control AUC 0-1 min
% of Control AUC 1-2 min
% of Control AUC 0-2 min
+ STO-609
Control
CCh 10-8
CCh 10-6
CCh 10-4

Combination Effects with Rho Kinase inhibition

CaMKK/AMPK inhibitor STO-609 was used in concert with Rho Kinase inhibitor Y27632 to observe any additive effect. In 7 strips so tested, both 10 µM STO-609 alone and 10 µM STO-609 with 10 µM Y27632 significantly inhibited peak contraction elicited by 1 µM CCh: 1.57 ± 0.32 grams for Control, 1.31 ± 0.24 grams for STO-609 alone ($P < 0.05$), 0.89 ± 0.18 grams for both inhibitors ($P < 0.01$). In addition, the contraction elicited by 1 µM CCh in the presence of both inhibitors was significantly lower than with STO-609 alone ($P < 0.05$). There is a significant additive effect of CaMKK/AMPK inhibition and Rho Kinase inhibition on peak contraction.

A similar additive effect was seen on AUC values 0-1 min and 0-2 min. For the 0-1 min AUC metric, control values (in gram-seconds) were 66.84 ± 14.99 versus 52.24 ± 10.47 for STO-609 alone ($P < 0.05$, n=7) and 28.17 ± 4.31 for both inhibitors. The value in the presence of both inhibitors was significantly less than with STO-609 alone ($P < 0.05$, n=7). For the 0-2 min AUC metric, control values (in gram-seconds) were 142.6 ± 131.86 versus 122.4 ± 26.22 for STO-609 alone ($P < 0.05$, n=7) and 68.36 ± 9.72 for both inhibitors ($P < 0.05$, n=7). The value in the presence of both inhibitors was significantly less than with STO-609 alone ($P < 0.05$, n=7). These results are visualized in Figure 35.

Figure 35. Combined Effects of CaMKK/AMPK and Rho Kinase Inhibition.

Top Panel: Effects of CaMKK/AMPK inhibition with Rho kinase inhibition on peak contraction are additive. (n=7, * indicates $P < 0.05$).

Middle Panel: Effects of CaMKK/AMPK inhibition with Rho kinase inhibition on AUC 0-1 min are additive. (n=7, * indicates $P < 0.05$).

Bottom Panel: Effects of CaMKK/AMPK inhibition with Rho kinase inhibition on AUC 0-2 min are additive. (n=7, * indicates $P < 0.05$).

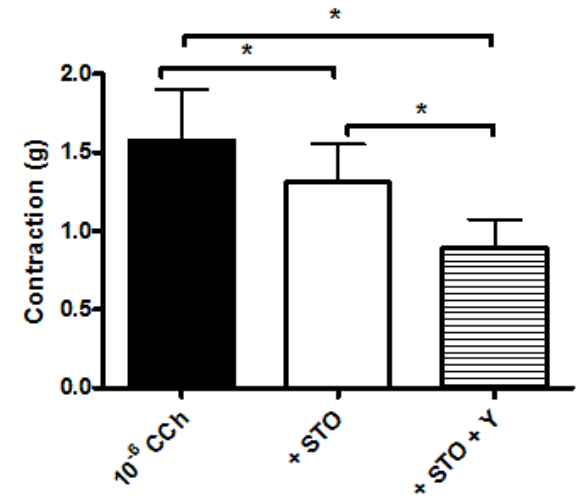
*
*
*
2.0
1.5
1.0
0.5
0.0
Contraction (g)
10-6 CCh
+ STO
+ STO + Y

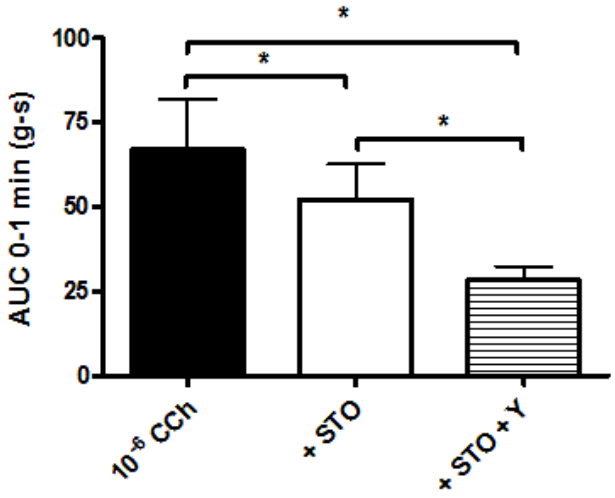
*
*
*
100
75
50
25
0
AUC 0-1 min (g-s)
10-6 CCh
+ STO
+ STO + Y

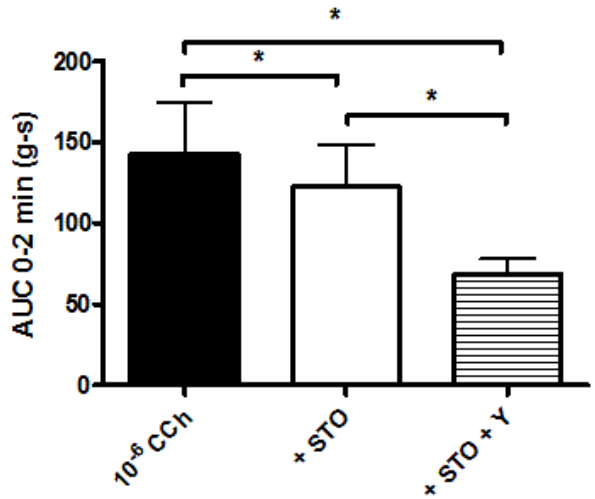
*
*
*
200
150
100
50
0
AUC 0-2 min (g-s)
10-6 CCh
+ STO
+ STO + Y

MLCK activity

The effect of CaMKK/AMPK inhibition on MLCK activity was measured using immunokinase assay. MLCK activity was measured in longitudinal muscle-myenteric plexus (LM-MP) strip homogenates of four groups: control, following 10 min incubation of 10 µM STO-609, 1 min post 1 µM CCh exposure, and 1 min post 1 µM CCh exposure following 10 min incubation with 10 µM STO-609. 1 µM CCh increased MLCK activity to 167% ± 21% of control activity ($P < 0.05$ versus control, $n = 12$). Incubation for 10 min with STO-609 reduced CCh-induced activity to 146% ± 19% of control activity ($P < 0.05$ versus control, $n = 8$). Incubation of STO-609 alone did not differ MLCK from control ($n = 12$ for control, $n = 4$ for STO-609 alone). CCh-induced activity was not significantly varied between strips with and without CaMKK/AMPK inhibition ($n = 12$ for CCh, $n = 8$ for CCh with STO-609 incubation). Results are shown in Figure 36.

Figure 36. Effect of CaMKK/AMPK inhibition on CCh-evoked MLCK activity.

1 µM CCh-induced MLCK activities with and without CaMKK/AMPK inhibition are presented. Values expressed as percentage ± SEM of control MLCK activity. Control, n = 12. CCh-induced activity is 167% ± 21% of control ($P < 0.05$, n = 12). CCh activity in the presence of 10 µM STO-609 reduces CCh-induced activity to 146% ± 19% of control ($P < 0.05$, n = 8).

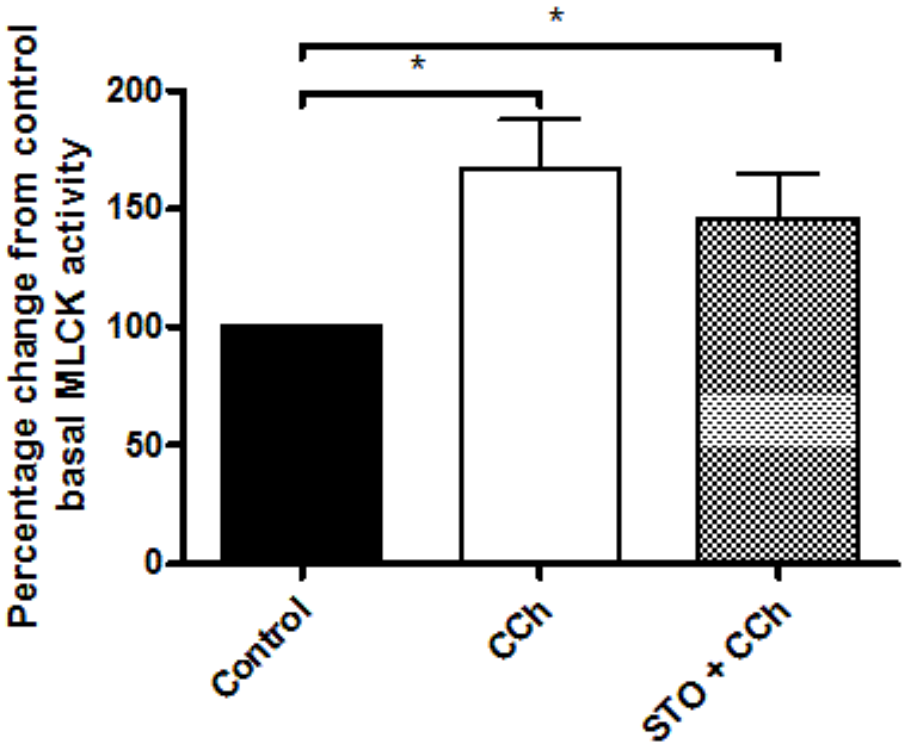
Percentage change from control basal MLCK activity
200
150
100
50
0
*
*
Control
CCh
STO + CCh

Effects of CaMKII Inhibition (KN62)

Incubation of strips for 15 minutes in 10 µM KN62 (a CaMKII inhibitor) allows for comparison of CaMKII inhibited contractions to control conditions. CaMKII inhibition was viewed from the contractile perspective of basal tone regulation, peak contraction, contraction at one and two minutes post CCh exposure, and area under the curve values. Additive effects of CaMKII inhibition with Rho Kinase inhibition were tested. The effect of CaMKII inhibition on MLCK activity was studied via molecular methods.

Basal Activity

CaMKII inhibition led to a significant decrease in basal tone after 10 minutes of incubation. In studied strips (n=8), administration of KN62 (CaMKII inhibition) resulted in a change of basal tone from 0.61 ± 0.07 grams to 0.53 ± 0.07 grams. A conducted paired t-test returned $P < 0.05$; the inhibition of CaMKII reduces basal tone. Data summarized and displayed in Figure 37.

Peak Contraction due to carbachol

CaMKII inhibition (via KN62 incubation) significantly reduced contraction for all concentrations of carbachol. Control peak contraction values (in grams) versus contractions following KN62

incubation are 0.52 ± 0.14 versus 0.34 ± 0.12 ($P < 0.05$, n=7) at 10 nM CCh; 0.74 ± 0.10 versus 0.46 ± 0.05 ($P < 0.01$, n=13) for 1 µM CCh; and 1.35 ± 0.32 versus 0.64 ± 0.15 ($P < 0.05$, n=7) at 100 µM CCh. Summary data are displayed in Figure 38.

Contraction at 1 min and 2 min minutes post exposure

CaMKII inhibition reduced the contraction at both 1 min and 2 min post CCh exposure for all concentrations of CCh. With 10 nM CCh, 1 minute control values (in grams) versus KN62 incubation were 0.71 ± 0.07 versus 0.52 ± 0.06 ($P < 0.05$), 2 minute values were 0.67 ± 0.07 for control versus 0.51 ± 0.07 for KN62 incubation ($P < 0.05$, both n=4); for 1 µM CCh, 1 minute control values (in grams) were 1.28 ± 0.10 versus 0.99 ± 0.11 ($P < 0.01$), 2 minute values were 1.15 ± 0.1 for control versus 0.94 ± 0.10 grams for KN62 incubation ($P < 0.05$, both n=11); for 100 µM CCh, 1 minute control values (in grams) versus KN62 incubation were 1.33 ± 0.18 versus 0.81 ± 0.08 ($P < 0.05$, n=5), 2 minute control values were 1.11 ± 0.16 versus 0.74 ± 0.08 for KN62 incubation ($P < 0.05$, n=4). Data summarized in Figure 39.

Area under curve for first two minutes

CaMKII inhibition caused a significant decrease in the area under the curve metric in the first (AUC 0-1), second (AUC 1-2), and first two minutes (AUC 0-2) for contractions elicited by 1 µM and 100 µM CCh. AUC data for 10 nM CCh contractions were significantly reduced only for the AUC 0-1 min measurement. For AUC 0-1 min, control versus KN62 incubation values (in gram-seconds): for 10 nM CCh, 8.59 ± 2.46 versus 5.48 ± 1.44 ($P < 0.05$, n=5); for 1 µM CCh, 36.98 ± 6.03 versus 20.89 ± 2.89 ($P < 0.05$, n=11); for 100 µM CCh, 58.47 ± 14.21 versus 33.00 ± 7.09 ($P < 0.05$, n=7). For AUC 1-2 min, control versus KN62 incubation values (in gram-seconds): for 10 nM CCh, 11.20 ± 4.73 versus 7.68 ± 3.45 ($P > 0.05$, n=5); for 1 µM CCh, 36.24 ± 5.62 versus 23.69 ± 3.6 ($P < 0.01$, n=11); for 100 µM CCh, 46.24 ± 4.25 versus 34.84 ± 3.33 ($P < 0.05$, n=7). For AUC 0-2 min, control versus KN62 incubation values (in gram-seconds): for 10 nM CCh, 22.13 ± 10.10 versus 16.14 ± 7.43 ($P > 0.05$, n=4); for 1 µM CCh, 69.38 ± 11.85 versus 42.11 ± 5.99 ($P < 0.05$, n=12); for 100 µM CCh, 100.7 ± 18.58 versus 63.46 ± 10.27 ($P < 0.05$, n=5). Summary data for AUC values is presented in Figure 40.

Figure 37. Effect of CaMKII inhibition on basal tone.

Administration of 10 μM KN62 for 10 min resulted in significant reduction of basal tone from 0.61 ± 0.07 grams to 0.53 ± 0.07 grams ($P < 0.05$, n=6). * = $P < 0.05$

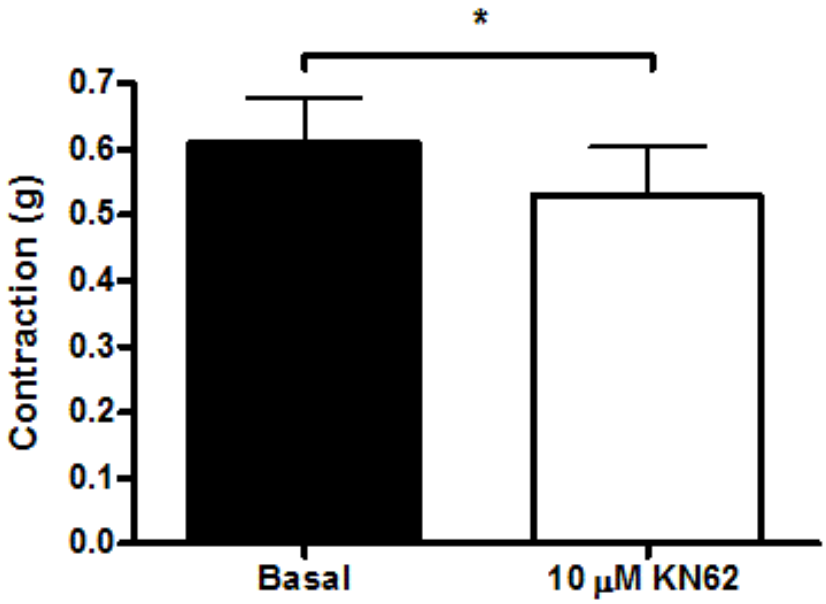
*
0.7
0.6
0.5
0.4
0.3
0.2
0.1
0.0
Contraction (g)
Basal
10 μM KN62

Figure 38. Effect of CaMKII inhibition on peak contraction.

Top Panel: CaMKII inhibition significantly reduced peak contraction elicited by 10 nM CCh (0.52 ± 0.14 versus 0.34 ± 0.12, n=7), 1 µM CCh (0.74 ± 0.10 versus 0.46 ± 0.05 grams, n=13) and by 100 µM CCh (1.35 ± 0.32 versus 0.64 ± 0.15 grams, n=7. (* = $P < 0.05$)

Bottom Panel: Summary data expressed as percentage of control. (* = $P < 0.05$)

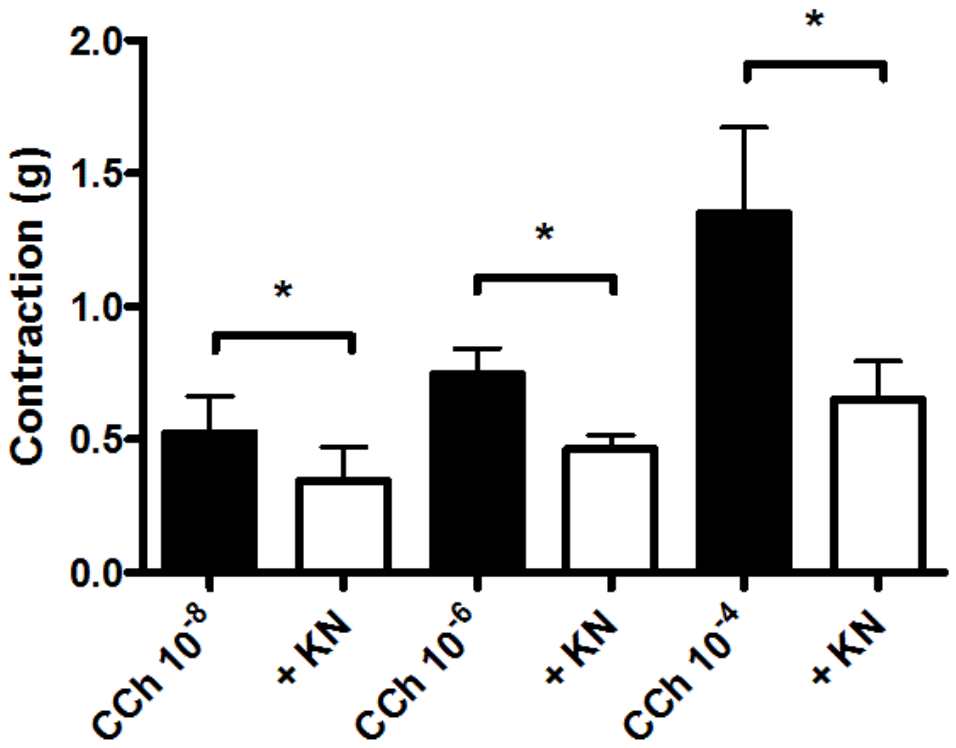
Contraction (g)
2.0
1.5
1.0
0.5
0.0
*
*
*
CCh 10-8
+ KN
CCh 10-6
+ KN
CCh 10-4
+ KN

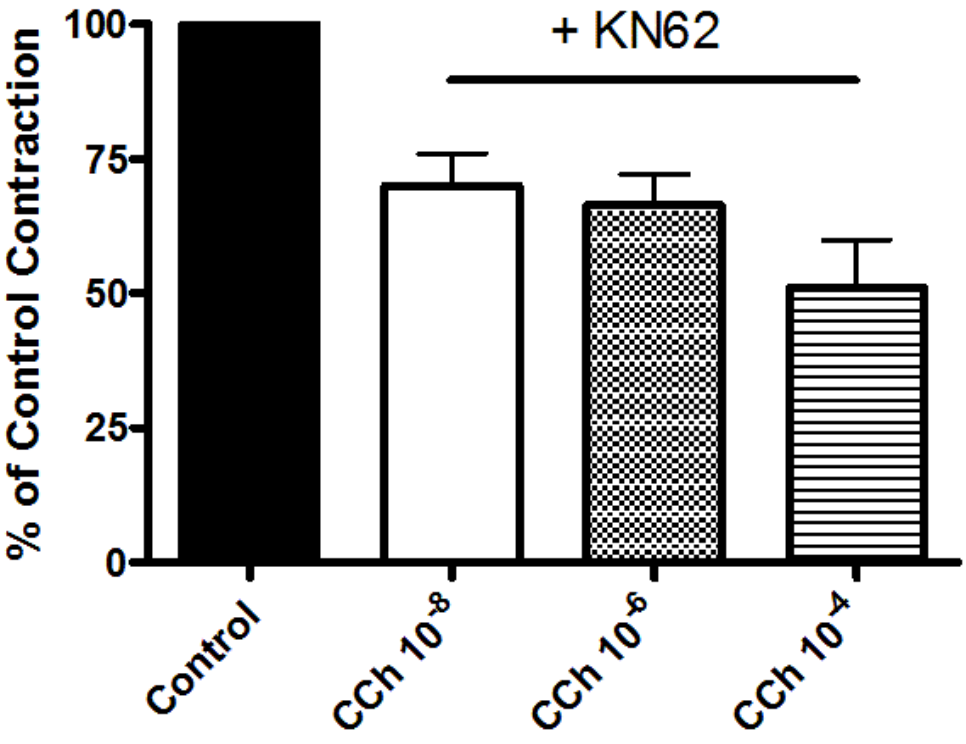
% of Control Contraction
100
75
50
25
0
+ KN62
Control
CCh 10-8
CCh 10-6
CCh 10-4

Figure 39. Effect of CaMKII inhibition on contractions at 1 min and 2 min post CCh exposure.

Top Panel: Tone was reduced at t = 1 min and t = 2 min with Rho kinase inhibition. Sample Sizes range from 4 to 11. (* = $P < 0.05$)

Bottom Panel: t = 1 min and t = 2 min data expressed by percentage of control.

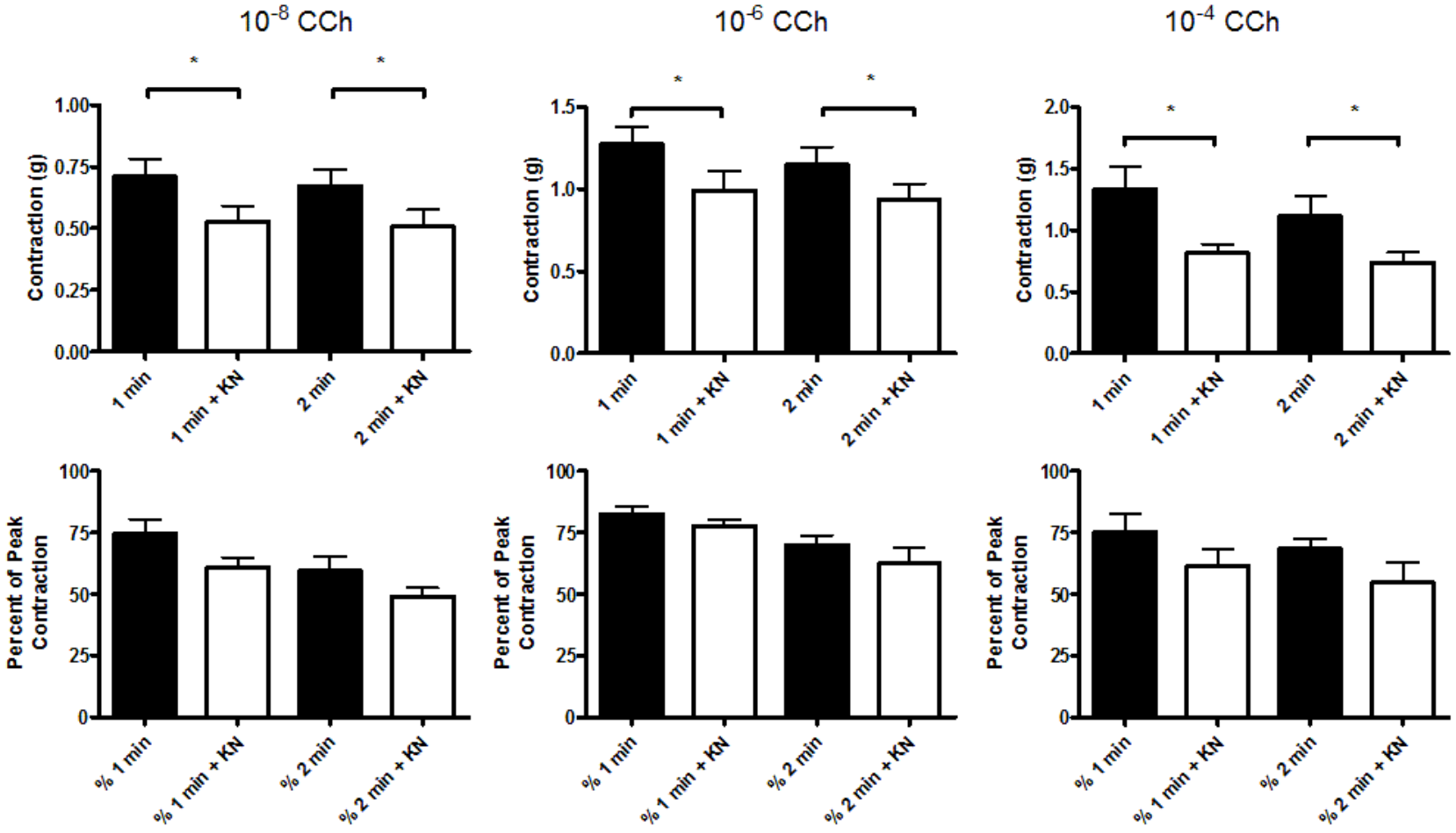
10-8 CCh
10-6 CCh
10-4 CCh
Contraction (g)
Percent of Peak Contraction
1 min
1 min + KN
2 min
2 min + KN
% 1 min
% 1 min + KN
% 2 min
% 2 min + KN
*

Figure 40. Effect of CaMKII inhibition on AUC values.

Top Panel: Raw data values of AUC 0-1 min, AUC 1-2 min, and AUC 0-2 min for CCh concentrations of 10 nM, 1 µM, and 100 µM. Sample sizes range from 5 to 16. (* indicates $P < 0.05$)

Bottom Panel: Data expressed as percentage of control.

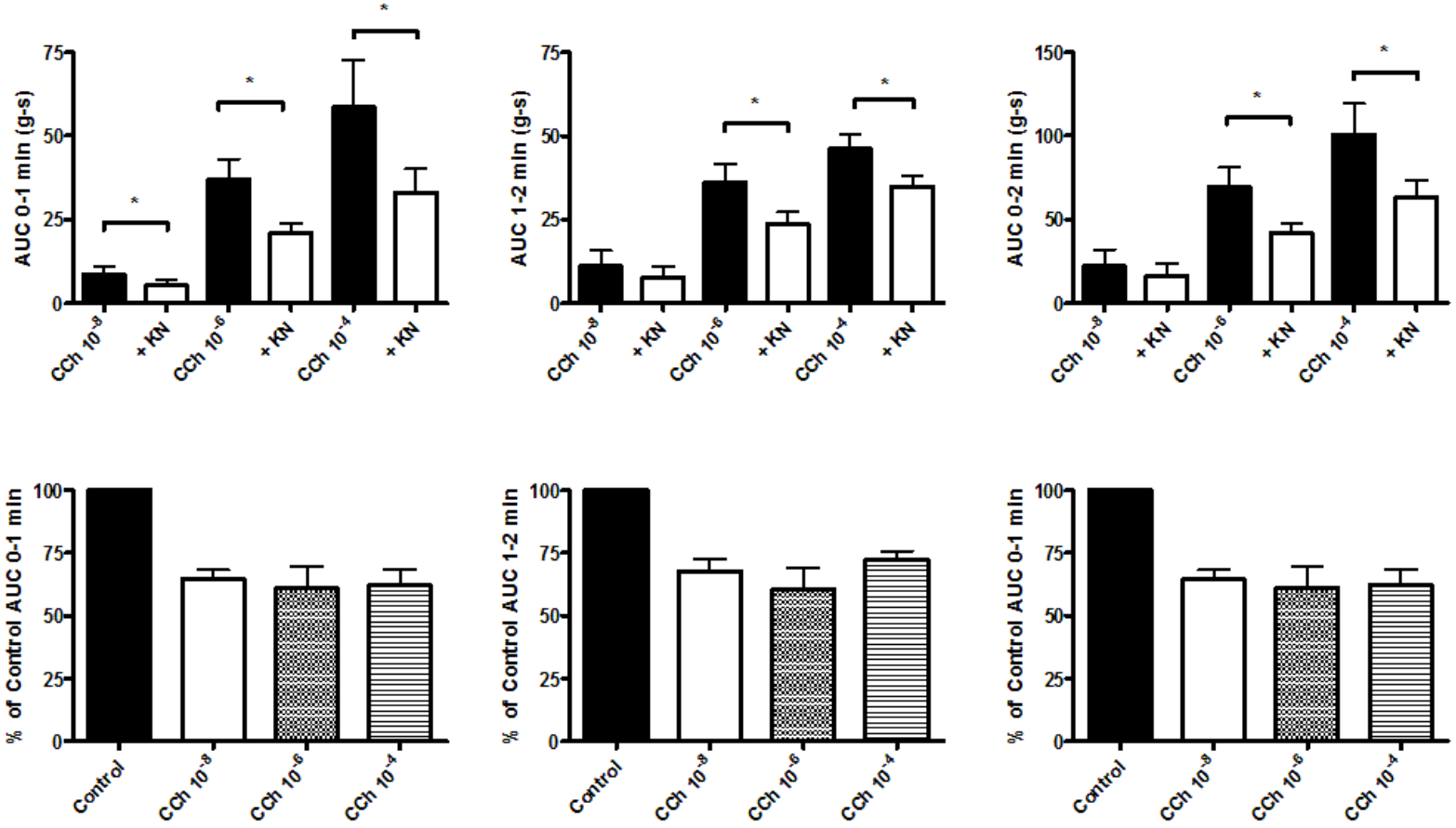
AUC 0-1 min (g-s)
AUC 1-2 min (g-s)
AUC 0-2 min (g-s)
CCh 10-8
+ KN
CCh 10-6
+ KN
CCh 10-4
+ KN
% of Control AUC 0-1 min
% of Control AUC 1-2 min
% of Control AUC 0-1 min
Control
CCh 10-8
CCh 10-6
CCh 10-4

Combination Effects with Rho Kinase inhibition

CaMKII inhibitor KN62 was used in concert with Rho Kinase inhibitor Y27632 to observe any additive effect. In 8 strips so tested, both 10 µM KN62 alone and 10 µM KN62 with 10 µM Y27632 significantly inhibited peak contraction elicited by 1 µM CCh: 0.92 ± 0.09 grams for Control, 0.60 ± 0.05 grams for KN62 alone ($P < 0.05$), 0.36 ± 0.06 grams for both inhibitors ($P < 0.05$). In addition, the contraction elicited by 1 µM CCh in the presence of both inhibitors was significantly lower than with KN62 alone ($P < 0.05$). There is a significant additive effect of CaMKII inhibition and Rho Kinase inhibition on peak contraction.

A similar additive effect was seen on AUC values 0-1 min and 0-2 min. For the 0-1 min AUC metric, control values (in gram-seconds) were 39.64 ± 5.21 versus 24.52 ± 2.67 for KN62 alone ($P < 0.05$, n=8) and 11.47 ± 2.89 for both inhibitors. The value in the presence of both inhibitors was significantly less than with KN62 alone ($P < 0.05$, n=8). For the 0-2 min AUC metric, control values (in gram-seconds) were 80.97 ± 11.84 versus 51.43 ± 4.00 for KN62 alone ($P < 0.05$, n=8) and 34.70 ± 3.18 for both inhibitors ($P < 0.05$, n=8). The value in the presence of both inhibitors was significantly less than with KN62 alone ($P < 0.05$, n=7). These results are summarized in Figure 41.

Figure 41. Combined Effects of CaMKII and Rho Kinase inhibition.

Top Panel: Effects of CaMKII inhibition with Rho kinase inhibition on peak contraction are additive. (n=8, * indicates $P < 0.05$).

Middle Panel: Effects of CaMKII inhibition with Rho kinase inhibition on AUC 0-1 min are additive. (n=8, * indicates $P < 0.05$).

Bottom Panel: Effects of CaMKII inhibition with Rho kinase inhibition on AUC 0-2 min are additive. (n=8, * indicates $P < 0.05$).

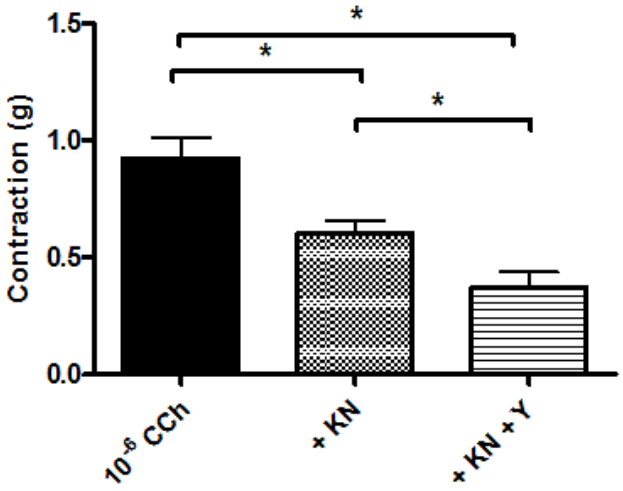
Contraction (g)
1.5
1.0
0.5
0.0
*
*
*
10-6 CCh
+ KN
+ KN + Y

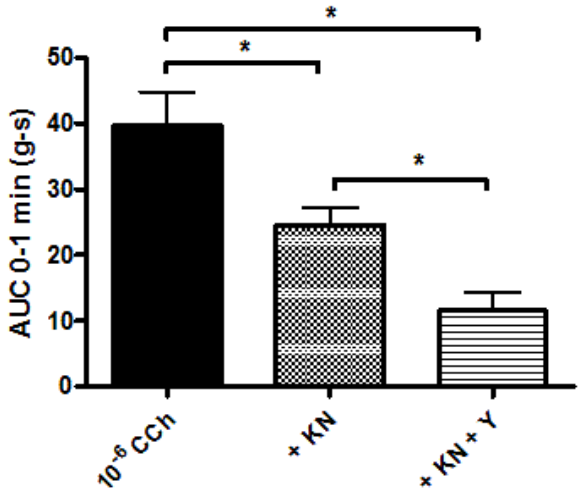
AUC 0-1 min (g-s)
50
40
30
20
10
0
*
*
*
10-6 CCh
+ KN
+ KN + Y

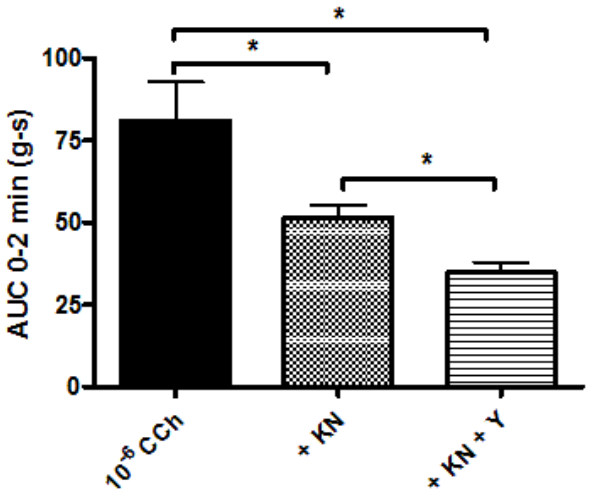
AUC 0-2 min (g-s)
100
75
50
25
0
*
*
*
10-6 CCh
+ KN
+ KN + Y

MLCK activity

The effect of CaMKII inhibition on MLCK activity was measured using immunokinase assay. MLCK activity was measured in longitudinal muscle-myenteric plexus (LM-MP) strip homogenates of four groups: control, following 10 min incubation of 10 µM KN62, 1 min post 1 µM CCh exposure, and 1 min post 1 µM CCh exposure following 10 min incubation with 10 µM KN62. 1 µM CCh increased MLCK activity to 167% ± 21% of control activity ($P < 0.05$ versus control, $n = 12$). Incubation for 10 min with Y27632 reduced CCh-induced activity to 140% ± 14% of control activity ($P < 0.05$ versus control, $n = 8$). Incubation of KN62 alone did not differ MLCK from control ($n = 12$ for control, $n = 3$ for KN62 alone). CCh-induced activity was not significantly varied between strips with and without Rho Kinase inhibition ($n = 12$ for CCh, $n = 8$ for CCh with KN62 incubation). Results are shown in Figure 42.

Figure 42. Effect of CaMKII inhibition on CCh-evoked MLCK activity.

1 µM CCh-induced MLCK activities with and without Rho Kinase inhibition are presented. Values expressed as percentage ± SEM of control MLCK activity. Control, n = 12. CCh-induced activity is 167% ± 21% of control ($P < 0.05$, n = 12). CCh activity in the presence of 10 µM KN62 reduces CCh-induced activity to 140% ± 14% of control ($P < 0.05$, n = 8).

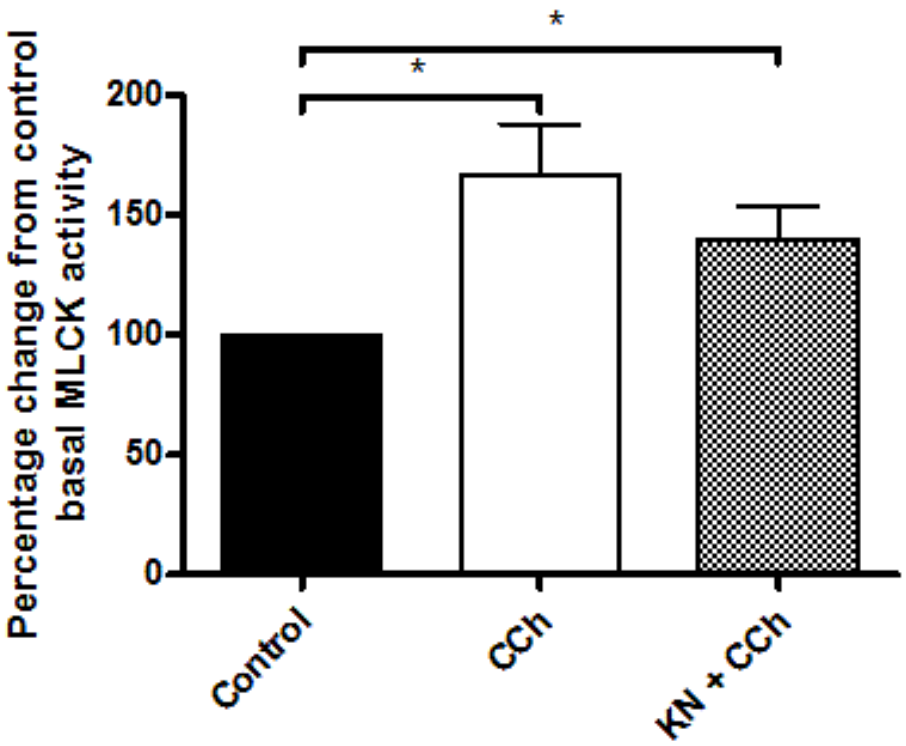
Percentage change from control basal MLCK activity
200
150
100
50
0
*
*
Control
CCh
KN + CCh

DISCUSSION

Strip Generalities

The strips obtained and studied were fairly consistent in their responses to carbachol and the kinase inhibitors used. Two distinct behavior patterns were noted – those with an early peak and moderate decay and those that displayed a slow rise of tension. Strips of each subpopulation were appropriately utilized. It is important before the data is explored and interpreted to make a distinction between the behaviors of these muscle strips, and, for the most part, data from biochemical assays completed on isolated muscle cells. Whereas the assays done in smooth muscle cells (particularly cultured cells) have as their samples uniform biochemical consistency and homogenous population, strips perform as functional tissue, with many different cell types. These strips have cells bound to extracellular matrix, orienting the cells in an organized fashion and altering their functional abilities as a whole. These strips of tissue may have some connective tissue attached and certainly have attached the myenteric plexus which can alter both the response of the strips to agents and the composition of any homogenate, as compared to a homogenate of isolated muscle cells. Differences in the possible amount of nerve tissue present or the tying/mounting of a particular strip could certainly affect the homogenate composition or the basic

contractile behavior of a given strip. However, since each strip serves as its own control when performing comparisons to the effects of inhibitors/blockers, these differences in strip behavior/composition are minimized.

Grand Means

Since there is variance within the performance of strips under control conditions, mean values of the utilized metrics were studied. The contractile response to carbachol of strips is concentration dependent as seen in Figure 11; there is some range of contractile values obtained. This is primarily a consequence of the reporting of tension as grams and not as grams per gram of tissue. Similar ranges of values are seen in the t = 1 min and t = 2 min values (Figure 12) and the area under the curve (AUC) values for the first, second, and first two minutes (Figure 13). These ranges also could have been minimized through normalization by mass; nonetheless, the use of a given strip as its own control enables the appropriate use of the dependent t-test (repeated measurement dependence). Sizable, measured differences can be certified significant even if the range of data suggests otherwise. Findings not found significant under these conditions can be viewed in the same manner – it is more likely that an effect is not present, than it is that significance was clouded by data variability.

Repeated Measures

Once mounted, strips spend considerable time equilibrating in bath solutions. This occurs following the initial mounting and immersion, as well as after washes to remove agonist or antagonist. So that the effects of the long term presence of strips can be eliminated as a factor in any change in their behavior, measurements similar to those conducted in the presence of inhibitor were performed on strips incubated only in standard Krebs solution. Figure 14 and Figure 15 demonstrate that after a 15 min incubation period, there is no significant effect on strip performance following incubation. Any effects of incubation on strip behavior are consequences of the presence of inhibitor in the bath, not the fatigue/deterioration of the strip.

Muscarinic Antagonism

Both M_2 and M_3 receptors are prevalent in muscle tissue, and the literature shows a higher density of M_2 receptors, but a greater functional role of M_3 receptors [86]. Modulation of contraction by both types of receptors has been studied, with some studies asserting no necessary role of M_2 or M_3 receptors in smooth muscle contraction [84, 165]. Data displayed in Figure 16 strengthens the idea that M_3 receptor activity is critical for the contractile behavior that this study measures. Blockade of M_2 causes little effect in CCh-induced contraction; such

contraction is abolished by M_3 blockade. Published data implicates M_1 receptors in human colonic myenteric plexus [166]. As these receptors are localized to nerves, neural contributions to observed contractile behaviors should be addressed.

Effects of Neural Inhibition

The effects of the attached plexus to strips may be the reason differences between strip behavior and isolated muscle cell behaviors are seen. Such differences in isolated cell/intact strip behavior have been reported – the presence of nerve in the strip was the explanation for observed differences [10]. Nerves constitute a minor percentage of the mass of intact muscle, but in this preparation, the mass percentage of nerve tissue may no longer be trivial. Tissue homogenates could have a substantial neural homogenate component. Treatment of strips with TTX following control CCh contractions allows for this effect to be determined. As shown in Figure 17, TTX incubation has no significant effect on the contractions induced by carbachol, although the data does trend to more contraction with TTX incubation. Such a finding would not be in conflict with the literature – longitudinal muscle possesses innervation pathways populated with many inhibitory interneurons [11]. This inhibition could be relieved by TTX. Figure 18 and Figure 19 demonstrate similar effects of TTX on t = 1 min and t = 2 min

data, as well as on AUC values. Again, AUC values did appear to trend higher, suggesting removal of inhibitory input by TTX.

Kinase Inhibition Housekeeping

The following table summarizes the findings of kinase inhibition on the contractile behavior of strips. The tabular format allows for later comparisons between kinases to be made. Peak and AUC data are expressed as percentages of control ± SEM. Sample sizes can be found in the results section. The reader is directed to Figures 22, 27, 33, and 39 in the results section for the percentage values of t = 1 min and t = 2 min experiments.

Table 1. Tabular representation of peak and AUC data for kinase inhibition experiments.

Values represent percentage of control. Sample sizes to be found in results section. Italics indicate $P < 0.05$, based on t-test of original raw data.

	Rho Kinase Inhibition	ERK1/2 Inhibition	CaMKK/AMPK Ihibition	CaMKII Inhibition
Peak				
10 nM CCh	70 ± 13	*60 ± 5*	64 ± 7	*70 ± 6*
1 µM CCh	*62 ± 9*	*64 ± 6*	*67 ± 5*	*66 ± 6*
100 µM CCh	*58 ± 8*	*65 ± 4*	*71 ± 7*	*51 ± 9*
AUC 0-1 min				
10 nM CCh	37 ± 5	60 ± 7	*59 ± 4*	*65 ± 4*
1 µM CCh	*33 ± 4*	*60 ± 6*	*73 ± 3*	*61 ± 9*
100 µM CCh	*50 ± 8*	*65 ± 4*	*70 ± 9*	*62 ± 6*
AUC 1-2 min				
10 nM CCh	32 ± 4	60 ± 4	*67 ± 6*	67 ± 5
1 µM CCh	*37 ± 4*	*59 ± 9*	*74 ± 4*	*61 ± 9*
100 µM CCh	*62 ± 12*	*55 ± 4*	*73 ± 7*	*72 ± 4*
AUC 0-2 min				
10 nM CCh	32 ± 6	64 ± 6	*65 ± 3*	69 ± 8
1 µM CCh	*37 ± 4*	*55 ± 4*	*74 ± 4*	*63 ± 8*
100 µM CCh	*55 ± 8*	*61 ± 3*	*71 ± 7*	*67 ± 5*

Effects of Rho Kinase Inhibition

In this study, inhibition of Rho kinase led to significant decreases in basal tone (Figure 20), peak contraction (Figure 21), contraction at 1 and 2 minutes post CCh administration (Figure 22), and AUC values (Figure 23). Rho kinase is known to promote MLC_{20} phosphorylation (and contraction) through its phosphorylation of MYPT1, regulating contraction through inhibition of MLCP. Rho kinase is also implicated in the activation of CPI-17, another MLCP inhibitor [73, 74, 167]. Rho kinase inhibition should have an obvious effect in promoting contraction, but its role seems more important in maintaining a sustained contraction, as its expression is heightened in tonic smooth muscle [112, 168]. Although Rho kinase inhibition shows decreases in tone as compared to control at t = 1 min, and t = 2 min (Figure 22), when these data are viewed as percentages of the control contraction, it can be inferred that this sustained phase may not be appreciably reduced – the initial contraction was smaller, so contraction values at t = 1 min and t = 2 min are obviously reduced, and the "sustained phase" similar to control. In this study, the more obvious finding is that Rho kinase is demonstrating an acute effect. Peak contractions are reduced, at a similar level (slightly greater) than the other inhibitors.

The literature as a whole focuses upon Rho kinase as a modulator of sustained contraction. Mbikou observed an acute effect of Rho kinase on contraction in airway smooth muscle, similar to findings of this study [169]. Frei found that the common Rho kinase inhibitor used in this study, Y27632, had no effect upon reducing CCh-induced contraction in colonic longitudinal muscle – the data of this study suggests a sizable effect [170]. The phosphorylation of MYTP1 and CPI-17 by Rho kinase can only aid in maintaining a level of tone; their inhibition (through Rho kinase inhibition) could not present itself as a decrease in induced contraction. From the perspective of phosphatase inhibition via Rho kinase, incubation with Y27632 would increase basal phosphatase activity – MLC_{20} phosphorylation would be decreased in resting state. Here, Y27632 incubation causes a decrease in basal tone *but* a reduction of peak contraction. Something else must be mediating this acute effect.

Hagerty offers a mechanism whereby Rho kinase increases the activity of ZIP kinase, known to effect Ca^{2+}-independent MLC_{20} phosphorylation [99, 115]. This is supported by Ihara and MacDonald, who find direct phosphorylation of MLC_{20} by ZIP kinase as well as phosphorylation of MYPT1 by ZIP kinase, which is the

possible mechanism connecting Rho kinase to its phosphorylation actions on the protein MYPT1 [75, 171, 172].

Another possibility is direct phosphorylation of MLC_{20} by Rho kinase. When Rho kinase is activated by Rho following M_3 activation, direct phosphorylation of MLC_{20} could take place. Inhibition of this possible phosphorylation mechanism would present itself as an acute effect. Such phosphorylation of MLC_{20} by Rho kinase has been reported [113]. The same group has implicated Rho kinase as an upstream mediator of a pathway that regulates nitric oxide production through eNOS in endothelial cells [114]. Although the muscle strips of this study possess no endothelial cells to generate NO, the nerves of the attached myenteric plexus are known to do so [11].

As compared to the other kinases, Rho kinase inhibition caused a far larger inhibition of all AUC values, and peak values except for those at the 10 nM CCh level. This may indicate an acute effect as evidenced by the reduced peak contraction. In addition, inhibition of the other kinases reduces the peak contraction by factor similar to their reduction in AUC values. Rho kinase inhibition causes far more reduction in AUC values as compared to its effect on the peak contraction. Possibly a hybrid/combined effect exists.

Effects of ERK1/2 Inhibition

Influence of ERK1/2 in smooth muscle contractile regulation is widely displayed in the literature. ERK1/2 is reported to have a presence in pathways of pathophysiological smooth muscle, either through its ability to phosphorylate directly a pertinent substrate or by its transcription factor behavior [87, 118]. It has roles in desensitization pathways in gastric smooth muscle and mediates contraction in vascular smooth muscle through endothelin signaling [119, 162]. ERK1/2 signaling can also be increased by muscarinic activation in a manner that increases cPLA2, a critical enzyme in longitudinal muscle calcium handling [120]. Its activity seems to be connected to contraction; ERK1/2 inhibition reduces contraction in this study and others [172].

ERK1/2 inhibition in this study produces a reduction in both peak contractile values and AUC values (Figure 26 and Figure 28). The degree of inhibition is second only to Rho kinase. ERK1/2 inhibition caused predictable concomitant decrease in contraction at t = 1 min and t = 2 min (Figure 27), with similar percentage of peak profiles as control. With ERK1/2 signaling/activity playing an established role in contractile regulation, its potential targets fall into several categories. Harnett verifies ERK1/2 phosphorylation of integrin-linked kinase (ILK) in esophagus, Muranyi links ILK to Ca^{2+}-independent

contraction via MYPT1 phosphorylation, and Deng offers direct phosphorylation of MLC_{20} by ILK [78, 81, 82]. Therefore ERK1/2 can be connected to actions on MLC_{20} directly and through phosphatase inhibition. Morrison from a biochemical standpoint and Klemke from a cell motility/proliferation angle both demonstrate that ERK1/2 directly phosphorylates MLCK and that this phosphorylation enhances MLCK activity [65, 66]. Others show similar effects that ERK1/2 can have modulatory effects on the MLCK as well. Immunokinase assay data from this study suggests a possible enhancement by ERK1/2. In addition to MLC_{20}, MYPT1, and MLCK modulation, ERK1/2 is also known to phosphorylate accessory proteins in the contractile mechanism or cytoskeleton. Both caldesmon and calponin are targeted by ERK1/2 [54, 117].

In conjunction with Rho kinase inhibition, ERK1/2 inhibition produced no additive reduction of contraction (Figure 29). This can be considered either a consequence of their shared effects upon MYPT1 phosphorylation (which does speak more to sustained aspects) or that the inhibition of peak contraction by ERK1/2 inhibition is mediated through its effects on direct phosphorylation of MLC_{20} via ILK, duplicated by the same actions through Rho kinase via ZIP kinase. Yet, it is more likely that an additive effect should exist, considering all avenues of

inhibition that ERK1/2 possesses, and that careful experimentation would illuminate these.

Effects of CaMKK/AMPK Inhibition

AMPK has implications in cellular metabolism in cells/tissues with metabolic needs that may have large variations with activity, such as muscle. Studies from tetanic electrical stimulation to hibernation to osmotic stress establish AMPK as a regulator/"switch" of glucose uptake, lipid metabolism, and mitochondrial manipulation [135, 142, 173]. CaMKK is an upstream effector of AMPK activity, with the beta isoform of CaMKK as the particular modulating kinase [134, 139]. This regulation of AMPK can be mediated through M_3 activation [136].

However, the upstream regulation of AMPK by CaMKKβ is time dependent. After sustained activation of AMPK by CaMKKβ, blockade of CaMKK no longer can affect AMPK activity in a model of tetanic contraction [174]. In addition, the alpha isoform of CaMKK does not modulate AMPK activity as it relates to metabolic processes [138]. The inhibitor used in this study (STO-609) targets both isoforms of CaMKK for inhibition, so use of this inhibitor does have consequences beyond AMPK [140, 141].

As a regulator of contraction, both Horman and Al-Shboul have shown that AMPK activity leads to phosphorylation of MLCK kinase

in a manner that reduces its ability to foster contraction [143, 175]. Bultot demonstrates that AMPK can directly phosphorylate MLC_{20}, but that such is unlikely to be its proper physiological function [144]. In this study, inhibition of CaMKK activity was found to reduce peak contraction and AUC values (Figure 32 and Figure 34). CaMKK inhibition caused predictable concomitant decrease in contraction at t = 1 min and t = 2 min (Figure 33), with similar percentage of peak profiles to control. MLCK activity was also decreased with CaMKK inhibition (Figure 36). Also, additive effects of CaMKK inhibition with Rho kinase inhibition were observed, implicating CaMKK effects on the kinase side of MLC_{20} phosphorylation regulation (Figure 35). These data are in conflict with Al-Shboul and Horman. Al-Shboul, however, made his findings in isolated circular muscle cells (no neural input) and Horman in chicken gizzard, a muscular structure with smooth muscle and innervation but little similarity to longitudinal muscle in gut. The findings of *this* study are in a model of different muscle type and are from strips, which may contract with different regulation than isolated cells (Al-Shboul) or have a different neural contribution as a homogenate for MLCK assay (Horman).

Furthermore, studies by Donsmark and Blair show that AMPK activity increases with electrically stimulated contraction

[176, 177]. It is conceivable that AMPK activity increases as a consequence of contraction, not as a modulator of contraction, but to evoke the metabolic modulatory effects in tissue whose metabolic needs have been advanced. The current study also used an inhibitor (STO-609) which does not discriminate between the alpha and beta isoforms. Only the beta isoform is an effector of AMPK, and any independent effects CaMKKα may have on contraction would be simultaneously affected. Schmitt shows ERK1/2 activation by CaMKK via calcium-calmodulin dependent kinase I (CaMKI), and this study has established the importance of ERK1/2 signaling in longitudinal muscle. CaMKK inhibition would affect this negatively [178]. Lastly, like CaMKII, this enzyme is dependent on calcium-calmodulin interactions for regulation of its activity, and with the unique calcium handling of longitudinal muscle, could conceivably have different effects as a result of different calcium dynamics.

Effects of CaMKII Inhibition

In this study, CaMKII inhibition by KN62 incubation caused decreases in basal tone (Figure 37), peak tension development (Figure 38), and AUC values (Figure 40). CaMKII inhibition caused predictable concomitant decrease in contraction at t = 1 min and t = 2 min (Figure 39), with similar percentage of peak profiles to control. CaMKII inhibition resulted in a decrease

of CCh-induced MLCK activity (Figure 42). These data are in conflict with Murthy, who found that CaMKII inhibition reduced MLCK activity and Tansey who found KN62 causes a decrease in calcium sensitization of MLCK, reducing its activity [84, 129]. Both of these studies were in isolated cells of muscle types (circular muscle, tracheal muscle) who differ in characteristics from longitudinal muscle. Hashimoto found that CaMKII can phosphorylate MLCK as a negative effector (in conflict the presented data), but that such phosphorylation could only occur before binding of calcium-calmodulin to MLCK [130]. As with CaMKK, differences in calcium handling in longitudinal muscle might preclude this effect, and the Hashimoto experiment was performed with purified protein (both MLCK and CaMKII). The additive effects of CaMKII inhibition with Rho kinase inhibition (Figure 41) suggests effects of CaMKII exist on kinase leg of regulation.

Studies by Henning and Pauly expose CaMKII as critical in the processes of migration and hypertrophy, where positive associations with myosin are more often observed than associations that decrease activity or important cooperative binding [125, 126]. Edelman and Kim demonstrate direct phosphorylation of MLC_{20} with CaMKII activation, which would

agree with the findings of decreased basal tone with incubation of CaMKII inhibitor (Figure 37) [132, 179].

CaMKII also has modulatory effects on ion channels and SR which would present heightened importance given the calcium handling modality of longitudinal muscle. McCarron implicates CaMKII in calcium channel regulation as a possible feed-forward mechanism, increasing calcium influx with CaMKII activity [180]. Greenwood shows that regulation of ion channels by CaMKII can differ between arterial and venous smooth cells [121]. It remains conceivable that calcium channel regulation could be different in longitudinal muscle (versus circular) where such effects would have larger consequences on calcium mobilization.

Moreover, CaMKII can modulate SR receptors. Witcher finds that CaMKII phosphorylation of cardiac ryanodine receptors leads to enhanced calcium release. This effect is not seen in skeletal muscle [127]. Given the similarities of calcium handling in cardiac and gut longitudinal muscle, such inhibition of CaMKII would reduce calcium mobilization and contractile activity, as findings in this study demonstrate. Lastly, CaMKII is an obvious upstream effector of ERK1/2. Marganski shows an essential role of CaMKII in regulation of downstream ERK1/2 activity [124]. ERK1/2 importance in contractile regulation in colonic longitudinal muscle has been established by the current

findings. Blockade of CaMKII would affect contraction in a manner similar to ERK1/2 regulation, and this is in concert with these data.

Putative Longitudinal Model

Because the contrary effects of CaMKK and CaMKII inhibition as compared to the circular muscle model (Figure 2), an updated model is offered for longitudinal muscle. The effects of CaMKK and CaMKII upon ERK1/2 activation, ion channels, SR receptors, and MLC_{20} phosphorylation have been added. The new model is offered in Figure 43, and both models together in Figure 44.

Figure 43. Model for Longitudinal Muscle Regulation.

Open Triangles indicate legacies of putative circular model roles of CaMKK/AMPK and CaMKII. Arrows indicate positive regulation.

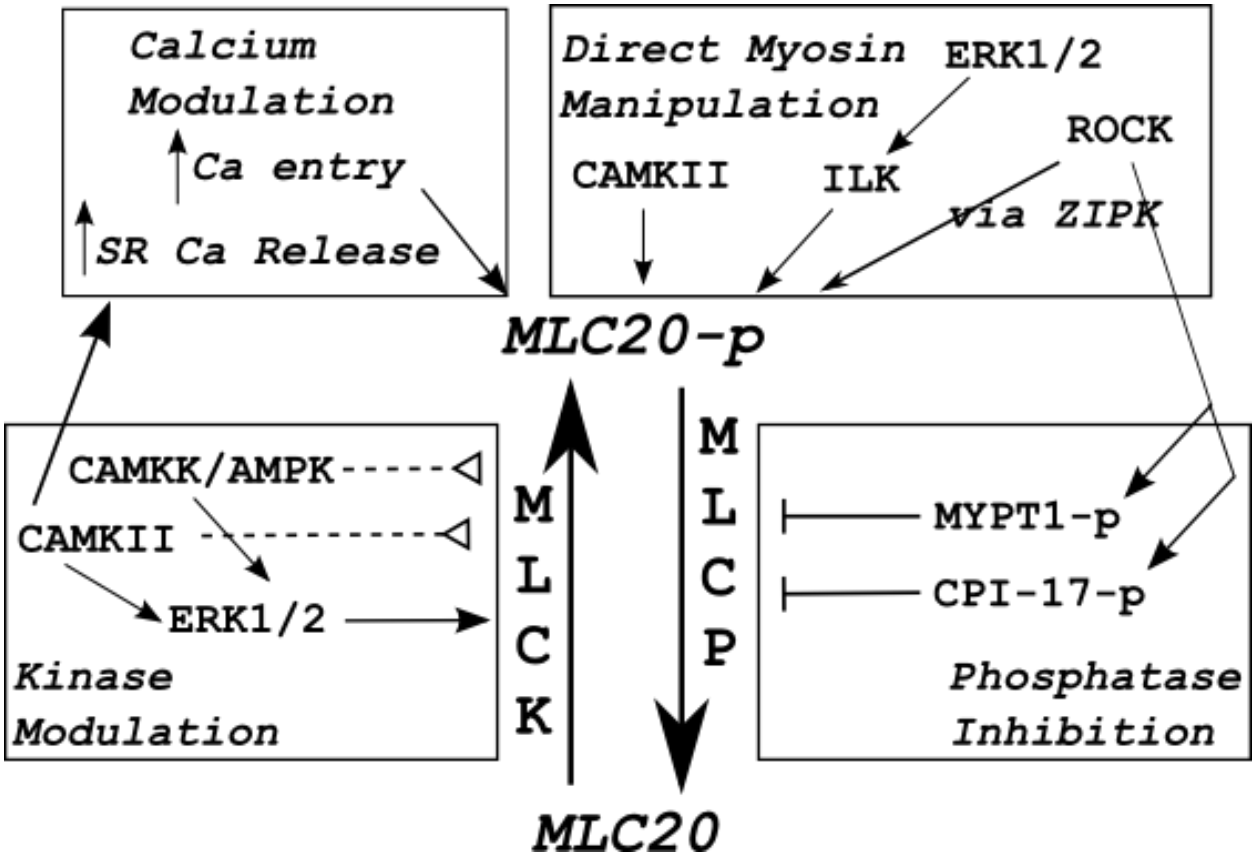
Calcium
Modulation
Ca entry
SR Ca Release
Direct Myosin
Manipulation
ERK1/2
ROCK
CAMKII
ILK
via ZIPK
MLC20-p
CAMKK/AMPK
CAMKII
ERK1/2
Kinase
Modulation
MLCK
MLCP
MYPT1-p
CPI-17-p
Phosphatase
Inhibition
MLC20

Figure 44. Circular and Longitudinal Muscle Regulation by Kinases.

Top Panel: Putative circular muscle model.

Bottom Panel: Putative longitudinal muscle model. Open triangles indicate contrary legacies from circular model.

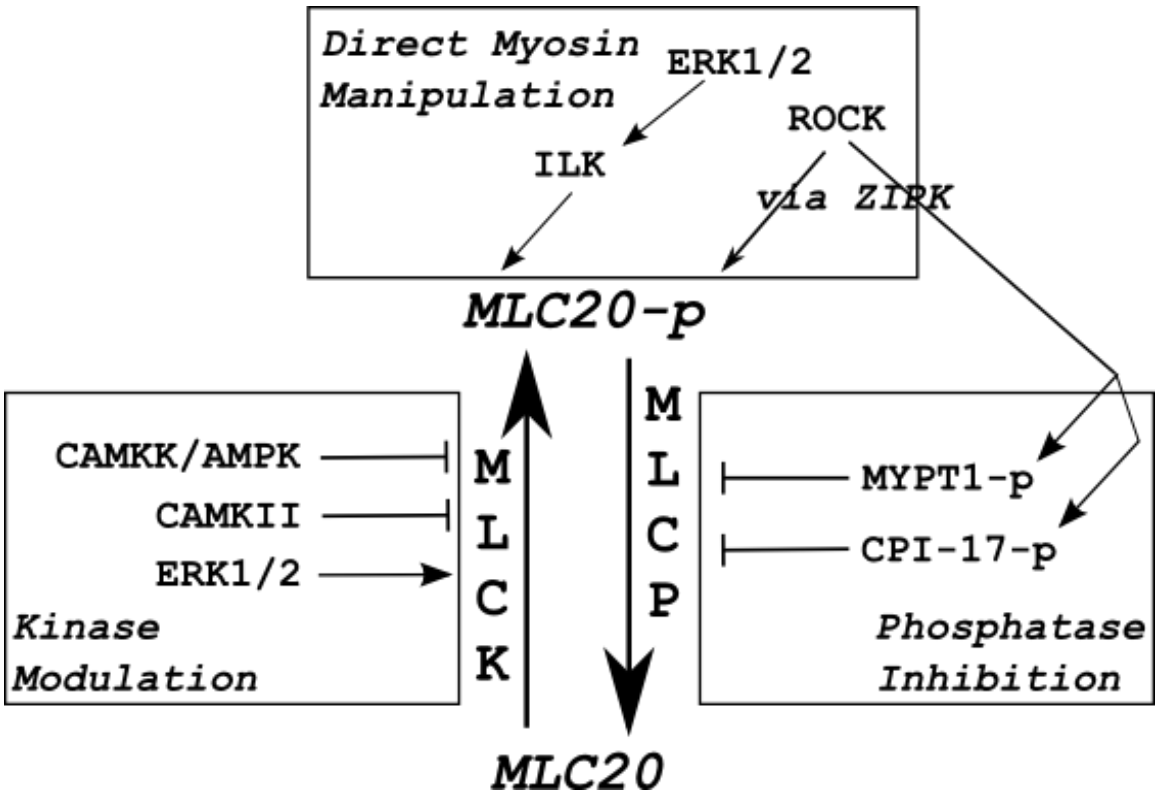
Direct Myosin Manipulation
ERK1/2
ROCK
ILK
via ZIPK
MLC20-p
CAMKK/AMPK
CAMKII
ERK1/2
Kinase Modulation
MLCK
MLCP
MYPT1-p
CPI-17-p
Phosphatase Inhibition
MLC20

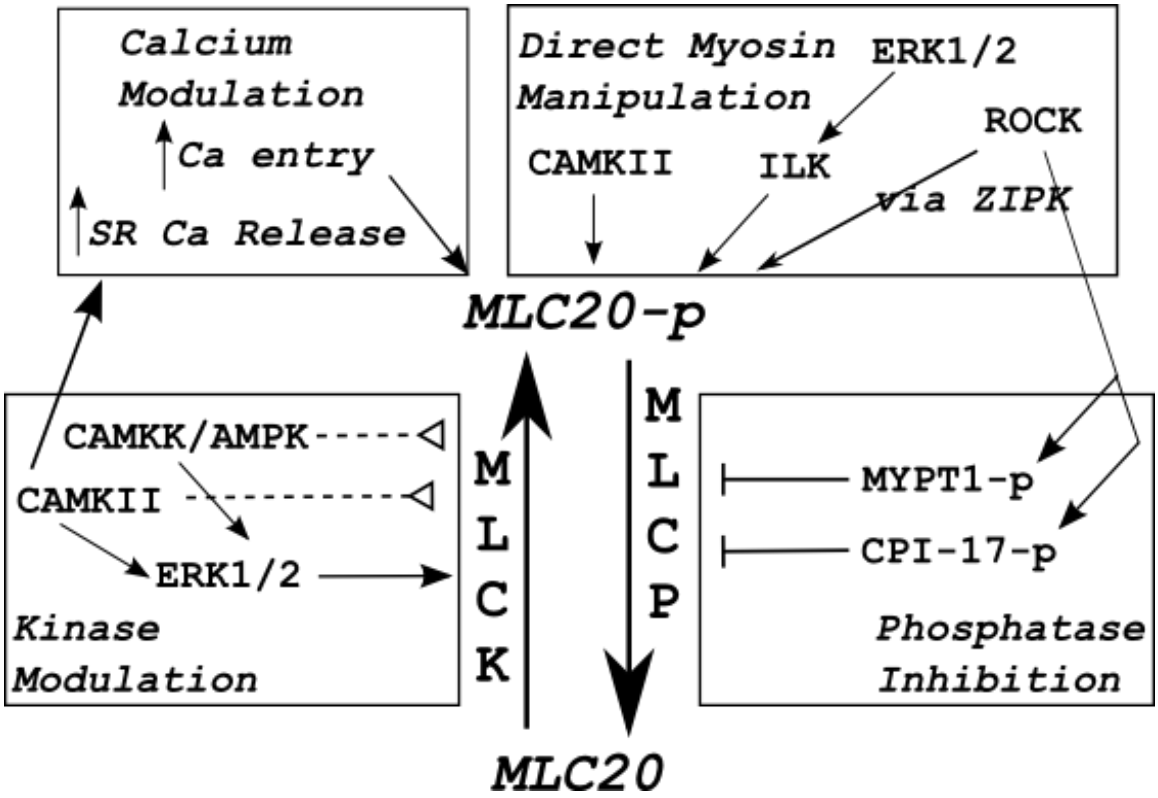
Calcium Modulation
Ca entry
SR Ca Release
Direct Myosin Manipulation
ERK1/2
ROCK
CAMKII
ILK
via ZIPK
MLC20-p
CAMKK/AMPK
CAMKII
ERK1/2
Kinase Modulation
MLCK
MLCP
MYPT1-p
CPI-17-p
Phosphatase Inhibition
MLC20

Avenues to Explore

To further and strengthen the model, the following experiments are proposed:

- Western Blot analysis to observe MLC_{20} phosphorylation levels directly under control conditions and in response to CCh, with and without kinase inhibition.
- Kinase assays for these candidate kinase, as well as ZIPK and ILK. These assays could offer information regarding Ca^{2+}-independent contraction regulation, and with appropriate use of inhibitors could sequence any possible cascades.
- Exploration of phosphatase activity by these kinases. This could be accomplished indirectly through observation of phosphorylation/activation of phosphatase inhibitors MYPT1 and CPI-17
- Experiments with kinase inhibition in conjunction with muscarinic antagonism and Na^{+} channel blockade via TTX, to determine neural contributions and possible modulation by M_2 signaling.
- Combination of kinase inhibition on contraction to determine possible additive effects or redundancies.

LIST OF REFERENCES

1. Pandol, S.J., H.E. Raybould, and J. Yee, Hal F., *Integrative responses of the gastrointestinal tract and liver to a meal.*, in *Textbook of gastroenterology*, T. Yamada and D.H. Alpers, Editors. 2009, Blackwell Pub.: Chichester, West Sussex ; Hoboken, NJ. p. 3-14.

2. Nagler-Anderson, C., *Man the barrier! strategic defences in the intestinal mucosa.* Nat Rev Immunol, 2001. **1**(1): p. 59-67.

3. Kokrashvili, Z., B. Mosinger, and R.F. Margolskee, *Taste signaling elements expressed in gut enteroendocrine cells regulate nutrient-responsive secretion of gut hormones.* Am J Clin Nutr, 2009. **90**(3): p. 822S-825S.

4. Egan, J.M. and R.F. Margolskee, *Taste Cells of the Gut and Gastrointestinal Chemosensation.* Molecular Interventions, 2008. **8**(2): p. 78-81.

5. Goyal, R.K. and A. Chaudhury, *Physiology of normal esophageal motility.* J Clin Gastroenterol, 2008. **42**(5): p. 610-9.

6. Rubin, D.C., *Small intestine: anatomy and structural anomalies*, in *Textbook of gastroenterology*, T. Yamada and D.H. Alpers, Editors. 2009, Blackwell Pub.: Chichester, West Sussex ; Hoboken, NJ. p. 1085-1108.

7. Rhoades, R. and G.A. Tanner, *Medical physiology*. 2nd ed. 2003, Philadelphia: Lippincott Williams & Wilkins. x, 781 p.

8. Kunze, W.A.A. and J.B. Furness, *THE ENTERIC NERVOUS SYSTEM AND REGULATION OF INTESTINAL MOTILITY.* Annual Review of Physiology, 1999. **61**(1): p. 117-142.

9. Makhlouf, G.M. and K.S. Murthy, *Signal Transduction in Gastrointestinal Smooth Muscle.* Cellular Signalling, 1997. **9**(3-4): p. 269-276.

10. Grider, J.R., *Regulation of excitatory neural input to longitudinal intestinal muscle by myenteric interneurons.* Am J Physiol, 1998. **275**(5 Pt 1): p. G973-8.

11. Grider, J.R., *Reciprocal activity of longitudinal and circular muscle during intestinal peristaltic reflex.* Am J Physiol Gastrointest Liver Physiol, 2003. **284**(5): p. G768-75.

12. Furness, J.B., *The enteric nervous system*. 2006, Malden, Mass.: Blackwell Pub. xiii, 274 p.

13. Sbarbati, A., et al., *The diffuse chemosensory system: exploring the iceberg toward the definition of functional roles.* Prog Neurobiol, 2010. **91**(1): p. 77-89.

14. Cominelli, F., et al., *The mucosal immune system and gastrointestinal inflammation.*, in *Textbook of gastroenterology*, T. Yamada and D.H. Alpers, Editors. 2009, Blackwell Pub.: Chichester, West Sussex ; Hoboken, NJ. p. 133-168.

15. Benarroch, E.E., *Enteric nervous system: functional organization and neurologic implications.* Neurology, 2007. **69**(20): p. 1953-7.

16. Furness, J.B., et al., *The enteric nervous system and its extrinsic connections.*, in *Textbook of gastroenterology*, T. Yamada and D.H. Alpers, Editors. 2009, Blackwell Pub.: Chichester, West Sussex ; Hoboken, NJ.

17. Sanders, K.M., S.D. Koh, and S.M. Ward, *INTERSTITIAL CELLS OF CAJAL AS PACEMAKERS IN THE GASTROINTESTINAL TRACT.* Annual Review of Physiology, 2006. **68**(1): p. 307-343.

18. Sanders, K.M. and S.M. Ward, *Interstitial cells of Cajal: a new perspective on smooth muscle function.* The Journal of Physiology, 2006. **576**(3): p. 721-726.

19. Liu, L.W., et al., *Interstitial cells of Cajal: mediators of communication between circular and longitudinal muscle layers of canine colon.* Cell Tissue Res, 1998. **294**(1): p. 69-79.

20. Liu, L.W. and J.D. Huizinga, *Electrical coupling of circular muscle to longitudinal muscle and interstitial cells of Cajal in canine colon.* J Physiol, 1993. **470**: p. 445-61.

21. Cobine, C., et al., *Relationship between interstitial cells of Cajal, fibroblast-like cells and inhibitory motor nerves*

in the internal anal sphincter. Cell and Tissue Research, 2011: p. 1-14.

22. Kurahashi, M., et al., *A functional role for the 'fibroblast-like cells' in gastrointestinal smooth muscles.* The Journal of Physiology, 2011. **589**(3): p. 697-710.

23. Rumessen, J.J., et al., *Ultrastructure of interstitial cells of Cajal in myenteric plexus of human colon.* Cell Tissue Res, 2009. **337**(2): p. 197-212.

24. Brookes, S.J., et al., *Identification of motor neurons to the longitudinal muscle of the guinea pig ileum.* Gastroenterology, 1992. **103**(3): p. 961-73.

25. Makhlouf, G.M. and J.R. Grider, *Nonadrenergic Noncholinergic Inhibitory Transmitters of the Gut.* N. Physiol Sci., 1993. **Volume 8**(October 1993): p. 195-199.

26. Murthy, K.S. and G.M. Makhlouf, *Opioid mu, delta, and kappa receptor-induced activation of phospholipase C-beta 3 and inhibition of adenylyl cyclase is mediated by Gi2 and G(o) in smooth muscle.* Mol Pharmacol, 1996. **50**(4): p. 870-7.

27. Murthy, K.S., D.H. Coy, and G.M. Makhlouf, *Somatostatin Receptor-mediated Signaling in Smooth Muscle.* Journal of Biological Chemistry, 1996. **271**(38): p. 23458-23463.

28. Misra, S., et al., *Differential expression of Y receptors and signaling pathways in intestinal circular and longitudinal smooth muscle.* Regul Pept, 2005. **125**(1-3): p. 163-72.

29. Dominguez, R. and K.C. Holmes, *Actin Structure And Function.* Annual Review of Biophysics, 2011. **40**(1): p. null.

30. Matsumura, F. and D.J. Hartshorne, *Myosin phosphatase target subunit: Many roles in cell function.* Biochemical and Biophysical Research Communications, 2008. **369**(1): p. 149-156.

31. Hall, J.E. and A.C. Guyton, *Guyton and Hall textbook of medical physiology*. 12th ed. 2011, Philadelphia, Pa.: Saunders/Elsevier. xix, 1091 p.

32. McPherson, P.S. and K.P. Campbell, *The ryanodine receptor/Ca2+ release channel.* Journal of Biological Chemistry, 1993. **268**(19): p. 13765-13768.

33. Hodgkinson, J.L., *Actin and the smooth muscle regulatory proteins: a structural perspective.* Journal of Muscle Research and Cell Motility, 2000. **21**(2): p. 115-130.

34. Ikebe, M., D.J. Hartshorne, and M. Elzinga, *Phosphorylation of the 20,000-dalton light chain of smooth muscle myosin by the calcium-activated, phospholipid-dependent protein kinase. Phosphorylation sites and effects of phosphorylation.* J Biol Chem, 1987. **262**(20): p. 9569-73.

35. Kamm, K.E. and J.T. Stull, *Dedicated Myosin Light Chain Kinases with Diverse Cellular Functions.* Journal of Biological Chemistry, 2001. **276**(7): p. 4527-4530.

36. SOMLYO, A.P. and A.V. SOMLYO, *Ca2+ Sensitivity of Smooth Muscle and Nonmuscle Myosin II: Modulated by G Proteins, Kinases, and Myosin Phosphatase.* Physiological Reviews, 2003. **83**(4): p. 1325-1358.

37. Kim, H.R., et al., *Smooth muscle signalling pathways in health and disease.* J Cell Mol Med, 2008. **12**(6A): p. 2165-80.

38. Furness, J.B., et al., *Plurichemical transmission and chemical coding of neurons in the digestive tract.* Gastroenterology, 1995. **108**(2): p. 554-563.

39. Murthy, K.S., *SIGNALING FOR CONTRACTION AND RELAXATION IN SMOOTH MUSCLE OF THE GUT.* Annual Review of Physiology, 2006. **68**(1): p. 345-374.

40. Walker, J.K., et al., *Mice lacking the dopamine transporter display altered regulation of distal colonic motility.* Am J Physiol Gastrointest Liver Physiol, 2000. **279**(2): p. G311-8.

41. Lv, Y., et al., *CCK mediated the inhibitory effect of oxytocin on the contraction of longitudinal muscle strips of duodenum in male rats.* Pflügers Archiv European Journal of Physiology, 2010. **460**(6): p. 1063-1071.

42. Bitar, K.N. and G.M. Makhlouf, *Selective presence of opiate receptors on intestinal circular muscle cells.* Life Sci, 1985. **37**(16): p. 1545-50.

43. Ma, T., et al., *Contractile effects and intracellular Ca2+ signalling induced by emodin in circular smooth muscle cells of rat colon.* World J Gastroenterol, 2003. **9**(8): p. 1804-7.

44. Somlyo, A.P. and A.V. Somlyo, *Signal transduction and regulation in smooth muscle.* Nature, 1994. **372**(6503): p. 231-236.

45. Matthijs, G., T.L. Peeters, and G. Vantrappen, *Effect of different calcium modulators on motilin-induced contractions of the rabbit duodenum. Comparison with acetylcholine.* Regul Pept, 1988. **21**(3-4): p. 321-30.

46. Hollenberg, M.D., *Tyrosine kinase pathways and the regulation of smooth muscle contractility.* Trends Pharmacol Sci, 1994. **15**(4): p. 108-14.

47. Jin, N., et al., *Communication between tyrosine kinase pathway and myosin light chain kinase pathway in smooth muscle.* American Journal of Physiology - Heart and Circulatory Physiology, 1996. **271**(4): p. H1348-H1355.

48. Urich, K., *Comparative animal biochemistry*. 1994, Berlin ; New York: Springer-Verlag. xvii, 782 p.

49. Milner, R.E., et al., *Calreticulin, and not calsequestrin, is the major calcium binding protein of smooth muscle sarcoplasmic reticulum and liver endoplasmic reticulum.* J Biol Chem, 1991. **266**(11): p. 7155-65.

50. Kuemmerle, J.F., K.S. Murthy, and G.M. Makhlouf, *Agonist-activated, ryanodine-sensitive, IP3-insensitive Ca2+ release channels in longitudinal muscle of intestine.* American Journal of Physiology - Cell Physiology, 1994. **266**(5): p. C1421-C1431.

51. Sanders, K.M., *Regulation of smooth muscle excitation and contraction.* Neurogastroenterology & Motility, 2008. **20**: p. 39-53.

52. Makhlouf, G. and K.S. Murthy, *Smooth Muscle of the Gut*, in *Textbook of gastroenterology*, T. Yamada and D.H. Alpers, Editors. 2009, Blackwell Pub.: Chichester, West Sussex ; Hoboken, NJ. p. 103-133.

53. Sakamoto, T., et al., *Three distinct muscarinic signalling pathways for cationic channel activation in mouse gut smooth muscle cells.* J Physiol, 2007. **582**(Pt 1): p. 41-61.

54. Gerthoffer, W.T., *Signal-Transduction Pathways that Regulate Visceral Smooth Muscle Function III. Coupling of muscarinic receptors to signaling kinases and effector proteins in gastrointestinal smooth muscles.* American Journal of Physiology - Gastrointestinal and Liver Physiology, 2005. **288**(5): p. G849-G853.

55. Akbarali, H.I., *Signal-Transduction Pathways that Regulate Smooth Muscle Function II. Receptor-ion channel coupling mechanisms in gastrointestinal smooth muscle.* American Journal of Physiology - Gastrointestinal and Liver Physiology, 2005. **288**(4): p. G598-G602.

56. Ozaki, H., et al., *Regulation of metabolism and contraction by cytoplasmic calcium in the intestinal smooth muscle.* Journal of Biological Chemistry, 1988. **263**(28): p. 14074-14079.

57. Wellman, G.C. and M.T. Nelson, *Signaling between SR and plasmalemma in smooth muscle: sparks and the activation of Ca2+-sensitive ion channels.* Cell Calcium, 2003. **34**(3): p. 211-229.

58. Wray, S., T. Burdyga, and K. Noble, *Calcium signalling in smooth muscle.* Cell Calcium, 2005. **38**(3-4): p. 397-407.

59. Triggle, C.R., V.C. Swamy, and D.J. Triggle, *Calcium antagonists and contractile responses in rat vas deferens and guinea pig ileal smooth muscle.* Can J Physiol Pharmacol, 1979. **57**(8): p. 804-18.

60. Murthy, K.S., et al., *Sustained muscle contraction induced by agonists, growth factors, and Ca2+ mediated by distinct PKC isozymes.* American Journal of Physiology - Gastrointestinal and Liver Physiology, 2000. **279**(1): p. G201-G210.

61. Gao, Y., et al., *Myosin Light Chain Kinase as a Multifunctional Regulatory Protein of Smooth Muscle Contraction.* IUBMB Life, 2001. **51**(6): p. 337-344.

62. Conti, M.A. and R.S. Adelstein, *The relationship between calmodulin binding and phosphorylation of smooth muscle myosin kinase by the catalytic subunit of 3':5' cAMP-*

dependent protein kinase. J Biol Chem, 1981. **256**(7): p. 3178-81.

63. Nishikawa, M., S. Shirakawa, and R.S. Adelstein, *Phosphorylation of smooth muscle myosin light chain kinase by protein kinase C. Comparative study of the phosphorylated sites.* J Biol Chem, 1985. **260**(15): p. 8978-83.

64. Goeckeler, Z.M., et al., *Phosphorylation of myosin light chain kinase by p21-activated kinase PAK2.* J Biol Chem, 2000. **275**(24): p. 18366-74.

65. Klemke, R.L., et al., *Regulation of Cell Motility by Mitogen-activated Protein Kinase.* The Journal of Cell Biology, 1997. **137**(2): p. 481-492.

66. Morrison, D.L., et al., *Phosphorylation and activation of smooth muscle myosin light chain kinase by MAP kinase and cyclin-dependent kinase-1.* Biochem Cell Biol, 1996. **74**(4): p. 549-57.

67. Hartshorne, D., M. Ito, and F. Erdo¨Di, *Myosin light chain phosphatase: subunit composition, interactions and regulation.* Journal of Muscle Research and Cell Motility, 1998. **19**(4): p. 325-341.

68. Terrak, M., et al., *Structural basis of protein phosphatase 1 regulation.* Nature, 2004. **429**(6993): p. 780-784.

69. Wooldridge, A.A., et al., *Smooth muscle phosphatase is regulated in vivo by exclusion of phosphorylation of threonine 696 of MYPT1 by phosphorylation of Serine 695 in response to cyclic nucleotides.* J Biol Chem, 2004. **279**(33): p. 34496-504.

70. Hartshorne, D.J., M. Ito, and F. Erdödi, *Role of Protein Phosphatase Type 1 in Contractile Functions: Myosin Phosphatase.* Journal of Biological Chemistry, 2004. **279**(36): p. 37211-37214.

71. Eto, M., et al., *Molecular cloning of a novel phosphorylation-dependent inhibitory protein of protein phosphatase-1 (CPI17) in smooth muscle: its specific localization in smooth muscle.* FEBS Lett, 1997. **410**(2-3): p. 356-60.

72. Kitazawa, T., et al., *Agonists trigger G protein-mediated activation of the CPI-17 inhibitor phosphoprotein of myosin light chain phosphatase to enhance vascular smooth muscle contractility.* J Biol Chem, 2000. **275**(14): p. 9897-900.

73. Hamaguchi, T., et al., *Phosphorylation of CPI-17, an inhibitor of myosin phosphatase, by protein kinase N.* Biochem Biophys Res Commun, 2000. **274**(3): p. 825-30.

74. Koyama, M., et al., *Phosphorylation of CPI-17, an inhibitory phosphoprotein of smooth muscle myosin phosphatase, by Rho-kinase.* FEBS Letters, 2000. **475**(3): p. 197-200.

75. MacDonald, J.A., et al., *Dual Ser and Thr phosphorylation of CPI-17, an inhibitor of myosin phosphatase, by MYPT-associated kinase.* FEBS Lett, 2001. **493**(2-3): p. 91-4.

76. Stevenson, A.S., et al., *Uncoupling of GPCR and RhoA-induced Ca2+-sensitization of chicken amnion smooth muscle lacking CPI-17.* FEBS Lett, 2004. **578**(1-2): p. 73-9.

77. He, W.-Q., et al., *Myosin Light Chain Kinase Is Central to Smooth Muscle Contraction and Required for Gastrointestinal Motility in Mice.* Gastroenterology, 2008. **135**(2): p. 610-620.e2.

78. Harnett, K.M., W. Cao, and P. Biancani, *Signal-Transduction Pathways that Regulate Smooth Muscle Function I. Signal transduction in phasic (esophageal) and tonic (gastroesophageal sphincter) smooth muscles.* American Journal of Physiology - Gastrointestinal and Liver Physiology, 2005. **288**(3): p. G407-G416.

79. Kitazawa, T., et al., *Receptor-coupled, permeabilized smooth muscle. Role of the phosphatidylinositol cascade, G-proteins, and modulation of the contractile response to Ca2+.* J Biol Chem, 1989. **264**(10): p. 5339-42.

80. Takeuchi, T., et al., *A minor role for Ca²⁺ sensitization in sustained contraction through activation of muscarinic receptor in circular muscle of rat distal colon.* Pflügers Archiv European Journal of Physiology, 2007. **454**(4): p. 565-574.

81. Deng, J.T., et al., *Phosphorylation of the myosin phosphatase inhibitors, CPI-17 and PHI-1, by integrin-linked kinase.* Biochem. J., 2002. **367**(2): p. 517-524.

82. Murányi, A., et al., *Phosphorylation of the myosin phosphatase target subunit by integrin-linked kinase.* Biochem. J., 2002. **366**(1): p. 211-216.

83. Woodsome, T.P., et al., *Expression of CPI-17 and myosin phosphatase correlates with Ca(2+) sensitivity of protein kinase C-induced contraction in rabbit smooth muscle.* J Physiol, 2001. **535**(Pt 2): p. 553-64.

84. Murthy, K.S., et al., *Differential signalling by muscarinic receptors in smooth muscle: m2-mediated inactivation of myosin light chain kinase via Gi3, Cdc42/Rac1 and p21-activated kinase 1 pathway, and m3-mediated MLC20 (20 kDa regulatory light chain of myosin II) phosphorylation via Rho-associated kinase/myosin phosphatase targeting subunit 1 and protein kinase C/CPI-17 pathway.* Biochem. J., 2003. **374**(1): p. 145-155.

85. Hersch, E., et al., *Gq/G13 signaling by ET-1 in smooth muscle: MYPT1 phosphorylation via ETA and CPI-17 dephosphorylation via ETB.* American Journal of Physiology - Cell Physiology, 2004. **287**(5): p. C1209-C1218.

86. Ehlert, F.J., et al., *Muscarinic Receptors and Gastrointestinal Smooth Muscle*, in *Muscarinic receptor subtypes in smooth muscle*, R.M. Eglen, Editor. 1997, CRC Press: Boca Raton, Fla. p. 195 p.

87. Kuemmerle, J.F., *Occupation of αvβ3-integrin by endogenous ligands modulates IGF-I receptor activation and proliferation of human intestinal smooth muscle.* American Journal of Physiology - Gastrointestinal and Liver Physiology, 2006. **290**(6): p. G1194-G1202.

88. Kuemmerle, J.F. and K.S. Murthy, *Coupling of the Insulin-like Growth Factor-I Receptor Tyrosine Kinase to Gi2 in Human Intestinal Smooth Muscle.* Journal of Biological Chemistry, 2001. **276**(10): p. 7187-7194.

89. Murthy, K.S. and G.M. Makhlouf, *Differential Coupling of Muscarinic m2 and m3 Receptors to Adenylyl Cyclases V/VI in Smooth Muscle.* Journal of Biological Chemistry, 1997. **272**(34): p. 21317-21324.

90. Murthy, K.S. and G.M. Makhlouf, *Phosphoinositide metabolism in intestinal smooth muscle: preferential production of Ins(1,4,5)P3 in circular muscle cells.* American Journal of

Physiology - Gastrointestinal and Liver Physiology, 1991. **261**(6): p. G945-G951.

91. Murthy, K.S. and G.M. Makhlouf, *Functional characterization of phosphoinositide-specific phospholipase C-beta 1 and -beta 3 in intestinal smooth muscle.* Am J Physiol, 1995. **269**(4 Pt 1): p. C969-78.

92. Foskett, J.K., et al., *Inositol Trisphosphate Receptor Ca2+ Release Channels.* Physiological Reviews, 2007. **87**(2): p. 593-658.

93. Murthy, K.S., J.R. Grider, and G.M. Makhlouf, *InsP3-dependent Ca2+ mobilization in circular but not longitudinal muscle cells of intestine.* American Journal of Physiology - Gastrointestinal and Liver Physiology, 1991. **261**(6): p. G937-G944.

94. Iino, M., *Molecular basis and physiological functions of dynamic Ca2+ signalling in smooth muscle cells.* Novartis Found Symp, 2002. **246**: p. 142-6; discussion 147-53, 221-7.

95. Taylor, C.W., *Regulation of Ca^{2+} entry pathways by both limbs of the phosphoinositide pathway.*, in *Novartis Research Symposium -- Role of the sarcoplasmic reticulum in smooth muscle*, D. Chadwick and J. Goode, Editors. 2002, J. Wiley: New York. p. ix, 285 p.

96. Taylor, C.W. and A.J. Laude, *IP3 receptors and their regulation by calmodulin and cytosolic Ca2+.* Cell Calcium, 2002. **32**(5-6): p. 321-34.

97. Murthy, K.S. and G.M. Makhlouf, *cGMP-mediated Ca2+ release from IP3-insensitive Ca2+ stores in smooth muscle.* Am J Physiol, 1998. **274**(5 Pt 1): p. C1199-205.

98. Huang, J., et al., *Gi-coupled receptors mediate phosphorylation of CPI-17 and MLC20 via preferential activation of the PI3K/ILK pathway.* Biochem J, 2006. **396**(1): p. 193-200.

99. Niiro, N. and M. Ikebe, *Zipper-interacting protein kinase induces Ca(2+)-free smooth muscle contraction via myosin light chain phosphorylation.* J Biol Chem, 2001. **276**(31): p. 29567-74.

100. Ihara, E. and J.A. MacDonald, *The regulation of smooth muscle contractility by zipper-interacting protein kinase.* Can J Physiol Pharmacol, 2007. **85**(1): p. 79-87.

101. Aslam, M., et al., *cAMP/PKA antagonizes thrombin-induced inactivation of endothelial myosin light chain phosphatase: role of CPI-17.* Cardiovasc Res, 2010. **87**(2): p. 375-84.

102. Sriwai, W., H. Zhou, and K.S. Murthy, *G(q)-dependent signalling by the lysophosphatidic acid receptor LPA(3) in gastric smooth muscle: reciprocal regulation of MYPT1 phosphorylation by Rho kinase and cAMP-independent PKA.* Biochem J, 2008. **411**(3): p. 543-51.

103. Murthy, K.S., et al., *Phosphorylation of GRK2 by PKA augments GRK2-mediated phosphorylation, internalization, and desensitization of VPAC2 receptors in smooth muscle.* Am J Physiol Cell Physiol, 2008. **294**(2): p. C477-87.

104. Bonnevier, J. and A. Arner, *Actions Downstream of Cyclic GMP/Protein Kinase G Can Reverse Protein Kinase C-mediated Phosphorylation of CPI-17 and Ca2+Sensitization in Smooth Muscle.* Journal of Biological Chemistry, 2004. **279**(28): p. 28998-29003.

105. Erdodi, F., et al., *Phosphorylation of protein phosphatase type-1 inhibitory proteins by integrin-linked kinase and cyclic nucleotide-dependent protein kinases.* Biochemical and Biophysical Research Communications, 2003. **306**(2): p. 382-387.

106. Riento, K. and A.J. Ridley, *ROCKs: multifunctional kinases in cell behaviour.* Nat Rev Mol Cell Biol, 2003. **4**(6): p. 446-456.

107. Mueller, B.K., H. Mack, and N. Teusch, *Rho kinase, a promising drug target for neurological disorders.* Nat Rev Drug Discov, 2005. **4**(5): p. 387-398.

108. Kume, H., *RhoA/Rho-kinase as a therapeutic target in asthma.* Curr Med Chem, 2008. **15**(27): p. 2876-85.

109. Fukumoto, Y., S. Tawara, and H. Shimokawa, *Recent progress in the treatment of pulmonary arterial hypertension: expectation for rho-kinase inhibitors.* Tohoku J Exp Med, 2007. **211**(4): p. 309-20.

110. Fernandes, L.B., P.J. Henry, and R.G. Goldie, *Review: Rho kinase as a therapeutic target in the treatment of asthma and chronic obstructive pulmonary disease.* Therapeutic Advances in Respiratory Disease, 2007. **1**(1): p. 25-33.

111. Kimura, K., et al., *Regulation of myosin phosphatase by Rho and Rho-associated kinase (Rho-kinase).* Science, 1996. **273**(5272): p. 245-8.

112. Patel, C.A. and S. Rattan, *Spontaneously tonic smooth muscle has characteristically higher levels of RhoA/ROK compared with the phasic smooth muscle.* American Journal of Physiology - Gastrointestinal and Liver Physiology, 2006. **291**(5): p. G830-G837.

113. Amano, M., et al., *Phosphorylation and activation of myosin by Rho-associated kinase (Rho-kinase).* J Biol Chem, 1996. **271**(34): p. 20246-9.

114. Sugimoto, M., et al., *Rho-kinase phosphorylates eNOS at threonine 495 in endothelial cells.* Biochemical and Biophysical Research Communications, 2007. **361**(2): p. 462-467.

115. Hagerty, L., et al., *ROCK1 Phosphorylates and Activates Zipper-interacting Protein Kinase.* Journal of Biological Chemistry, 2007. **282**(7): p. 4884-4893.

116. Roux, P.P. and J. Blenis, *ERK and p38 MAPK-Activated Protein Kinases: a Family of Protein Kinases with Diverse Biological Functions.* Microbiol. Mol. Biol. Rev., 2004. **68**(2): p. 320-344.

117. Kordowska, J., R. Huang, and C.L. Wang, *Phosphorylation of caldesmon during smooth muscle contraction and cell migration or proliferation.* J Biomed Sci, 2006. **13**(2): p. 159-72.

118. Ihara, E., et al., *Mitogen-activated protein kinase pathways contribute to hypercontractility and increased Ca2+ sensitization in murine experimental colitis.* Mol Pharmacol, 2009. **75**(5): p. 1031-41.

119. Cain, A.E., D.M. Tanner, and R.A. Khalil, *Endothelin-1--induced enhancement of coronary smooth muscle contraction via MAPK-dependent and MAPK-independent [Ca(2+)](i) sensitization pathways.* Hypertension, 2002. **39**(2 Pt 2): p. 543-9.

120. Zhou, H., S. Das, and K.S. Murthy, *Erk1/2- and p38 MAP kinase-dependent phosphorylation and activation of cPLA2 by m3 and m2 receptors.* American Journal of Physiology - Gastrointestinal and Liver Physiology, 2003. **284**(3): p. G472-G480.

121. Greenwood, I.A., J. Ledoux, and N. Leblanc, *Differential regulation of Ca(2+)-activated Cl(-) currents in rabbit arterial and portal vein smooth muscle cells by Ca(2+)-calmodulin-dependent kinase.* J Physiol, 2001. **534**(Pt. 2): p. 395-408.

122. Ledoux, J., D. Chartier, and N. Leblanc, *Inhibitors of calmodulin-dependent protein kinase are nonspecific blockers of voltage-dependent K+ channels in vascular myocytes.* J Pharmacol Exp Ther, 1999. **290**(3): p. 1165-74.

123. Lu, K.K., et al., *Adhesion-dependent activation of CaMKII and regulation of ERK activation in vascular smooth muscle.* American Journal of Physiology - Cell Physiology, 2005. **289**(5): p. C1343-C1350.

124. Marganski, W.A., et al., *Targeting of a novel Ca+2/calmodulin-dependent protein kinase II is essential for extracellular signal-regulated kinase-mediated signaling in differentiated smooth muscle cells.* Circ Res, 2005. **97**(6): p. 541-9.

125. Pauly, R.R., et al., *Role of Calcium/Calmodulin-Dependent Protein Kinase II in the Regulation of Vascular Smooth Muscle Cell Migration.* Circulation, 1995. **91**(4): p. 1107-1115.

126. Henning, R.J., et al., *Cocaine Activates Calcium/Calmodulin Kinase II and Causes Cardiomyocyte Hypertrophy.* Journal of Cardiovascular Pharmacology, 2006. **48**(1): p. 802-813 10.1097/01.fjc.0000211796.45281.46.

127. Witcher, D.R., et al., *Unique phosphorylation site on the cardiac ryanodine receptor regulates calcium channel activity.* J Biol Chem, 1991. **266**(17): p. 11144-52.

128. Mattiazzi, A., L. Hove-Madsen, and D.M. Bers, *Protein kinase inhibitors reduce SR Ca transport in permeabilized cardiac myocytes.* Am J Physiol, 1994. **267**(2 Pt 2): p. H812-20.

129. Tansey, M.G., et al., *Phosphorylation of myosin light chain kinase by the multifunctional calmodulin-dependent protein kinase II in smooth muscle cells.* Journal of Biological Chemistry, 1992. **267**(18): p. 12511-12516.

130. Hashimoto, Y. and T.R. Soderling, *Phosphorylation of smooth muscle myosin light chain kinase by Ca2+/calmodulin-dependent protein kinase II: Comparative study of the phosphorylation sites.* Archives of Biochemistry and Biophysics, 1990. **278**(1): p. 41-45.

131. Tansey, M.G., et al., *Ca(2+)-dependent phosphorylation of myosin light chain kinase decreases the Ca2+ sensitivity of light chain phosphorylation within smooth muscle cells.* Journal of Biological Chemistry, 1994. **269**(13): p. 9912-9920.

132. Kim, I., et al., *Ca2+-calmodulin-dependent protein kinase II-dependent activation of contractility in ferret aorta.* J Physiol, 2000. **526 Pt 2**: p. 367-74.

133. Rokolya, A. and H.A. Singer, *Inhibition of CaM kinase II activation and force maintenance by KN-93 in arterial smooth muscle.* American Journal of Physiology - Cell Physiology, 2000. **278**(3): p. C537-C545.

134. Abbott, M.J., A.M. Edelman, and L.P. Turcotte, *CaMKK is an upstream signal of AMP-activated protein kinase in regulation of substrate metabolism in contracting skeletal muscle.* American Journal of Physiology - Regulatory, Integrative and Comparative Physiology, 2009. **297**(6): p. R1724-R1732.

135. Horman, S., et al., *Evaluation of the role of AMP-activated protein kinase and its downstream targets in mammalian hibernation.* Comparative Biochemistry and Physiology Part B: Biochemistry and Molecular Biology, 2005. **142**(4): p. 374-382.

136. Merlin, J., et al., *The M3-muscarinic acetylcholine receptor stimulates glucose uptake in L6 skeletal muscle cells by a CaMKK-AMPK-dependent mechanism.* Cellular Signalling, 2010. **22**(7): p. 1104-1113.

137. Woods, A., et al., *Ca2+/calmodulin-dependent protein kinase kinase-[beta] acts upstream of AMP-activated protein kinase in mammalian cells.* Cell Metabolism, 2005. **2**(1): p. 21-33.

138. Witczak, C.A., et al., *Ca2+/Calmodulin-Dependent Protein Kinase Kinase-α Regulates Skeletal Muscle Glucose Uptake Independent of AMP-Activated Protein Kinase and Akt Activation.* Diabetes, 2007. **56**(5): p. 1403-1409.

139. Hurley, R.L., et al., *The Ca2+/Calmodulin-dependent Protein Kinase Kinases Are AMP-activated Protein Kinase Kinases.* Journal of Biological Chemistry, 2005. **280**(32): p. 29060-29066.

140. Tokumitsu, H., et al., *A Single Amino Acid Difference between α and β Ca2+/Calmodulin-dependent Protein Kinase Kinase Dictates Sensitivity to the Specific Inhibitor, STO-609.* Journal of Biological Chemistry, 2003. **278**(13): p. 10908-10913.

141. Tokumitsu, H., et al., *STO-609, a Specific Inhibitor of the Ca2+/Calmodulin-dependent Protein Kinase Kinase.* Journal of Biological Chemistry, 2002. **277**(18): p. 15813-15818.

142. Miranda, L., et al., *AMP-activated protein kinase induces actin cytoskeleton reorganization in epithelial cells.* Biochemical and Biophysical Research Communications, 2010. **396**(3): p. 656-661.

143. Horman, S., et al., *AMP-activated protein kinase phosphorylates and desensitizes smooth muscle myosin light chain kinase.* J Biol Chem, 2008. **283**(27): p. 18505-12.

144. Bultot, L., et al., *Myosin light chains are not a physiological substrate of AMPK in the control of cell structure changes.* FEBS Letters, 2009. **583**(1): p. 25-28.

145. Lukas, T.J., *A Signal Transduction Pathway Model Prototype II: Application to Ca2+-Calmodulin Signaling and Myosin Light Chain Phosphorylation.* Biophysical Journal, 2004. **87**(3): p. 1417-1425.

146. Akata, T., *Cellular and molecular mechanisms regulating vascular tone. Part 1: basic mechanisms controlling cytosolic Ca^{2+} concentration and the Ca^{2+} dependent regulation of vascular tone.* Journal of Anesthesia, 2007. **21**(2): p. 220-231.

147. Akata, T., *Cellular and molecular mechanisms regulating vascular tone. Part 2: regulatory mechanisms modulating Ca^{2+} mobilization and/or myofilament Ca^{2+} sensitivity in vascular*

smooth muscle cells. Journal of Anesthesia, 2007. **21**(2): p. 232-242.

148. Wallace, A.S. and A.J. Burns, *Development of the enteric nervous system, smooth muscle and interstitial cells of Cajal in the human gastrointestinal tract.* Cell and Tissue Research, 2005. **319**(3): p. 367-382.

149. McHugh, K.M., *Molecular analysis of gastrointestinal smooth muscle development.* J Pediatr Gastroenterol Nutr, 1996. **23**(4): p. 379-94.

150. Young, H.M., *On the outside looking in: longitudinal muscle development in the gut.* Neurogastroenterology & Motility, 2008. **20**(5): p. 431-433.

151. McHugh, K.M., *Molecular analysis of smooth muscle development in the mouse.* Dev Dyn, 1995. **204**(3): p. 278-90.

152. Torihashi, S., et al., *Blockade of kit signaling induces transdifferentiation of interstitial cells of Cajal to a smooth muscle phenotype.* Gastroenterology, 1999. **117**(1): p. 140-148.

153. McLin, V.A., S.J. Henning, and M. Jamrich, *The Role of the Visceral Mesoderm in the Development of the Gastrointestinal Tract.* Gastroenterology, 2009. **136**(7): p. 2074-2091.

154. Kurahashi, M., et al., *Platelet-derived growth factor signals play critical roles in differentiation of longitudinal smooth muscle cells in mouse embryonic gut.* Neurogastroenterol Motil, 2008. **20**(5): p. 521-31.

155. Lesh, R.E., et al., *Localization of Ryanodine Receptors in Smooth Muscle.* Circ Res, 1998. **82**(2): p. 175-185.

156. Guerrero-Hernandez, A., et al., *Ryanodine receptors in smooth muscle.* Front Biosci, 2002. **7**: p. d1676-88.

157. Kotlikoff, M.L., et al., *Calcium release by ryanodine receptors in smooth muscle.* Novartis Found Symp, 2002. **246**: p. 108-19; discussion 119-24, 221-7.

158. Grider, J.R. and G.M. Makhlouf, *Contraction mediated by Ca++ release in circular and Ca++ influx in longitudinal intestinal muscle cells.* Journal of Pharmacology and Experimental Therapeutics, 1988. **244**(2): p. 432-437.

159. Murthy, K.S., J.F. Kuemmerle, and G.M. Makhlouf, *Agonist-mediated activation of PLA2 initiates Ca2+ mobilization in intestinal longitudinal smooth muscle.* American Journal of Physiology - Gastrointestinal and Liver Physiology, 1995. **269**(1): p. G93-G102.

160. Kuemmerle, J., K. Murthy, and G. Makhlouf, *Longitudinal smooth muscle of the mammalian intestine.* Cell Biochemistry and Biophysics, 1998. **28**(1): p. 31-44.

161. Hu, W., et al., *Characterization of S1P1 and S1P2 receptor function in smooth muscle by receptor silencing and receptor protection.* Am J Physiol Gastrointest Liver Physiol, 2006. **291**(4): p. G605-10.

162. Huang, J., et al., *Cross-regulation of VPAC(2) receptor desensitization by M(3) receptors via PKC-mediated phosphorylation of RKIP and inhibition of GRK2.* Am J Physiol Gastrointest Liver Physiol, 2007. **292**(3): p. G867-74.

163. Warner, F.J., et al., *Circular muscle contraction, messenger signalling and localization of binding sites for neurokinin A in human sigmoid colon.* Clin Exp Pharmacol Physiol, 2000. **27**(11): p. 928-33.

164. Hwang, S.J., et al., *beta-nicotinamide adenine dinucleotide is an enteric inhibitory neurotransmitter in human and nonhuman primate colons.* Gastroenterology, 2011. **140**(2): p. 608-617 e6.

165. Matsui, M., et al., *Mice Lacking M2 and M3 Muscarinic Acetylcholine Receptors Are Devoid of Cholinergic Smooth Muscle Contractions But Still Viable.* The Journal of Neuroscience, 2002. **22**(24): p. 10627-10632.

166. Harrington, A.M., et al., *Localization of muscarinic receptors M1R, M2R and M3R in the human colon.* Neurogastroenterology & Motility, 2010. **22**(9): p. 999-e263.

167. Sward, K., et al., *The role of RhoA and Rho-associated kinase in vascular smooth muscle contraction.* Curr Hypertens Rep, 2003. **5**(1): p. 66-72.

168. Al-Shboul, O., et al., *Agonist-Induced Rho Kinase and ZIP kinase Activity Levels in Different Regions of the Stomach.* The FASEB Journal, 2011. **25**(1_MeetingAbstracts): p. 1059.3.

169. Mbikou, P., et al., *Contribution of Rho kinase to the early phase of the calcium–contraction coupling in airway smooth muscle.* Experimental Physiology, 2011. **96**(2): p. 240-258.

170. Frei, E., et al., *Calcium-dependent and calcium-independent inhibition of contraction by cGMP/cGKI in intestinal smooth muscle.* American Journal of Physiology - Gastrointestinal and Liver Physiology, 2009. **297**(4): p. G834-G839.

171. Ihara, E., et al., *Ca2+-independent contraction of longitudinal ileal smooth muscle is potentiated by a zipper-interacting protein kinase pseudosubstrate peptide.* American Journal of Physiology - Gastrointestinal and Liver Physiology, 2009. **297**(2): p. G361-G370.

172. Ihara, E., et al., *Characterization of protein kinase pathways responsible for Ca2+ sensitization in rat ileal longitudinal smooth muscle.* American Journal of Physiology - Gastrointestinal and Liver Physiology, 2007. **293**(4): p. G699-G710.

173. Kahn, B.B., et al., *AMP-activated protein kinase: ancient energy gauge provides clues to modern understanding of metabolism.* Cell Metab, 2005. **1**(1): p. 15-25.

174. Jensen, T.E., et al., *Possible CaMKK-dependent regulation of AMPK phosphorylation and glucose uptake at the onset of mild tetanic skeletal muscle contraction.* American Journal of Physiology - Endocrinology And Metabolism, 2007. **292**(5): p. E1308-E1317.

175. Al-Shboul, O., et al., *269 Expression of AMP-Activated Kinase (AMP Kinase) and Inactivation of Myosin Light Chain (MLC) Kinase By AMP Kinase Determines the Magnitude of Smooth Muscle Contraction in Different Regions of the Stomach.* Gastroenterology, 2009. **136**(5): p. A-52.

176. Blair, D.R., et al., *A myosin II ATPase inhibitor reduces force production, glucose transport, and phosphorylation of AMPK and TBC1D1 in electrically stimulated rat skeletal muscle.* American Journal of Physiology - Endocrinology And Metabolism, 2009. **296**(5): p. E993-E1002.

177. Donsmark, M., et al., *Contractions induce phosphorylation of the AMPK site Ser565 in hormone-sensitive lipase in muscle.* Biochemical and Biophysical Research Communications, 2004. **316**(3): p. 867-871.

178. Schmitt, J.M., et al., *Calcium Activation of ERK Mediated by Calmodulin Kinase I.* Journal of Biological Chemistry, 2004. **279**(23): p. 24064-24072.

179. Edelman, A.M., et al., *Phosphorylation of smooth muscle myosin by type II Ca2+/calmodulin-dependent protein kinase.* Mol Cell Biochem, 1990. **97**(1): p. 87-98.

180. McCarron, J.G., et al., *Calcium-dependent enhancement of calcium current in smooth muscle by calmodulin-dependent protein kinase II.* Nature, 1992. **357**(6373): p. 74-7.

VITA

Charles Dudley Anderson, Jr. ("Andy") was born October 31, 1974 in Henrico County, Virginia. Raised in Hanover County, he graduated from Lee-Davis High School in 1992. Andy received his Bachelor of Science in Physics from the University of Richmond in 1996. Following coursework at the College of William and Mary to earn his teacher certification, he taught high school physics and leadership civics at Douglas Southall Freeman High School in Henrico County for four years. Returning to graduate school in 2002, he received his Master of Science in Biomedical Engineering in 2004 from Virginia Commonwealth University. Following the awarding of his Doctor of Philosophy degree from the Department of Physiology and Biophysics, School of Medicine, Virginia Commonwealth University in May 2011, he will assume a faculty position in the Department of Nurse Anesthesia, School of Allied Health Professions, Virginia Commonwealth University. He was never been more pleased or relieved than he was when he wrote this vita.